

# Estimation of Latent Group Structures in Time-Varying Panel Data Models

Paul Haimerl<sup>\*1</sup>, Stephan Smeekes<sup>†2</sup>, and Ines Wilms<sup>‡2</sup>

<sup>1</sup>Department of Economics and Business Economics, CoRE Center for Research in Energy: Economics and Markets, Aarhus University, Fuglesangs Allé 4, 8210 Aarhus V, Denmark

<sup>2</sup>Department of Quantitative Economics, Maastricht University, Tongersestraat 53, 6211 ML Maastricht, The Netherlands

March, 2025

**Abstract.** We introduce a panel data model where coefficients vary both over time and the cross-section. Slope coefficients change smoothly over time and follow a latent group structure, being homogeneous within but heterogeneous across groups. The group structure is identified using a pairwise adaptive group fused-Lasso penalty. The trajectories of time-varying coefficients are estimated via polynomial spline functions. We derive the asymptotic distributions of the penalized and post-selection estimators and show their oracle efficiency. A simulation study demonstrates excellent finite sample properties. An application to the emission intensity of GDP highlights the relevance of addressing cross-sectional heterogeneity and time-variance in empirical settings.

**Keywords.** Panel data model, time-varying coefficients, classification, basis splines.

**JEL classification.** C22, C23, C38.

## 1 Introduction

Panel datasets span multiple cross-sectional units and time periods. When analyzing such data, it is crucial to account for any heterogeneity that arises as a function of the different environments and time periods from which the observations are sampled: economic regimes vary across countries and industries (Kose et al., 2003); business cycles induce short-run fluctuations and technological innovations spur persistent structural shifts (Harvey, 1985; Cogley and Sargent, 2005); the distribution of environmental variables depends on the precise physical location, season, and time of day (Rahmstorf et al., 2017; Chang et al., 2020).

Ignoring heterogeneity along the cross-section can yield misleading inference, even in large samples (Galvao and Kato, 2014; Wang et al., 2019). Moreover, neglecting structural breaks or smooth variation over time may result in inconsistent and insignificant estimates (Chow, 1960; Hastie and Tibshirani, 1993; Perron and Wada, 2009). Consequently, statistical approaches that can accommodate heterogeneity across both the cross-sectional and the temporal dimensions are needed (Lee et al., 1997; Pesaran, 2006). This paper introduces

---

\*Correspondence to [paul.haimerl@econ.au.dk](mailto:paul.haimerl@econ.au.dk)

†[s.smeekes@maastrichtuniversity.nl](mailto:s.smeekes@maastrichtuniversity.nl)

‡[i.wilms@maastrichtuniversity.nl](mailto:i.wilms@maastrichtuniversity.nl)

We are grateful to Martin Schumann, the participants of the National Econometrics Study Group (NESG 2024), the Econometric Models of Climate Change conference (EMCC VIII), and the Aarhus Workshop in Econometrics (AWE V) for valuable comments. We thank Ali Mehrabani and Xia Wang for providing helpful code. Ines Wilms is supported by a grant from the Dutch Research Council (NWO), research program Vidi under the grant number VI.Vidi.211.032.

a panel data model that provides such flexibility: slope coefficients vary both along the cross-section and smoothly over time. We offer a penalized sieve estimation procedure leveraging a pairwise adaptive group fused-Lasso (*PAGFL*) penalty to jointly identify a latent group structure among the cross-sectional units and estimate group-specific time-varying coefficients.

Panel data models with latent group structures strike a good balance between capturing cross-sectional heterogeneity and maintaining parsimony by allocating cross-sectional units into groups where coefficients vary across but not within groups. Two primary sub-strands emerge from the literature. The first uses traditional clustering algorithms (e.g. *K*-means or hierarchical classifiers) on either test statistics, coefficient estimates, or fixed effects to estimate the group structure. Group-specific coefficients are obtained in a subsequent post-selection step (see [Lin and Ng, 2012](#); [Bonhomme and Manresa, 2015](#); [Sarafidis and Weber, 2015](#); [Ando and Bai, 2016](#); [Vogt and Linton, 2017](#); [Chen, 2019](#); [Liu et al., 2020](#); [Chetverikov and Manresa, 2022](#); [Lumsdaine et al., 2023](#), among others). The second strand employs penalization schemes to jointly trace out the latent grouping and group-specific coefficients, commonly complemented by a post-selection estimator to mitigate finite sample penalty bias ([Ke et al., 2015](#); [Su et al., 2016](#); [Wang et al., 2018](#); [Chernozhukov et al., 2019](#); [Miao et al., 2023](#); [Mehrabani, 2023](#)).

The recent literature has seen parallel advancements in time-varying panel data models, which describe temporal heterogeneity either through smoothly changing coefficients ([Huang et al., 2004](#); [Cai, 2007](#); [Su and Jin, 2012](#); [Robinson, 2012](#)) or discrete structural breaks ([Bai, 2010](#); [Qian and Su, 2016a](#)). Notably, the latter encompasses a large intersection with panel data models that are subject to latent group structures. Structural breaks are commonly estimated using shrinkage techniques like the fused-Lasso ([Okui and Wang, 2021](#); [Wang et al., 2024](#)) or by minimizing a criterion function that takes the break date as an explicit argument ([Baltagi et al., 2016](#); [Mugnier, 2022](#); [Lumsdaine et al., 2023](#)). Conversely, smoothly changing coefficients are modeled using nonparametric techniques such as local linear smoothers or splines ([Cai, 2007](#); [Robinson, 2012](#); [Su et al., 2019](#); [Friedrich et al., 2020](#); [Friedrich and Lin, 2024](#)).

We contribute to the literature on time-varying panel data models with latent group structures by introducing a novel estimation technique we term the *time-varying PAGFL* estimator. The method simultaneously obtains consistent estimates of the latent grouping and group-specific time-varying slope coefficients. The group structure is retrieved using the *PAGFL* penalty, which first appeared in [Qian and Su \(2016a,b\)](#) and was more recently used by [Mehrabani \(2023\)](#) to identify latent group patterns in time-constant panel data models. The *PAGFL* penalizes all pairwise coefficient vector differences. Subsequently, two cross-sectional units are assigned to the same group if the distance between their respective coefficient vectors is shrunk to zero. The group structure and the total number of groups are data-driven and require no prior specification.

To accommodate time-varying panel data models, we propose to approximate the time-varying coefficient functions using polynomial basis splines (B-splines), taking inspiration from [Huang et al. \(2004\)](#); [Su et al. \(2019\)](#). B-splines offer two decisive advantages over typically employed kernel estimators. First, spline functions are computationally efficient, parsimonious, and numerically stable while maintaining good approx-

imation properties. Second, B-splines can be expressed as linear combinations of polynomial basis functions. The basis functions vary across the domain of a B-spline but remain independent of its concrete functional form; that is, distinct B-splines can share the same underlying basis functions. Constant control points act as weights on each basis function and thus construct a unique linear combination that shapes the functional form of each B-spline. The possibility of separating a time-varying element, which does not have to be estimated, the set of basis functions, from individual time-constant components which are estimated, the control points, makes B-splines particularly convenient to use in conjunction with the *PAGFL* penalty. Additionally, we propose a *post-Lasso* estimator and introduce a consistent BIC-type information criterion (IC) to select the fused-Lasso tuning parameter. We show that both the penalized estimator and the post-selection estimator achieve the oracle property, being asymptotically equivalent to an infeasible oracle estimator based on the true grouping.

We compare the finite sample performance of our proposal to its most natural benchmark, namely the method of [Su et al. \(2019\)](#). Their approach differs from ours in that they employ the Classifier Lasso (*C-Lasso*; [Su et al., 2016](#)) to identify the latent group structure rather than a *PAGFL* penalty. We find that the *time-varying PAGFL* exhibits considerably better classification performance than the *C-Lasso* benchmark. This also holds for the estimation accuracy of the time-varying coefficients. Generally our method demonstrates good results in various simulation settings. Additionally, we demonstrate the merits of our methodology by analyzing trends in the carbon dioxide (CO<sub>2</sub>) intensity of Gross Domestic Product (GDP), the amount of CO<sub>2</sub> emitted per unit of GDP produced. In a panel dataset of 92 countries spanning 1960 to 2023, the model identifies five groups, each group with a unique trend of CO<sub>2</sub> intensity.

The plan for the remainder of this paper is as follows. Section 2 introduces the model along with our estimation procedure. The asymptotic theory is developed in Section 3. Section 4 investigates the finite sample performance via a simulation study. Section 5 presents the empirical illustration. The [final section](#) concludes. We provide a software implementation in our companion R-package *PAGFL* ([Haimerl et al., 2025](#)). Replication files of the simulation study and empirical application are available at [GitHub](#).<sup>1</sup>

**Notation.** Throughout, we denote vectors by boldface small letters and matrices by boldface capital letters. For a real matrix  $\mathbf{A}$ , the Frobenius norm is written as  $\|\mathbf{A}\|_F = \sqrt{\text{tr}(\mathbf{A}\mathbf{A}^\top)}$ .  $\mu_{\max}(\mathbf{A})$  and  $\mu_{\min}(\mathbf{A})$  denote the largest and smallest eigenvalues, respectively.  $\|\mathbf{A}\|_{\text{sp}} = \sqrt{\mu_{\max}(\mathbf{A}\mathbf{A}^\top)}$  gives the spectral norm.  $\text{vec}(\mathbf{A})$  describes a column-wise vectorization of  $\mathbf{A}$ .  $\|\mathbf{a}\|_2$  denotes the Euclidian norm for a real vector  $\mathbf{a}$ . The operators  $\xrightarrow{P}$ ,  $\xrightarrow{D}$ , and  $\text{plim}$  signal convergence in probability, convergence in distribution, and the probability limit.  $\otimes$  represents the Kronecker product. The superscript zero, or index when appropriate, marks a true quantity.  $\mathbf{I}_a$  and  $\mathbf{0}_a$  denote an  $a \times a$  identity matrix and an  $a \times 1$  vector of zeros. ‘With probability approaching one’ is abbreviated as w.p.a.1. For two sequences of positive (random) numbers  $a_n$  and  $b_n$ ,  $a_n \lesssim b_n$  indicates that  $a_n/b_n$  is (stochastically) bounded and  $a_n \asymp b_n$  signals that both  $a_n \lesssim b_n$  and  $b_n \lesssim a_n$  hold.

<sup>1</sup>R-Notebooks and a Dockerfile with replication material are published at [github.com/Paul-Haimerl/replication-tv-pagfl](https://github.com/Paul-Haimerl/replication-tv-pagfl).

## 2 Model and Estimation

In this section, we introduce the time-varying panel data model (Section 2.1) and our penalized sieve estimation procedure (Section 2.2).

### 2.1 The Model

Consider the time-varying panel data model

$$y_{it} = \gamma_i^0 + \boldsymbol{\beta}_{it}^{0'} \mathbf{x}_{it} + \epsilon_{it}, \quad i = 1, \dots, N, \quad t = 1, \dots, T, \quad (2.1)$$

where  $y_{it}$  is the response,  $\mathbf{x}_{it}$  is a  $p \times 1$  vector of explanatory variables, the  $\gamma_i^0$ 's denote the unobserved individual fixed effects, and  $\epsilon_{it}$  represents a zero mean idiosyncratic error. The fixed effects  $\gamma_i^0$  may correlate with some elements of  $\mathbf{x}_{it}$  and are independently distributed across individuals. We assume that the  $p$ -dimensional vector of slope coefficients  $\boldsymbol{\beta}_{it}^0$  varies smoothly over time. In particular, we take

$$\boldsymbol{\beta}_{it}^0 = \boldsymbol{\beta}_i^0(t/T), \quad (2.2)$$

where the superscript 0 denotes the true parameter value. Furthermore, we assume that the time-varying slope parameters adhere to the following latent group structure

$$\boldsymbol{\beta}_i^0\left(\frac{t}{T}\right) = \sum_{k=1}^{K_0} \boldsymbol{\alpha}_k^0\left(\frac{t}{T}\right) \mathbf{1}\{i \in G_k^0\}, \quad (2.3)$$

where  $\boldsymbol{\alpha}_k^0(t/T)$  is a  $p \times 1$  vector of group-specific time-varying functional coefficients and  $\mathbf{1}\{\cdot\}$  denotes the indicator function. The grouping structure  $\mathcal{G}_K^0 = \{G_1^0, \dots, G_{K_0}^0\}$  results in a partition of the cross-sectional units into disjoint sets;  $\cup_{k=1}^{K_0} G_k^0 = \{1, \dots, N\}$  and  $G_j^0 \cap G_k^0 = \emptyset$  for any  $j \neq k$ . We denote the cardinality of group  $G_k^0$  as  $N_k$ .

*Remark 2.1.* The group-specific functional coefficients  $\boldsymbol{\alpha}_k^0(\cdot)$  are smooth functions of  $t/T$  (see Assumption A.1(vi)). As a consequence, the data generating process (DGP) in (2.1) does not describe discrete structural breaks in the slope parameters but rather smooth variations over time. Nevertheless, our model is general and nests many previously studied specifications, including time-constant panel data models with latent group structures.

### 2.2 Penalized Sieve Estimation of Time-Varying Coefficients

Taking inspiration from Huang et al. (2004); Su et al. (2019), we approximate the  $p \times 1$  functional coefficient vector  $\boldsymbol{\beta}_i^0(t/T)$  in (2.2) using an  $M$ -dimensional vector  $\mathbf{b}(t/T)$  of polynomial spline basis functions

$$\boldsymbol{\beta}_i^{0'}\left(\frac{t}{T}\right) \mathbf{x}_{it} \approx \left[ \boldsymbol{\Pi}_i^{0'} \mathbf{b}\left(\frac{t}{T}\right) \right]' \mathbf{x}_{it} = \text{vec}(\boldsymbol{\Pi}_i^0)' \left[ \mathbf{x}_{it} \otimes \mathbf{b}\left(\frac{t}{T}\right) \right] = \boldsymbol{\pi}_i^{0'} z_{it}, \quad (2.4)$$

where  $\mathbf{\Pi}_i^0 = (\boldsymbol{\pi}_{i1}^0, \dots, \boldsymbol{\pi}_{ip}^0)$  denotes a  $M \times p$  matrix of B-spline control points,  $\boldsymbol{\pi}_i^0 = \text{vec}(\mathbf{\Pi}_i^0)$ , and  $\mathbf{z}_{it} = \mathbf{x}_{it} \otimes \mathbf{b}(t/T)$  is a  $Mp \times 1$  vector.  $\mathbf{\Pi}_i^{0'} \mathbf{b}(t/T)$  is a function in the sieve-space  $\mathbb{B}_M$  that is spanned by the  $M$  basis functions in  $\mathbf{b}(t/T)$ . By increasing the polynomial degree  $d$  (order  $d + 1$ ) and the number of interior knots  $M^*$  of the spline basis, we extend  $M = M^* + d + 1$  along with  $\mathbb{B}_M$  and obtain closer approximations of  $\boldsymbol{\beta}_i^0$ . Appendix B contains full details on the spline basis functions.

Plugging (2.4) into model (2.1) then yields

$$y_{it} = \gamma_i^0 + \boldsymbol{\pi}_i^{0'} \mathbf{z}_{it} + u_{it}, \quad u_{it} = \epsilon_{it} + \eta_{it}, \quad (2.5)$$

where  $u_{it}$  collects the idiosyncratic error  $\epsilon_{it}$  and the sieve approximation error  $\eta_{it} = \boldsymbol{\beta}_i^{0'}(t/T) \mathbf{x}_{it} - \boldsymbol{\pi}_i^{0'} \mathbf{z}_{it}$ . To obtain an estimate of the time-varying slope parameters  $\boldsymbol{\beta}_i^0(t/T)$  in model (2.1), we estimate the time-constant vector  $\boldsymbol{\pi}_i^0$  in model (2.5) and take  $\hat{\boldsymbol{\beta}}_i(t/T) = \hat{\mathbf{\Pi}}_i' \mathbf{b}(t/T)$ , where  $\hat{\boldsymbol{\pi}}_i = \text{vec}(\hat{\mathbf{\Pi}}_i)$ .

Joint identification of the time-varying coefficients and latent group structure in (2.3) is achieved through *penalized* sieve estimation, leveraging the *PAGFL* penalty (Qian and Su, 2016a; Mehrabani, 2023). In what follows, we introduce this estimation procedure in the context of the time-varying panel data model (2.1). Beyond this baseline, our proposal can readily accommodate extensions, as discussed in Appendix D.

First, we concentrate out the individual fixed effects  $\gamma_i^0$  in (2.5) using  $\tilde{y}_{it} = y_{it} - T^{-1} \sum_{t=1}^T y_{it}$ , with  $\tilde{\mathbf{z}}_{it}$  and  $\tilde{\epsilon}_{it}$  defined analogously. Let  $\boldsymbol{\pi} = (\boldsymbol{\pi}'_1, \dots, \boldsymbol{\pi}'_N)'$  collect all individual parameters. We then take as objective function

$$\mathcal{F}_{NT}(\boldsymbol{\pi}, \lambda) = \frac{1}{T} \sum_{i=1}^N \sum_{t=1}^T (\tilde{y}_{it} - \boldsymbol{\pi}'_i \tilde{\mathbf{z}}_{it})^2 + \frac{\lambda}{N} \sum_{i=1}^{N-1} \sum_{j=i+1}^N \dot{\omega}_{ij} \|\boldsymbol{\pi}_i - \boldsymbol{\pi}_j\|_2, \quad (2.6)$$

where the first part is the usual sum of squared residuals and the second part is the *time-varying PAGFL* penalty term with tuning parameter  $\lambda > 0$  and adaptive penalty weights  $\dot{\omega}_{ij}$ . The weights are set to  $\dot{\omega}_{ij} = \|\hat{\boldsymbol{\pi}}_i - \hat{\boldsymbol{\pi}}_j\|_2^{-\kappa}$ , where  $\hat{\boldsymbol{\pi}}_i$  represents an initial consistent estimate  $\hat{\boldsymbol{\pi}} = \arg \min_{\boldsymbol{\pi}} T^{-1} \sum_{i=1}^N \sum_{t=1}^T (\tilde{y}_{it} - \boldsymbol{\pi}'_i \tilde{\mathbf{z}}_{it})^2$  and  $\kappa$  is specified by the user; we maintain  $\kappa = 2$  throughout the paper. Objective (2.6) generalizes the objective function in Mehrabani (2023, eq. 2.6) from a *time-constant PAGFL* to a *time-varying PAGFL*. The penalized sieve estimator (*PSE*)  $\hat{\boldsymbol{\pi}}_\lambda$  is then obtained by minimizing (2.6), namely

$$\hat{\boldsymbol{\pi}}_\lambda = \arg \min_{\boldsymbol{\pi}} \mathcal{F}_{NT}(\boldsymbol{\pi}, \lambda).$$

In the following, unless required, we suppress the dependence of  $\hat{\boldsymbol{\pi}}$  on  $\lambda$  to lighten the notation.

The *time-varying PAGFL* penalty encourages sparsity in the difference between two coefficient vectors, and this across all  $N(N - 1)/2$  pairs of cross-sectional individuals. For large  $\lambda$ , some of these differences will be shrunken to exactly zero, implying that the corresponding cross-sectional units feature identical parameter estimates.

Cross-sectional units with identical slope estimates are assigned to the same group by collecting all  $\hat{K}$

unique subvectors  $\hat{\boldsymbol{\pi}}_i$  of  $\hat{\boldsymbol{\pi}}$  in the vector  $\hat{\boldsymbol{\xi}} = (\hat{\boldsymbol{\xi}}'_1, \dots, \hat{\boldsymbol{\xi}}'_{\hat{K}})'$  and defining the set  $\hat{G}_k = \{i : \hat{\boldsymbol{\pi}}_i = \hat{\boldsymbol{\xi}}_k, 1 \leq i \leq N\}$  for each  $k = 1, \dots, \hat{K}$ . Subsequently, the group-specific *PSE* coefficient function equals  $\hat{\boldsymbol{\alpha}}_k(t/T) = \hat{\boldsymbol{\Xi}}'_k \mathbf{b}(t/T)$ , where  $\hat{\boldsymbol{\xi}}_k = \text{vec}(\hat{\boldsymbol{\Xi}}_k)$ . As such, parameter estimation and identification of the latent group structure are performed simultaneously. The total number of clusters  $\hat{K}$  is determined by the tuning parameter  $\lambda$ . We propose to select  $\lambda$  using the consistent information criterion (IC) introduced in Section 3.

*Remark 2.2.* The penalty term in criterion (2.6) is time-invariant and, therefore, also the grouping structure. Nevertheless, cross-sectional units switching groups do not lead to inconsistent estimates of the time-varying coefficients but only to a larger number of groups  $\hat{K}$ , since each distinct combination of the time of the switch, origin group, and destination group implies one excess estimated group. Alternatively, one can define the penalty in (2.6) over each of the  $M$  rows in  $\mathbf{\Pi}_i$  individually, implying groupings specific to each basis function and thus allowing for time-varying group membership. Such an extension is further discussed in Appendix D.1.

*Remark 2.3.* The *time-varying PAGFL* shows similarities with the proposal in Su et al. (2019). However, they use a different approach to identify the latent group structure, namely the *C-Lasso* of Su et al. (2016). The *C-Lasso* shrinks  $N$  individual coefficients towards  $K$  group-level coefficients and requires an additional tuning parameter to explicitly determine  $K$ . Moreover, it is involved to transform the *C-Lasso* objective into a convex problem. These two constraints do not apply to our routine. In addition, we allow  $K$  to diverge to infinity and let the minimum group separability to tend to zero asymptotically (see Section 3).

Objective function (2.6) is convex in  $\boldsymbol{\pi}$ . To solve for  $\boldsymbol{\pi}$ , we employ a computationally efficient alternating direction method of moments (*ADMM*) algorithm, adapted from Mehrabani (2023, sec. 5) and detailed in Appendix C. An open-source implementation of this algorithm is provided in our companion companion R-package *PAGFL* (Haimerl et al., 2025).

To omit finite sample penalty bias from the *PAGFL* term in (2.6), we propose a post-selection fused-Lasso estimator, labeled *post-Lasso* estimator for brevity,

$$\hat{\boldsymbol{\xi}}_{\hat{G}_k}^p = \left( \sum_{i \in \hat{G}_k} \sum_{t=1}^T \tilde{\mathbf{z}}_{it} \tilde{\mathbf{z}}'_{it} \right)^{-1} \sum_{i \in \hat{G}_k} \sum_{t=1}^T \tilde{\mathbf{z}}_{it} \tilde{y}_{it} \quad \text{for } k = 1, \dots, \hat{K},$$

for the given estimated group pattern  $\hat{\mathcal{G}} = \{\hat{G}_1, \dots, \hat{G}_{\hat{K}}\}$ . Subsequently, the final *post-Lasso* time-varying coefficient estimates follow as  $\hat{\boldsymbol{\alpha}}_{\hat{G}_k}^p(t/T) = \hat{\boldsymbol{\Xi}}_{\hat{G}_k}^{p'} \mathbf{b}(t/T)$ , using  $\hat{\boldsymbol{\xi}}_{\hat{G}_k}^p = \text{vec}(\hat{\boldsymbol{\Xi}}_{\hat{G}_k}^p)$ .

### 3 Asymptotic Properties

In this section, we study the consistency of the coefficient estimates and the classification procedure. Furthermore, we establish the limiting distribution of the *PSE* and the *post-Lasso* estimator. Formal proofs appear in Appendix A.

### 3.1 Preliminary Convergence Rates

Let  $\mathbb{C}^\theta[0, 1]$  denote the space of functions that are  $\theta$ -times continuously differentiable on the unit interval. Moreover, if  $\mathbf{x}_{it}$  includes an intercept terms, let  $\mathbf{x}_{it} = (1, \mathbf{x}_{it}^{(2)})$  and  $\mathbf{x}_{it}^{(2)} = \mathbf{x}_{it}$  else.

#### Assumption 1.

- (i) There exists a positive constant  $c_{\epsilon\epsilon} < \infty$  such that  $N^{-1} \sum_{i=1}^N \sum_{j=1}^N |\max_t E(\epsilon_{it}\epsilon_{jt})| \leq c_{\epsilon\epsilon}$ .<sup>2</sup>
- (ii)  $\{(\mathbf{x}_{it}^{(2)}, \epsilon_{it}), t = 1, \dots, T\}$  is a strong mixing process with geometric decay such that the mixing coefficient  $\phi(j)$  satisfies  $\phi(j) \leq c_\phi \varphi^j$  for some  $c_\phi < \infty$ ,  $0 \leq \varphi < 1$ , and each  $i = 1, \dots, N$ .
- (iii) There exist two positive constants  $c_x < \infty$  and  $c_\epsilon < \infty$  such that  $\max_{i,t} E\|\mathbf{x}_{it}\|_2^q \leq c_x$  and  $\max_{i,t} E|\epsilon_{it}|^q \leq c_\epsilon$  for some  $q \geq 6$ , when  $\mathbf{x}_{it} \neq 1$ .
- (iv) There exist a lower and upper bound  $0 < \underline{c}_{xx} \leq \bar{c}_{xx} < \infty$  such that  $\underline{c}_{xx} \leq \min_{i,t} \mu_{\min}(\text{Var}(\mathbf{x}_{it}^{(2)})) \leq \max_{i,t} \mu_{\max}(E(\mathbf{x}_{it}^{(2)} \mathbf{x}_{it}^{(2)'})) \leq \bar{c}_{xx}$ .
- (v)  $\lim_{N \rightarrow \infty} N_k/N \in [0, 1)$  for each  $k = 1, \dots, K_0$  and  $N_k > 1$  for all  $k \in \{k : \lim_{N \rightarrow \infty} N_k/N = 0, 1 \leq k \leq K_0\}$ .
- (vi)  $\boldsymbol{\alpha}_k^0(v) \in \mathbb{C}^\theta[0, 1]$  for each  $k = 1, \dots, K_0$  and some  $1 < \theta \leq d + 2$ .

Assumption 1(i) is standard in the factor model literature and limits cross-sectional dependence (cf. Bai and Ng, 2002). This condition is trivially satisfied if the idiosyncratic errors are independently distributed, an assumption frequently made for similar panel data models with latent group structures (cf. Su et al., 2016; Qian and Su, 2016a; Su et al., 2019). Assumptions 1(ii)-(iv) loosely follow Su et al. (2019, Assumption 1(ii)-(iv)). Assumption 1(ii) imposes a strong mixing process, which nests a multitude of popular and extensively studied time series processes with geometrically decaying innovations, such as common ARMA, GARCH, Markov-switching, or threshold autoregressive models. Serial correlation as well as conditional heteroscedasticity in the error process comply with this assumption.

As Su et al. (2019) point out, Assumption 1(ii) restricts the fixed effects  $\gamma_i$  in dynamic panels to be either nonrandom and the idiosyncratic error processes having a Lebesgue-integrable characteristic function or the mixing coefficients to be conditioned on the fixed effects (see Andrews, 1984; Hahn and Kuersteiner, 2011). Assumptions 1(i)-(ii) can also be replaced by similar primitive (Bonhomme and Manresa, 2015, A.1(d)-(f)) or higher-level assumptions (Mehrabani, 2023, A.1(i)-(iii)) that impose a sufficient degree of independence across time and the cross-section such that a central limit theorem can be applied.

Assumptions 1(iii)-(iv) place common moment conditions on the regressors and innovations. The conditions on the regressors in Assumptions 1(iii)-(iv) are redundant if  $\mathbf{x}_{it}$  is deterministic. Assumption 1(v) allows group sizes to remain constant or to diverge at a speed slower or equal to  $N$ . Assumption 1(vi) imposes

<sup>2</sup>We abbreviate  $\max_{1 \leq i \leq N}$ ,  $\max_{1 \leq t \leq T}$ , and  $\max_{1 \leq i \leq N, 1 \leq t \leq T}$  with  $\max_i$ ,  $\max_t$ , and  $\max_{i,t}$ , respectively.  $\min_i$ ,  $\min_t$ , and  $\min_{i,t}$  are defined likewise.

smoothness on the true functional coefficients and ensures that they can be well approximated by polynomial splines.

Let  $J_{\min}$  indicate the minimum group separability in the sieve-space  $\mathbb{B}_M$ ,  $J_{\min} = \min_{i \in G_k^0, j \notin G_k^0} \|\pi_i^0 - \pi_j^0\|_2$ .

**Assumption 2.**

- (i)  $\lim_{T \rightarrow \infty} MT^{-1/2} = 0$ .
- (ii)  $\lim_{T \rightarrow \infty} (MT^{-1/2} + M^{-\theta+1/2})^{-1} J_{\min} = \infty$ .
- (iii)  $\text{plim}_{T \rightarrow \infty} (T^{-1/2} + M^{-\theta-1/2})^{-1} \lambda J_{\min}^{-\kappa} = c_\lambda$  for some constant  $c_\lambda > 0$ .
- (iv)  $\text{plim}_{(N,T) \rightarrow \infty} (MT^{-1/2} + M^{-\theta+1/2})^{-\kappa-1} M^{1/2} \lambda N_k / N = \infty$  for each  $k = 1, \dots, K_0$ .

Assumption 2(i) controls the size of the spline basis system. Assumption 2(ii) determines the rate at which the minimum group separability in  $\mathbb{B}_M$  may shrink to zero. Assumption 2(iii) governs the speed at which the tuning parameter  $\lambda$  must shrink to zero. Assumption 2(iv) places conditions on the relative rates of the number of coefficients to be estimated, coefficient convergence, and  $\lambda$  so that group-specific trajectories can still be consistently estimated. In sum,  $N$ ,  $T$ ,  $M$ , and  $K_0$  diverge to infinity, whereas  $\lambda$  and  $J_{\min}$  tend to zero in the limit.

**Theorem 3.1.** *Given that Assumptions 1 and 2(i)-(iii) are satisfied,*

- (i)  $\|\hat{\pi}_i - \pi_i^0\|_2 = O_p(MT^{-1/2} + M^{-\theta+1/2})$ ,
- (ii)  $N^{-1} \sum_{i=1}^N \|\hat{\pi}_i - \pi_i^0\|_2^2 = O_p(M^2T^{-1} + M^{-2\theta+1})$ ,

for  $i = 1, \dots, N$ .

Theorem 3.1 establishes pointwise and mean-square convergence of  $\hat{\pi}_i$ . The first summand in the rates of Theorem 3.1 reflects the stochastic error. The second summand corresponds to the asymptotic bias of the sieve technique. Increasing the complexity of the spline system  $M$  involves a bias-variance trade-off. On the one hand, the larger  $M$ , the slower the convergence due to the increased size of the coefficient vector.<sup>3</sup> On the other, increasing  $M$  reduces the asymptotic sieve bias. Moreover, the greater the order of continuous differentiability of the true coefficient functions  $\theta$ , the faster the sieve bias shrinks in  $M$ .

**Corollary 3.2.** *Given that Assumptions 1 and 2(i)-(iii) are satisfied,*

- (i)  $\sup_{v \in [0,1]} \|\hat{\beta}_i(v) - \beta_i^0(v)\|_2 = O_p(MT^{-1/2} + M^{-\theta+1/2})$ ,
- (ii)  $\int_0^1 \|\hat{\beta}_i(v) - \beta_i^0(v)\|_2^2 dv = O_p(MT^{-1} + M^{-2\theta})$ ,

for  $i = 1, \dots, N$ .

---

<sup>3</sup>Note that  $O_p(MT^{-1/2} + M^{-\theta+1/2}) = o_p(1)$  by Assumptions 1(vi) and 2(i).



Corollary 3.2 relates the results of Theorem 3.1 to the actual functional coefficients. Note that the true coefficient functions are time-continuous. As a consequence, we report the supremum and integral over the unit interval. Interestingly, the pointwise rates of  $\hat{\pi}_i$  and  $\hat{\beta}_i(v)$  match, whereas the  $L_2$  rate of  $\hat{\beta}_i(v)$  is faster in  $M$ . This result is caused by the boundedness property of B-splines (see Lemma A.1(ii)).

## 3.2 Classification Consistency

This subsection studies the asymptotic behavior of the classification procedure.

**Theorem 3.3.** *Given that Assumptions 1 and 2 are satisfied,  $\Pr(\|\hat{\pi}_i - \hat{\pi}_j\|_2 = 0 \forall i, j \in G_k^0, 1 \leq k \leq K_0) \rightarrow 1$ , as  $(N, T) \rightarrow \infty$ .*

Theorem 3.3 establishes that, in the limit, every cross-sectional unit is simultaneously placed into the correct group.

**Corollary 3.4.** *Given that Assumptions 1 and 2 are satisfied,*

- (i)  $\lim_{(N, T) \rightarrow \infty} \Pr(\hat{K} = K_0) = 1$ ,
- (ii)  $\lim_{(N, T) \rightarrow \infty} \Pr(\hat{\mathcal{G}}_{K_0} = \mathcal{G}_{K_0}^0) = 1$ .

Based on Theorem 3.3, Corollary 3.4 shows that the correct number of groups and group structure will be derived asymptotically. This result is intuitive since, given Theorem 3.3,  $\hat{\pi}$  can only hold  $K_0$  distinct elements and all homogenous individuals are assigned to the same group as  $(N, T) \rightarrow \infty$ . Since the latent grouping will be identified w.p.a.1, Corollary 3.4 motivates the oracle property of the procedure. This implies that the estimation procedure is asymptotically equivalent to an infeasible oracle estimator based on the true grouping.

## 3.3 Limiting Distribution of the *PSE* and *Post-Lasso* Estimators

In the following, we derive the asymptotic distribution of the *PSE* and the *post-Lasso*.

**Assumption 3.**  $\text{plim}_{(N, T) \rightarrow \infty} (N_k T M)^{1/2} \lambda J_{\min}^{-\kappa} = 0$  for each  $k = 1, \dots, K_0$ .

The penalty term in (2.6) grows quadratically in  $N$ . Hence, Assumption 3 strengthens Assumption 2(iii) and imposes conditions for the penalty term to vanish asymptotically, resulting in coinciding limiting distributions for the *PSE* and the *post-Lasso*. To this end, Assumption 3 specifies a larger group separation or a faster rate at which  $\lambda$  converges to zero. Assumption 3 is only relevant for the *PSE* and need not hold for the asymptotic properties of the *post-Lasso*.

Let  $\epsilon_i = (\epsilon_{i1}, \dots, \epsilon_{iT})'$ .

**Assumption 4.**

- (i) There exists a positive constant  $\bar{c}_{\epsilon\epsilon} < \infty$  such that  $\lim_{(N, T) \rightarrow \infty} \max_{i \in G_k^0} \mu_{\max}(E(\epsilon_i \epsilon_i')) \leq \bar{c}_{\epsilon\epsilon}$  for each  $k = 1, \dots, K_0$ .

(ii)  $\lim_{(N,T) \rightarrow \infty} NTM^{-2\theta} = 0$ .

Assumption 4(i) imposes a mild restriction on the error process, enabling the use of the Lindeberg condition to derive the limiting distribution in Theorem 3.5. Assumption 4(ii) provides an additional regularity condition that precludes the sieve approximation error from dominating the limiting distributions of the *PSE* and the *post-Lasso*. Let  $\hat{\mathbf{Q}}_{G_k^0, \tilde{z}\tilde{z}} = \sum_{i \in G_k^0} \hat{\mathbf{Q}}_{i, \tilde{z}\tilde{z}}$  with  $\hat{\mathbf{Q}}_{i, \tilde{z}\tilde{z}} = T^{-1} \sum_{t=1}^T \tilde{z}_{it} \tilde{z}'_{it}$  and  $\tilde{\mathbf{Z}}_i = (\tilde{z}_{i1}, \dots, \tilde{z}_{iT})$ . Furthermore, define the variance-covariance matrix  $\hat{\mathbf{\Omega}}_{G_k^0} = \hat{\nu}'_{G_k^0} \hat{\mathbf{\Xi}}_{G_k^0} \hat{\nu}_{G_k^0}$  with

$$\hat{\nu}_{G_k^0} = \left( MN_k^{-1} \hat{\mathbf{Q}}_{G_k^0, \tilde{z}\tilde{z}} \right)^{-1} (\mathbf{I}_p \otimes \mathbf{b}(v)),$$

$$\hat{\mathbf{\Xi}}_{G_k^0} = \frac{M}{N_k T} \sum_{i \in G_k^0} \tilde{\mathbf{Z}}'_i E(\epsilon_i \epsilon'_i) \tilde{\mathbf{Z}}_i,$$

and  $\mathbf{q}_{G_k^0} = \sqrt{M/(N_k T)} \sum_{i \in G_k^0} \sum_{t=1}^T E(\tilde{z}_{it} \tilde{\epsilon}_{it})$ .

**Theorem 3.5.** *Given that Assumptions 1-4 are satisfied,*

- (i)  $\sqrt{N_k T/M} \hat{\mathbf{\Omega}}_{G_k^0}^{-1/2} (\hat{\boldsymbol{\alpha}}_k(v) - \boldsymbol{\alpha}_k^0(v)) - \hat{\mathbf{\Xi}}_{G_k^0}^{-1/2} \mathbf{q}_{G_k^0} \xrightarrow{D} N(0, \mathbf{I}_p),$
- (ii)  $\sqrt{N_k T/M} \hat{\mathbf{\Omega}}_{\hat{G}_k}^{-1/2} (\hat{\boldsymbol{\alpha}}_{\hat{G}_k}^p(v) - \boldsymbol{\alpha}_k^0(v)) - \hat{\mathbf{\Xi}}_{G_k^0}^{-1/2} \mathbf{q}_{G_k^0} \xrightarrow{D} N(0, \mathbf{I}_p).$

$\mathbf{q}_{G_k^0}$  equals zero in the case of strictly exogenous regressors. However, commonly referred to as the Nickell bias,  $\mathbf{q}_{G_k^0}$  is nonzero and of order  $O(\sqrt{N_k/T})$  for dynamic panel data models (Nickell, 1981; Phillips and Sul, 2007). The bias emerges when  $T$  remains fixed or grows slower than  $N_k$ . The within-transformation nets out the fixed effect  $\gamma_i$  but simultaneously induces a contemporaneous correlation between the error term and the autoregressive regressor, thus biasing the coefficient estimate if  $T$  does not grow fast enough relative to the number of individuals that feed into the group-specific autoregressive coefficient function (Nickell, 1981; Kiviet, 1995; Hahn and Kuersteiner, 2011; Su et al., 2016).

The *PSE* and the *post-Lasso* estimators are asymptotically equivalent to the true coefficient function and achieve oracle efficiency. Furthermore, given Assumption A.3, both estimators feature the same asymptotic distribution. Nevertheless, despite their equivalence in the limit, we recommend using the *post-Lasso* in finite sample applications. The penalty term of the *PSE* can lead to non-negligible bias, particularly in small samples. The simulation study in Section 4 corroborates this finding.

Given a consistent estimator  $\hat{\mathbf{\Xi}}_{\hat{G}_k}$  and exploiting the oracle property in Corollary 3.4, the variance of the limiting distribution can be estimated consistently. Potential techniques to derive  $\hat{\mathbf{\Xi}}_{\hat{G}_k}$  are numerous. We follow the literature on heteroscedasticity and autocorrelation robust estimation of covariance matrices and take

$$\hat{\mathbf{\Xi}}_{\hat{G}_k} = \hat{\mathbf{\Xi}}_{\hat{G}_k}^{(0)} + \sum_{h=1}^{H_T} w(h, H_T) \left( \hat{\mathbf{\Xi}}_{\hat{G}_k}^{(h)} + \hat{\mathbf{\Xi}}_{\hat{G}_k}^{(h)'} \right),$$

where  $H_T$  is the window size,  $\hat{\mathbf{\Xi}}_{\hat{G}_k}^{(h)} = N_k^{-1} \sum_{i \in \hat{G}_k} T^{-1} \sum_{t=h+1}^T \tilde{z}_{it} \tilde{z}'_{it-1} \hat{\epsilon}_{it} \hat{\epsilon}'_{it-1}$ , and  $\hat{\epsilon}_{it} = \tilde{y}_{it} - \hat{\boldsymbol{\alpha}}_{\hat{G}_k}^{p'}(t/T) \tilde{\mathbf{x}}_{it}$  (Newey and West, 1987; Hahn and Kuersteiner, 2002; Pesaran, 2006; Müller, 2014).  $w(h, H_T)$  denotes a

weighting function subject to  $\sup_h |w(h, H_T)| < \infty$  and  $\lim_{T \rightarrow \infty} w(h, H_T) = 1$ . It is common to specify  $w(h, H_T) = 1 - h/(H_T + 1)\mathbf{1}\{h \leq H_T\}$  (Newey and West, 1987). A rigorous derivation of the consistency of  $\hat{\mathcal{E}}_{\hat{G}_k}$  and required primitive conditions are beyond the scope of this paper and are left for future work (see, e.g., Su and Jin, 2012, Theorem 4.3 for further reference).

### 3.4 Selecting the Tuning Parameter $\lambda$

In the remainder of this section, we make the dependence of  $\hat{K}_\lambda$  and  $\hat{G}_{k,\lambda}$  on  $\lambda$  explicit. We choose the tuning parameter  $\lambda$  that minimizes the following BIC-type IC

$$IC(\lambda) = \ln \left( \hat{\sigma}_{\hat{G}_{\hat{K},\lambda}}^2 \right) + \rho_{NT} p M \hat{K}_\lambda, \quad (3.1)$$

where  $\hat{\sigma}_{\hat{G}_{\hat{K},\lambda}}^2 = (NT)^{-1} \sum_{k=1}^{\hat{K}_\lambda} \sum_{i \in \hat{G}_{k,\lambda}} \sum_{t=1}^T \left( \tilde{y}_{it} - \boldsymbol{\alpha}_{\hat{G}_{k,\lambda}}^{p'}(t/T) \tilde{\boldsymbol{x}}_{it} \right)^2$  and  $\rho_{NT}$  represents a tuning parameter (see Qian and Su, 2016a; Su et al., 2019; Mehrabani, 2023, for similar approaches). Define the set  $\Lambda = [0, \lambda_{\max}]$  for some sufficiently large  $\lambda_{\max} < \infty$  and partition  $\Lambda$  into  $\Lambda_{0,NT}$ ,  $\Lambda_{-,NT}$ , and  $\Lambda_{+,NT}$ , such that  $\Lambda_{0,NT} = \{\lambda \in \Lambda : \hat{K}_\lambda = K_0\}$ ,  $\Lambda_{-,NT} = \{\lambda \in \Lambda : \hat{K}_\lambda < K_0\}$ , and  $\Lambda_{+,NT} = \{\lambda \in \Lambda : \hat{K}_\lambda > K_0\}$ .<sup>4</sup> In addition, assume that all  $\lambda \in \Lambda_0$  comply with the regularity conditions stated in Assumptions 2-3. Denote the set of all  $K$ -partitions of  $\{1, \dots, N\}$  as  $\mathbb{G}$ .

**Assumption 5.**  $\text{plim}_{(N,T) \rightarrow \infty} \min_{1 \leq K < K_0} \inf_{\mathcal{G}_K \in \mathbb{G}} \hat{\sigma}_{\mathcal{G}_K}^2 = \underline{\sigma}^2 > \sigma_0^2$ .

Assumption 5 is standard in the literature and implies that the mean squared error (*MSE*) of an underfitted model is asymptotically larger than  $\sigma_0^2$ , the *MSE* of the true model.

**Assumption 6.**

(i)  $\lim_{(N,T) \rightarrow \infty} \rho_{NT} M K_0 = 0$ .

(ii)  $\lim_{(N,T) \rightarrow \infty} T \rho_{NT} = \infty$ .

Assumption 6 collects conditions such that the penalty term in (3.1) either dominates the *MSE* or vanishes in the limit, depending on if  $\hat{K} > K_0$  or  $\hat{K} \leq K_0$ , respectively.

**Theorem 3.6.** *Given that Assumptions 1-6 are satisfied,  $\Pr \left( \inf_{\lambda \in \Lambda_{-,NT} \cup \Lambda_{+,NT}} IC(\lambda) > \sup_{\lambda \in \Lambda_{0,NT}} IC(\lambda) \right) \rightarrow 1$  as  $(N, T) \rightarrow \infty$ .*

From Theorem 3.6 follows that neither an underfitted nor an overfitted model maximizes the IC as  $N$  and  $T$  diverge to infinity. Consequently, the IC in (3.1) uncovers the true model asymptotically. When applying the IC, a practitioner must select  $\rho_{NT}$ . After some preliminary experiments and in line with previous literature, we recommend specifying  $\rho_{NT} = c_\lambda \log(NT)(NT)^{-1/2}$  with  $c_\lambda = 0.04$ .

<sup>4</sup>We index the three subsets of  $\Lambda$  with  $NT$  to make it apparent that  $\hat{K}$  is obtained from a random sample of dimension  $(N, T)$ .

## 4 Monte Carlo Simulation Study

In this section, we study the finite sample properties of the *time-varying PAGFL* using several Monte Carlo simulation studies. In Section 4.1, we describe the DGPs. In Section 4.2, we discuss implementation details and evaluation metrics. In Section 4.3, we present the results.

### 4.1 The Data Generation Processes

We consider three DGPs for all  $(N, T)$  combinations of  $N = \{50, 100\}$  and  $T = \{50, 100\}$ . The cross-sectional individuals are sampled from three groups with the proportions 0.3, 0.3, and 0.4. Throughout the simulation study, we draw the individual fixed effects  $\gamma_i^0$  and the idiosyncratic innovations  $\epsilon_{it}$  from mutually independent standard normal distributions. Following Su et al. (2019, sec. 6), the DGPs are constructed as follows:

**DGP 1:** Trending panel data model

$$y_{it} = \gamma_i^0 + \beta_{i,0}^0(t/T) + \epsilon_{it}.$$

The coefficient functions are given by

$$\beta_{i,0}^0(v) = \begin{cases} \alpha_{1,0}^0(v) = 6F(v; 0.5, 0.1) & \text{if } i \in G_1^0 \\ \alpha_{2,0}^0(v) = 6 [2v - 6v^2 + 4v^3 + F(v; 0.7, 0.05)] & \text{if } i \in G_2^0 \\ \alpha_{3,0}^0(v) = 6 [4v - 8v^2 + 4v^3 + F(v; 0.6, 0.05)] & \text{if } i \in G_3^0, \end{cases}$$

where  $F(v; a, b) = [1 + \exp(-(v - a)/b)]^{-1}$  denotes a cumulative logistic function.

**DGP 2:** Trending panel with an exogenous regressor

$$y_{it} = \gamma_i^0 + \beta_{i,1}^0(t/T) + \beta_{i,2}^0(t/T)x_{it} + \epsilon_{it},$$

that augments DGP 1 with a scalar exogenous explanatory variable  $x_{it}$  which is generated from a standard normal distribution. Let  $\beta_{i,1}^0(t/T) = 1/2\beta_{i,0}^0(t/T)$  (and hence  $\alpha_{i,1}^0(t/T) = 1/2\alpha_{i,0}^0(t/T)$ ), where  $\beta_{i,0}^0$  and  $\alpha_{i,0}^0$  are as defined in DGP 1 and

$$\beta_{i,2}^0(v) = \begin{cases} \alpha_{1,2}^0(v) = 3 [2v - 4v^2 + 2v^3 + F(v; 0.6, 0.1)] & \text{if } i \in G_1^0 \\ \alpha_{2,2}^0(v) = 3 [v - 3v^2 + 2v^3 + F(v; 0.7, 0.04)] & \text{if } i \in G_2^0 \\ \alpha_{3,2}^0(v) = 3 [0.5v - 0.5v^2 + F(v; 0.4, 0.07)] & \text{if } i \in G_3^0. \end{cases}$$

**DGP 3:** Dynamic panel data model

$$y_{it} = \gamma_i^0 + \beta_{i,3}^0(t/T)y_{it-1} + \epsilon_{it},$$

featuring a time-varying autoregressive functional relationship. In order to comply with the strong mixing condition in Assumption A.1(ii),  $\sup_{v \in [0,1]} |\alpha_{k,3}^0(v)| < 1$  for all  $k = 1, \dots, K_0$ . The autoregressive coefficient is simulated as

$$\beta_{i,3}^0(v) = \begin{cases} \alpha_{1,3}^0(v) = 1.5 [-0.5 + 2v - 5v^2 + 2v^3 + F(v; 0.6, 0.03)] & \text{if } i \in G_1^0 \\ \alpha_{2,3}^0(v) = 1.5 [-0.5 + v - 3v^2 + 2v^3 + F(v; 0.2, 0.04)] & \text{if } i \in G_2^0 \\ \alpha_{3,3}^0(v) = 1.5 [-0.5 + 0.5v - 0.5v^2 + F(v; 0.8, 0.07)] & \text{if } i \in G_3^0. \end{cases}$$

Figure 1 presents the sample paths of the simulated coefficient functions.

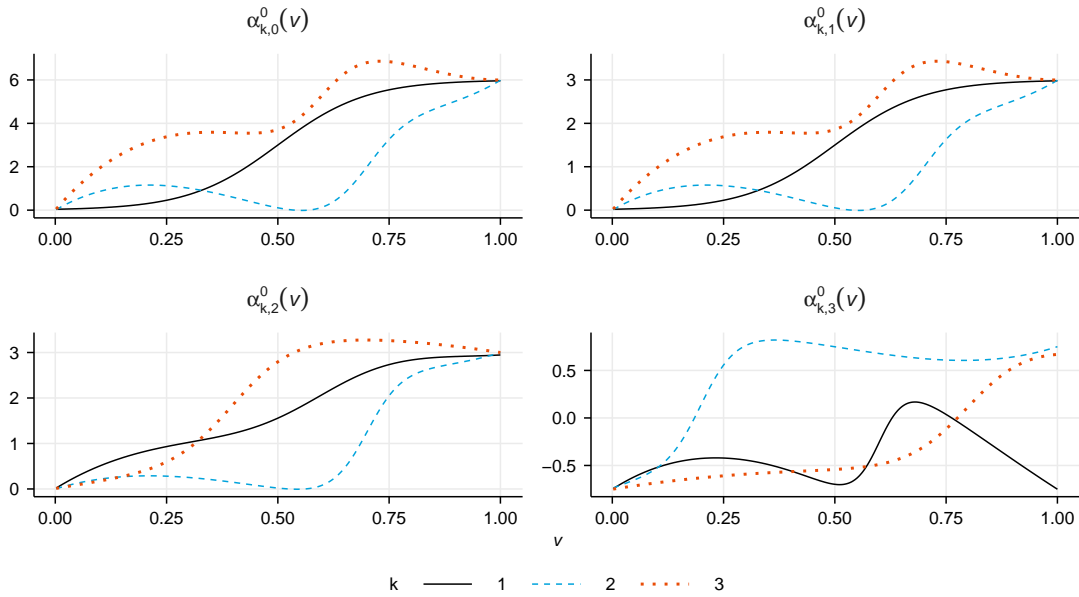


Figure 1: Simulated group-specific coefficient functions.

## 4.2 Implementation and Evaluation

We obtain the *time-varying PAGFL* estimator as described in Section 2.2. We select the number of interior knots  $M^*$  of the spline system  $\mathbf{b}(t/T)$  by taking  $M^* = \max \{ \lfloor (NT)^{1/7} - \log(p) \rfloor, 1 \}$ , where  $\lfloor \cdot \rfloor$  rounds to the lower integer. When  $T$  is small, large  $M^*$  tend to overfit the individual time-varying coefficients and pollute the group classification. Conversely, a small  $M^*$  caps the flexibility of the time-varying coefficients and may complicate the group differentiation in large panels with many latent groups. Furthermore, we set  $d = 3$  since cubic splines offer a good trade-off between flexibility and parsimony. This gives a  $M^* + d + 1 = M$ -dimensional vector of spline basis functions.

We compute the *PAGFL* estimator for a grid of  $\lambda$  values; the grids are specified in Table 3 of Appendix E for the three DGPs. To select the tuning parameter, we then use the IC in equation (3.1). We hereby set  $\rho_{NT} = c_\lambda \log(NT)(NT)^{-1/2}$  with  $c_\lambda = 0.04$  as described in Section 3.4. In large samples, the results do not vary substantially in  $c_\lambda$ .

To evaluate the performance of the estimators, we inspect classification and estimation accuracy. We evaluate the classification performance across  $n_{\text{sim}}$  Monte Carlo experiments according to the following criteria:

- (i) Frequency of  $\hat{K} = K_0$ ,  $n_{\text{sim}}^{-1} \sum_{j=1}^{n_{\text{sim}}} \mathbf{1}\{\hat{K}_j = K_0\}$ .
- (ii) Frequency of  $\hat{\mathcal{G}}_{\hat{K}} = \mathcal{G}^0$ ,  $n_{\text{sim}}^{-1} \sum_{j=1}^{n_{\text{sim}}} \mathbf{1}\{\hat{\mathcal{G}}_{\hat{K},j} = \mathcal{G}_j^0\}$ .
- (iii) Adjusted Rand Index (*ARI*). The *ARI* ranges from minus one to one and measures the similarity between two groupings; one signals total agreement, minus one total disagreement, and zero reflects random assignment. We report the average *ARI* over all Monte Carlo iterations  $ARI = n_{\text{sim}}^{-1} \sum_{j=1}^{n_{\text{sim}}} ARI_j(\hat{\mathcal{G}}_{\hat{K},j}, \mathcal{G}_j^0)$ .
- (iv) Average  $\hat{K}$ ,  $\bar{K} = n_{\text{sim}}^{-1} \sum_{j=1}^{n_{\text{sim}}} \hat{K}_j$ .

The root mean square error (*RMSE*) quantifies the estimation accuracy of the time-varying coefficient functions and is computed as

$$RMSE(\hat{\alpha}_l(t/T)) = N^{-1} \sum_{i=1}^N \sqrt{T^{-1} \sum_{t=1}^T \left[ \hat{\alpha}_{i,l}(t/T) - \alpha_{i,l}^0(t/T) \right]^2},$$

where  $\hat{\alpha}_{i,l}(t/T) = \hat{\alpha}_{k,l}(t/T)$  if  $i \in \hat{G}_k$  and  $\alpha_{i,l}^0(t/T) = \alpha_{j,l}^0(t/T)$  if  $i \in G_j^0$ .

When reporting results on estimation accuracy, note that we explicitly distinguish between the proposed *PSE* and the *post-Lasso* estimator as defined in Section 2.2; whereas throughout the rest of the paper we refer to the latter as the *time-varying PAGFL*. We compare their performance to two benchmarks. The first is the infeasible oracle estimator that is based on the true latent grouping  $\mathcal{G}_0$ , averaged across all  $n_{\text{sim}}$  experiments. The second, is the *time-varying C-Lasso* by Su et al. (2019). Appendix E.3 lists details on the implementation of the *time-varying C-Lasso*.

### 4.3 Simulation Study Results

We simulate all DGPs  $n_{\text{sim}} = 300$  times and apply the *time-varying PAGFL* as well as the *time-varying C-Lasso* procedures. Table 1 reports the classification metrics. The classification accuracy improves quickly with increasing  $T$ , but not in  $N$ . This is intuitive since the classification routine is driven by the estimated individual control points  $\hat{\boldsymbol{\pi}}_i$ , which are not consistent with respect to the cross-sectional dimension (see Theorem 3.1). Accordingly, when  $T$  is small, the estimation of individual coefficient functions is highly noisy, complicating correct group assignment. This property is particularly evident when comparing DGP 1 and DGP 2. The latter involves estimating a second regression curve, which introduces additional uncertainty and subsequently does not lead to the near-perfect classification observed in DGP 1. Nevertheless, DGP 2 still exhibits excellent classification performance. In contrast, the dynamic panel data model applied to DGP 3 performs markedly worse than the other settings, especially when  $T = 50$ . Similar estimation devices have previously reported decreased performance for dynamic panel data models (see Mehrabani, 2023).

Table 1: Classification accuracy

	N	T	Freq. $\hat{K} = K_0$		Freq. $\hat{\mathcal{G}}_{\hat{K}} = \mathcal{G}_{K_0}^0$		ARI		$\bar{K}$	
			<i>PAGFL</i>	<i>C-Lasso</i>	<i>PAGFL</i>	<i>C-Lasso</i>	<i>PAGFL</i>	<i>C-Lasso</i>	<i>PAGFL</i>	<i>C-Lasso</i>
DGP 1	50	50	1.000	0.947	0.960	0.867	0.997	0.974	3.000	2.980
	50	100	1.000	1.000	1.000	1.000	1.000	1.000	3.000	3.000
	100	50	1.000	0.900	0.943	0.667	0.998	0.940	3.000	2.900
	100	100	1.000	1.000	1.000	1.000	1.000	1.000	3.000	3.000
DGP 2	50	50	0.937	0.430	0.623	0.140	0.949	0.691	2.957	2.430
	50	100	1.000	0.357	0.983	0.320	0.999	0.725	3.000	2.357
	100	50	0.943	0.523	0.487	0.023	0.951	0.618	2.957	2.523
	100	100	1.000	0.973	0.977	0.540	0.999	0.960	3.000	2.973
DGP 3	50	50	0.713	0.000	0.120	0.000	0.838	0.503	3.280	2.000
	50	100	0.937	0.000	0.677	0.000	0.974	0.541	3.063	2.000
	100	50	0.750	0.000	0.047	0.000	0.829	0.485	2.810	2.000
	100	100	0.993	0.000	0.633	0.000	0.983	0.542	2.993	2.000

*Notes:* Frequency of obtaining the correct number of groups  $\hat{K} = K_0$  and the correct grouping  $\hat{\mathcal{G}}_{\hat{K}} = \mathcal{G}_{K_0}^0$ , the ARI, and the average estimated number of total groups  $\bar{K}$  based on a Monte Carlo study with 300 replications. *PAGFL* denotes our proposed *time-varying PAGFL* methodology. *C-Lasso* refers to the benchmark model by [Su et al. \(2019\)](#).

Nevertheless, as indicated by the *ARI* measure, even when individual cross-sectional units are misclassified, the estimated grouping remains a close approximation of the true unobserved group structure. Furthermore, our *time-varying PAGFL* convincingly outperforms the *C-Lasso* benchmark, particularly in smaller samples and in the dynamic panel data model DGP 3.

Table 2 reports the *RMSE* for each time-varying coefficient. Figure 2 provides the estimated sample paths of the functional coefficients for each DGP and  $N, T = 50$ . The *RMSE* results largely align with the classification performance. This also holds for the comparison with the *time-varying C-Lasso*, which returns considerably poorer results regarding the *RMSE* as well. Unlike classification accuracy, the *post-Lasso RMSE* also improves with  $N$  due to the larger number of cross-sectional units available for pooling when estimating group-specific trajectories. Notably, the *post-Lasso* performs well relative to the oracle estimator, even in cases where the classification results may suggest a poor fit. This finding is likely because misclassified units tend to feature sample paths that are particularly similar to other groups, leading to a minor impact on the *RMSE* compared to the oracle estimation. Precise identification of group-specific coefficients despite several misclassifications has been previously reported by [Bonhomme and Manresa \(2015\)](#). Table 2 further highlights that the shrinkage penalty leads to a sizeable finite samples bias in the *PSE*, even though the *PSE* and the *post-Lasso* share the same asymptotic distribution (see Theorem 3.5). This motivates our exclusive reliance on the *post-Lasso* for empirical applications.

A glance at Figure 2 corroborates the previous findings: while minor deviations occur—partly due to misclassified units—the estimated trajectories closely follow the true underlying function.

Additionally, we also simulate the three DGPs with idiosyncratic errors that follow an *AR(1)* process with a  $a(L) = 1 - 0.3L$  lag polynomial and, to mimic an empirical application, generate sample paths that randomly discard 30% of the observations. In the latter scenario, the simulation results largely mirror the ones presented here. Discarding part of the sample has a similar effect to decreasing  $T$  in a balanced panel.

Table 2: *RMSE* of coefficient estimates

		N	T	<i>PSE</i>		<i>post-Lasso</i>		oracle
				<i>PAGFL</i>	<i>C-Lasso</i>	<i>PAGFL</i>	<i>C-Lasso</i>	
DGP 1	$\hat{\alpha}_{k,0}(t/T)$	50	50	0.274	0.915	0.160	0.311	0.159
		50	100	0.197	1.037	0.146	0.277	0.146
		100	50	0.274	1.034	0.146	0.299	0.146
		100	100	0.190	1.095	0.139	0.271	0.139
DGP 2	$\hat{\alpha}_{k,1}(t/T)$	50	50	0.263	0.432	0.154	0.231	0.130
		50	100	0.189	0.453	0.140	0.209	0.117
		100	50	0.275	0.433	0.146	0.226	0.117
		100	100	0.189	0.529	0.134	0.153	0.079
DGP 2	$\hat{\alpha}_{k,2}(t/T)$	50	50	0.306	0.655	0.153	0.231	0.135
		50	100	0.207	0.698	0.127	0.186	0.116
		100	50	0.321	0.662	0.139	0.220	0.119
		100	100	0.206	0.836	0.121	0.075	0.085
DGP 3	$\hat{\alpha}_{k,3}(t/T)$	50	50	0.217	0.422	0.145	0.418	0.074
		50	100	0.168	0.457	0.119	0.423	0.059
		100	50	0.243	0.413	0.147	0.416	0.060
		100	100	0.153	0.422	0.052	0.412	0.050

Notes: *RMSE* of the *PSE*, the *post-Lasso*, and an infeasible oracle estimator based on a Monte Carlo study with 300 replication. *PAGFL* denotes our proposed *time-varying PAGFL* methodology. *C-Lasso* refers to the benchmark model by Su et al. (2019).

However, when the innovations follow an *AR*(1) process, the performance decreases markedly, particularly when  $T$  is small. Introducing autocorrelation to the errors increases the estimation uncertainty and thus contaminates the classification mechanism. However, even when the grouping is correctly estimated, the coefficient trajectories offer a significantly poorer fit than the base case. Detailed results are relegated to Appendix E.

## 5 Empirical Illustration

Many major economies pledge to reduce the emission of harmful greenhouse gases, a key driver of global warming. Achieving this objective without impeding economic growth requires emissions per unit of GDP to decrease. CO<sub>2</sub> accounts for approximately 66% of the anthropogenic contribution to global warming and is a ubiquitous by-product of economic activity and energy production (Bennedsen et al., 2023). Consequently, understanding the relationship between CO<sub>2</sub> pollution and economic growth is crucial for effective policy and climate action. We contribute by applying our *time-varying PAGFL* procedure to identify trends in the CO<sub>2</sub> emission intensity of GDP, the CO<sub>2</sub> emitted per unit of GDP produced.

The CO<sub>2</sub> intensity of GDP is determined by the structural composition of an economy and the “greenness” of its energy production (Bella et al., 2014). For instance, transitioning from a production-based to a services-orientated economy reduces energy consumption and direct emissions from high-pollution industries. Likewise, shifting from emission-intensive solid fuels, such as coal or biomass, to cleaner carriers, like natural gas or renewables, lowers the elasticity between energy demand and associated pollution. The combined effects of economic restructuring and energy source optimization are often credited with driving the



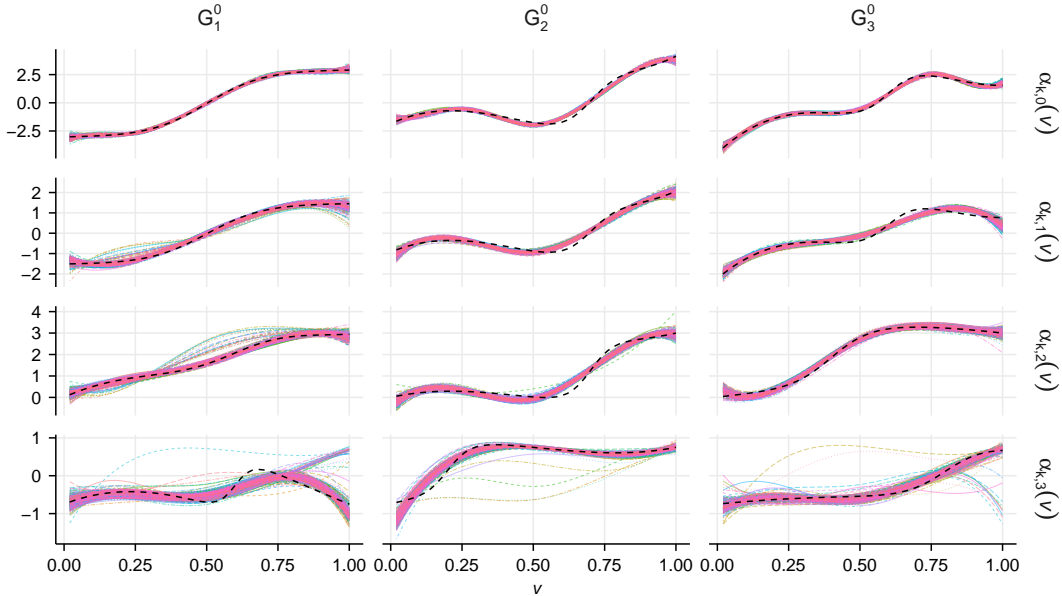


Figure 2: Estimated *time-varying PAGFL post-Lasso* functional coefficients when  $N, T = 50$  and  $n_{\text{sim}} = 300$ . The true coefficient functions are shown in black (dashed).

decoupling of GDP growth from production-based emissions in high-income countries (Jakob et al., 2012; Wang et al., 2017; Hannesson, 2020). This decoupling pattern has inspired an extensive literature on the inverted U-shaped environmental Kuznets curve (ECK), which posits a positive elasticity between income and emissions during the early stages of economic development, turning negative as technological progress and greater prosperity take hold (see Grossman and Krueger, 1995; Azomahou et al., 2006; Wagner, 2015; Magazzino et al., 2023; Bennedsen et al., 2023, among other). However, as (log) GDP, an integrated process, clearly does not satisfy the regularity conditions in Assumption 1, we instead study the relationship between emissions and income by estimating trends in CO<sub>2</sub> intensity. Trend functions capture the long-term behavior of CO<sub>2</sub> intensity by smoothing over short-run fluctuations such as business cycles, fuel price volatility or temporary energy supply disruptions. Moreover, it is well-established that economies exhibit significant heterogeneity in their developmental trajectories over time (Kose et al., 2003; Azomahou et al., 2006). Consequently, the assumption of a common CO<sub>2</sub> intensity trend across a large panel is implausible. Nevertheless, much of the existing empirical literature imposes cross-sectional homogeneity or homogeneity conditional on an exogenous grouping (Churchill et al., 2018; Kang and Kang, 2022; Bennedsen et al., 2023). We relax this condition. Using our *time-varying PAGFL* procedure, different economies only share a common trend if the consistent grouping mechanism identifies homogenous coefficients, enabling us to exploit the cross-sectional dimension without imposing restrictive homogeneity assumptions. In addition, given the small number of group-specific trend functions relative to the cross-sectional dimension, it becomes feasible to interpret the long-term behavior of CO<sub>2</sub> intensity for a large number of economies.

To estimate trends in the CO<sub>2</sub> intensity of GDP, we employ production-based CO<sub>2</sub> emissions data from the Global Carbon Project (Friedlingstein et al., 2024).<sup>5</sup> GDP series are obtained from the World Bank

<sup>5</sup>Dataset *National fossil carbon emissions v2024*, available at [globalcarbonbudgetdata.org](https://globalcarbonbudgetdata.org). Accessed November 14, 2024.

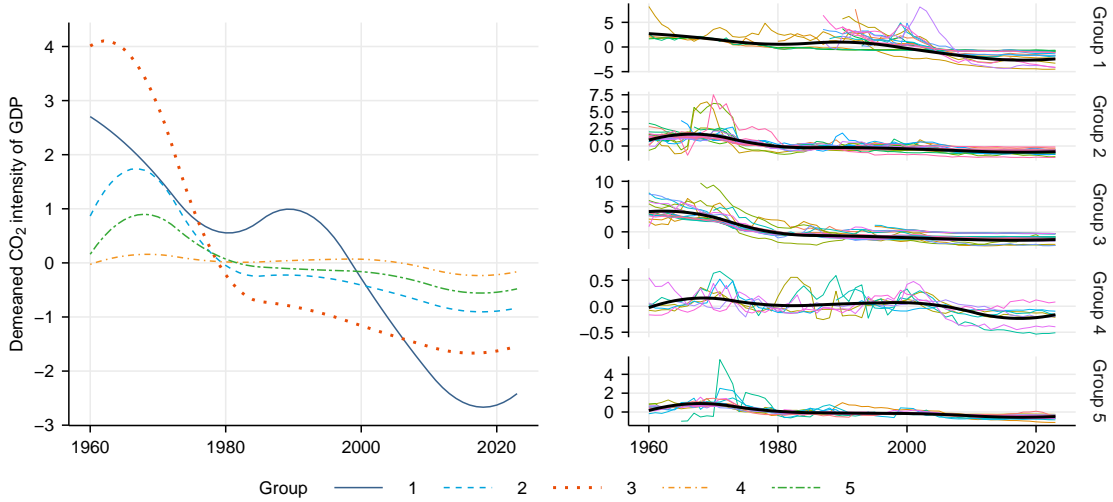


Figure 3: The left panel displays the group-specific *post-Lasso* trend functions. The right panel contrasts the estimated trend functions (black, thick) with the demeaned data of CO<sub>2</sub> intensity (colored, thin).

Development Indicators database.<sup>6</sup> Both datasets are in annual frequency and span the time period from 1960 to 2023 for 92 countries. Details on the countries included in the sample and descriptive statistics are provided in Appendix F. Using this data, we compute the CO<sub>2</sub> intensity and construct an unbalanced panel where the individual series range from 29 to 64 years in length.

Let  $y_{it} = \text{CO}_{2it}/\text{GDP}_{it}$ , with CO<sub>2</sub> measured in million tonnes and GDP in billion 2024 U.S. dollar. We formulate the time-varying panel data model subject to a latent grouping

$$y_{it} = \gamma_i + \beta_i \left( \frac{t}{T} \right) + \epsilon_{it},$$

where  $\beta_i(t/T)$  represents the trend function of interest (time-varying intercept).

Searching over a dense grid of  $d$ ,  $M^*$ , and  $\lambda$  values,  $d = 2$ ,  $M^* = 4$ , and  $\lambda = 0.72$  yield the lowest IC, implying five latent groups. Figure 3 presents the estimated group-specific trend functions  $\hat{\alpha}_{G_k}^p(t/T)$  and fit of the model. Figure 4 sketches the spatial pattern in the group structure. Table 9 in Appendix F provides a detailed record of which countries are assigned to which group.

Group 1 predominantly comprises middle-to-high-income economies in Eastern Europe and Asia, which have exhibited a substantial and ongoing decline in CO<sub>2</sub> emission intensity since the 1990s. Structural changes and rapid technological advances following the fall of the USSR and the economic liberalization of China may drive this trend. Notably, only Group 1 experiences a significant and persistent increase in emissions throughout the entire observational horizon. However, the steep income growth outpaces the increasing emissions, producing a declining emission intensity. Group 2 largely includes low-to-middle-income economies, with outliers such as Switzerland, Hong Kong, and Singapore. The trend of Group 2 features a much more gradual decrease compared to the first group due to more moderate growth in both income and emissions. Group 3 primarily consists of high-income countries that experienced a sharp decline in emission

<sup>6</sup>Series *NY.GDP.MKTP.CD*, available at [data.worldbank.org/indicator/NY.GDP.MKTP.CD](https://data.worldbank.org/indicator/NY.GDP.MKTP.CD). Accessed November 12, 2024.

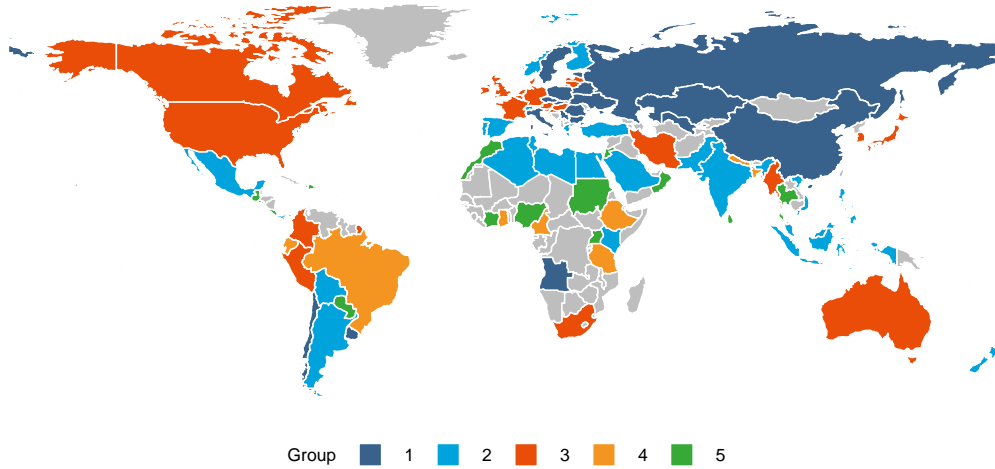


Figure 4: Estimated group structure in the trends of CO<sub>2</sub> intensity.

intensity pre-1980, followed by a continued but more dampened decline thereafter. This pattern reflects a stark reduction in emissions until the 1980s, accompanied by consistent GDP growth throughout the entire sample period, aligning with a transition to service-based economies and the off-shoring of emission- and energy-intensive sectors to low-income countries. Group 4 contains low-income and developing economies, characterized by a laterally moving trend. In these economies, technological progress has yet to reduce emission intensity significantly or, as in the case of Brazil, income growth is largely driven by the exploitation of natural resources. Group 5, which is made up of low-income economies, exhibits a similar but slightly more attenuated trend compared to Group 2.

## 6 Conclusion

This article introduces a novel technique, the *time-varying PAGFL*, to estimate panel data models with smoothly time-varying coefficient functions that are subject to an unobserved group structure. Our approach simultaneously identifies the functional coefficients, the number of latent groups, and group compositions. In addition, we propose a BIC-type IC that determines the penalty tuning parameter, introduce a *post-Lasso* estimator, and proof oracle-efficiency. Monte Carlo simulation studies confirm strong finite sample performance across a wide range of scenarios. We apply our method to analyze trends in the CO<sub>2</sub> emission intensity of GDP.

An extension still largely unexplored in the literature regards inference methods for (time-varying) panel data models with a latent group pattern. The estimated grouping is an inherently noisy representation of the true unobserved structure. Subsequently, the classification introduces uncertainty to the slope coefficients, analogous to the well-established problem of non-uniform convergence of post-selection estimation (see

[Greenshtein and Ritov, 2004](#); [Leeb and Pötscher, 2008](#); [Adamek et al., 2023](#)). To the best of our knowledge, [Dzemski and Okui \(2024\)](#) provide the only approach to creating confidence sets of the grouping by inverting poolability tests to date. Subsequently, the development of inference methods for penalized panel data models that admit a latent grouping, including confidence intervals for the group structure and coefficients, as well as tests for coefficient poolability and constancy akin to [Friedrich and Lin \(2024\)](#), remains an important direction for future research.

## References

- Adamek, R., Smeekes, S., and Wilms, I. (2023). Lasso inference for high-dimensional time series. *Journal of Econometrics*, 235(2):1114–1143.
- Ando, T. and Bai, J. (2016). Panel data models with grouped factor structure under unknown group membership. *Journal of Applied Econometrics*, 31(1):163–191.
- Andrews, D. W. (1984). Non-strong mixing autoregressive processes. *Journal of Applied Probability*, 21(4):930–934.
- Azomahou, T., Laisney, F., and Van, P. N. (2006). Economic development and co2 emissions: A nonparametric panel approach. *Journal of Public Economics*, 90(6-7):1347–1363.
- Bai, J. (2010). Common breaks in means and variances for panel data. *Journal of Econometrics*, 157(1):78–92.
- Bai, J. and Ng, S. (2002). Determining the number of factors in approximate factor models. *Econometrica*, 70(1):191–221.
- Baltagi, B. H., Feng, Q., and Kao, C. (2016). Estimation of heterogeneous panels with structural breaks. *Journal of Econometrics*, 191(1):176–195.
- Bella, G., Massidda, C., and Mattana, P. (2014). The relationship among co2 emissions, electricity power consumption and gdp in oecd countries. *Journal of Policy Modeling*, 36(6):970–985.
- Bennedsen, M., Hillebrand, E., and Jensen, S. (2023). A neural network approach to the environmental kuznets curve. *Energy Economics*, 126:106985.
- Bernstein, D. S. (2009). *Matrix Mathematic, Theory, Facts, and Formulas with Application to Linear Systems Theory*. Princeton University Press.
- Bonhomme, S. and Manresa, E. (2015). Grouped patterns of heterogeneity in panel data. *Econometrica*, 83(3):1147–1184.
- Cai, Z. (2007). Trending time-varying coefficient time series models with serially correlated errors. *Journal of Econometrics*, 136(1):163–188.
- Cashin, P., Mohaddes, K., Raissi, M., and Raissi, M. (2014). The differential effects of oil demand and supply shocks on the global economy. *Energy Economics*, 44:113–134.
- Chang, Y., Kaufmann, R. K., Kim, C. S., Miller, J. I., Park, J. Y., and Park, S. (2020). Evaluating trends in time series of distributions: A spatial fingerprint of human effects on climate. *Journal of Econometrics*, 214(1):274–294.
- Chen, J. (2019). Estimating latent group structure in time-varying coefficient panel data models. *The Econometrics Journal*, 22(3):223–240.
- Chernozhukov, V., Hansen, C. B., Liao, Y., and Zhu, Y. (2019). Inference for heterogeneous effects using low-rank estimations. Technical report, CEMMAP working paper.
- Chetverikov, D. and Manresa, E. (2022). Spectral and post-spectral estimators for grouped panel data models. *arXiv preprint arXiv:2212.13324*.
- Chow, G. C. (1960). Tests of equality between sets of coefficients in two linear regressions. *Econometrica*, pages 591–605.
- Churchill, S. A., Inekwe, J., Ivanovski, K., and Smyth, R. (2018). The environmental kuznets curve in the oecd: 1870–2014. *Energy Economics*, 75:389–399.
- Cogley, T. and Sargent, T. J. (2005). Drifts and volatilities: monetary policies and outcomes in the post wwii us. *Review of Economic Dynamics*, 8(2):262–302.
- De Boor, C. (2001). *A practical guide to splines*. springer-verlag New York.
- Diebold, F. X., Li, C., and Yue, V. Z. (2008). Global yield curve dynamics and interactions: a dynamic nelson–siegel approach. *Journal of Econometrics*, 146(2):351–363.
- Dung, V. T. and Tjahjowidodo, T. (2017). A direct method to solve optimal knots of b-spline curves: An application for non-uniform b-spline curves fitting. *PloS one*, 12(3):e0173857.
- Dzemeski, A. and Okui, R. (2024). Confidence set for group membership. *Quantitative Economics*, 15(2):245–277.

- Freyaldenhoven, S. (2022). Factor models with local factors—determining the number of relevant factors. *Journal of Econometrics*, 229(1):80–102.
- Friedlingstein, P., O’Sullivan, M., Jones, M. W., Andrew, R. M., Hauck, J., Landschützer, P., Le Quéré, C., Li, H., Luijkx, I. T., Olsen, A., Peters, G. P., Peters, W., Pongratz, J., Schwingshackl, C., Sitch, S., Canadell, J. G., Ciais, P., Jackson, R. B., Alin, S. R., Arneth, A., Arora, V., Bates, N. R., Becker, M., Bellouin, N., Berghoff, C. F., Bittig, H. C., Bopp, L., Cadule, P., Campbell, K., Chamberlain, M. A., Chandra, N., Chevallier, F., Chini, L. P., Colligan, T., Decayeux, J., Djoutchouang, L., Dou, X., Duran Rojas, C., Enyo, K., Evans, W., Fay, A., Feely, R. A., Ford, D. J., Foster, A., Gasser, T., Gehlen, M., Gkritzalis, T., Grassi, G., Gregor, L., Gruber, N., Gürses, O., Harris, I., Hefner, M., Heinke, J., Hurtt, G. C., Iida, Y., Ilyina, T., Jacobson, A. R., Jain, A., Jarníková, T., Jersild, A., Jiang, F., Jin, Z., Kato, E., Keeling, R. F., Klein Goldewijk, K., Knauer, J., Korsbakken, J. L., Lauvset, S. K., Lefèvre, N., Liu, Z., Liu, J., Ma, L., Maksyutov, S., Marland, G., Mayot, N., McGuire, P., Metzl, N., Monacci, N. M., Morgan, E. J., Nakaoka, S.-I., Neill, C., Niwa, Y., Nützel, T., Olivier, L., Ono, T., Palmer, P. I., Pierrot, D., Qin, Z., Resplandy, L., Roobaert, A., Rosan, T. M., Rödenbeck, C., Schwinger, J., Smallman, T. L., Smith, S., Sospedra-Alfonso, R., Steinhoff, T., Sun, Q., Sutton, A. J., Séférian, R., Takao, S., Tatebe, H., Tian, H., Tilbrook, B., Torres, O., Tourigny, E., Tsujino, H., Tubiello, F., van der Werf, G., Wanninkhof, R., Wang, X., Yang, D., Yang, X., Yu, Z., Yuan, W., Yue, X., Zaehle, S., Zeng, N., and Zeng, J. (2024). Supplemental data of global carbon budget 2024. *Earth System Science Data Discussions*, 2024:1–133.
- Friedrich, M., Beutner, E., Reuvers, H., Smeekes, S., Urbain, J.-P., Bader, W., Franco, B., Lejeune, B., and Mahieu, E. (2020). A statistical analysis of time trends in atmospheric ethane. *Climatic Change*, 162:105–125.
- Friedrich, M. and Lin, Y. (2024). Sieve bootstrap inference for linear time-varying coefficient models. *Journal of Econometrics*, 239(1):105345. *Climate Econometrics*.
- Galvao, A. F. and Kato, K. (2014). Estimation and inference for linear panel data models under misspecification when both  $n$  and  $t$  are large. *Journal of Business & Economic Statistics*, 32(2):285–309.
- Greenshtein, E. and Ritov, Y. (2004). Persistence in high-dimensional linear predictor selection and the virtue of overparametrization. *Bernoulli*, 10(6):971–988.
- Grossman, G. M. and Krueger, A. B. (1995). Economic growth and the environment. *The Quarterly Journal of Economics*, 110(2):353–377.
- Hahn, J. and Kuersteiner, G. (2002). Asymptotically unbiased inference for a dynamic panel model with fixed effects when both  $n$  and  $t$  are large. *Econometrica*, 70(4):1639–1657.
- Hahn, J. and Kuersteiner, G. (2011). Bias reduction for dynamic nonlinear panel models with fixed effects. *Econometric Theory*, 27(6):1152–1191.
- Haimerl, P., Smeekes, S., Wilms, I., and Mehrabani, A. (2025). *R-Package ‘PAGFL’*. R package version 1.1.3.
- Hannesson, R. (2020). Co2 intensity and gdp per capita. *International Journal of Energy Sector Management*, 14(2):372–388.
- Hansen, M. H. and Kooperberg, C. (2002). Spline adaptation in extended linear models (with comments and a rejoinder by the authors). *Statistical Science*, 17(1):2–51.
- Harvey, A. C. (1985). Trends and cycles in macroeconomic time series. *Journal of Business & Economic Statistics*, 3(3):216–227.
- Hastie, T. and Tibshirani, R. (1993). Varying-coefficient models. *Journal of the Royal Statistical Society Series B: Statistical Methodology*, 55(4):757–779.
- Huang, J. Z., Wu, C. O., and Zhou, L. (2004). Polynomial spline estimation and inference for varying coefficient models with longitudinal data. *Statistica Sinica*, 14(3):763–788.
- Jakob, M., Haller, M., and Marschinski, R. (2012). Will history repeat itself? economic convergence and convergence in energy use patterns. *Energy Economics*, 34(1):95–104.
- Kang, M. and Kang, S. (2022). Energy intensity efficiency and the effect of changes in gdp and co2 emission. *Energy Efficiency*, 15(1):8.
- Ke, Z. T., Fan, J., and Wu, Y. (2015). Homogeneity pursuit. *Journal of the American Statistical Association*, 110(509):175–194.
- Kiviet, J. F. (1995). On bias, inconsistency, and efficiency of various estimators in dynamic panel data models. *Journal of Econometrics*, 68(1):53–78.

- Kose, M. A., Otrok, C., and Whiteman, C. H. (2003). International business cycles: World, region, and country-specific factors. *American Economic Review*, 93(4):1216–1239.
- Lee, K., Pesaran, M. H., and Smith, R. (1997). Growth and convergence in a multi-country empirical stochastic solow model. *Journal of Applied Econometrics*, 12(4):357–392.
- Leeb, H. and Pötscher, B. M. (2008). Sparse estimators and the oracle property, or the return of hedges’ estimator. *Journal of Econometrics*, 142(1):201–211.
- Lin, C.-C. and Ng, S. (2012). Estimation of panel data models with parameter heterogeneity when group membership is unknown. *Journal of Econometric Methods*, 1(1):42–55.
- Liu, R., Shang, Z., Zhang, Y., and Zhou, Q. (2020). Identification and estimation in panel models with overspecified number of groups. *Journal of Econometrics*, 215(2):574–590.
- Lumsdaine, R. L., Okui, R., and Wang, W. (2023). Estimation of panel group structure models with structural breaks in group memberships and coefficients. *Journal of Econometrics*, 233(1):45–65.
- Ma, S. and Huang, J. (2017). A concave pairwise fusion approach to subgroup analysis. *Journal of the American Statistical Association*, 112(517):410–423.
- Magazzino, C., Gallegati, M., and Giri, F. (2023). The environmental kuznets curve in a long-term perspective: Parametric vs semi-parametric models. *Environmental Impact Assessment Review*, 98:106973.
- Mehrabani, A. (2023). Estimation and identification of latent group structures in panel data. *Journal of Econometrics*, 235(2):1464–1482.
- Miao, K., Phillips, P. C., and Su, L. (2023). High-dimensional vars with common factors. *Journal of Econometrics*, 233(1):155–183.
- Mugnier, M. (2022). Unobserved clusters of time-varying heterogeneity in nonlinear panel data models.
- Müller, U. K. (2014). Hac corrections for strongly autocorrelated time series. *Journal of Business & Economic Statistics*, 32(3):311–322.
- Newey, W. K. and West, K. D. (1987). A simple, positive semi-definite, heteroskedasticity and autocorrelation consistent covariance matrix. *Econometrica*, 55(3):703–708.
- Nickell, S. (1981). Biases in dynamic models with fixed effects. *Econometrica*, pages 1417–1426.
- Okui, R. and Wang, W. (2021). Heterogeneous structural breaks in panel data models. *Journal of Econometrics*, 220(2):447–473.
- Perron, P. and Wada, T. (2009). Let’s take a break: Trends and cycles in us real gdp. *Journal of Monetary Economics*, 56(6):749–765.
- Pesaran, M. H. (2006). Estimation and inference in large heterogeneous panels with a multifactor error structure. *Econometrica*, 74(4):967–1012.
- Phillips, P. C. and Sul, D. (2007). Bias in dynamic panel estimation with fixed effects, incidental trends and cross section dependence. *Journal of Econometrics*, 137(1):162–188.
- Qian, J. and Su, L. (2016a). Shrinkage estimation of common breaks in panel data models via adaptive group fused lasso. *Journal of Econometrics*, 191(1):86–109.
- Qian, J. and Su, L. (2016b). Shrinkage estimation of regression models with multiple structural changes. *Econometric Theory*, 32(6):1376–1433.
- Rahmstorf, S., Foster, G., and Cahill, N. (2017). Global temperature evolution: recent trends and some pitfalls. *Environmental Research Letters*, 12(5):054001.
- Robinson, P. M. (2012). Nonparametric trending regression with cross-sectional dependence. *Journal of Econometrics*, 169(1):4–14.
- Sarafidis, V. and Weber, N. (2015). A partially heterogeneous framework for analyzing panel data. *Oxford Bulletin of Economics and Statistics*, 77(2):274–296.
- Scarpiniti, M., Communiello, D., Parisi, R., and Uncini, A. (2013). Nonlinear spline adaptive filtering. *Signal Processing*, 93(4):772–783.
- Su, L. and Jin, S. (2012). Sieve estimation of panel data models with cross section dependence. *Journal of Econometrics*, 169(1):34–47.

- Su, L., Shi, Z., and Phillips, P. C. (2016). Identifying latent structures in panel data. *Econometrica*, 84(6):2215–2264.
- Su, L., Wang, X., and Jin, S. (2019). Sieve estimation of time-varying panel data models with latent structures. *Journal of Business & Economic Statistics*, 37(2):334–349.
- Vogt, M. and Linton, O. (2017). Classification of non-parametric regression functions in longitudinal data models. *Journal of the Royal Statistical Society Series B: Statistical Methodology*, 79(1):5–27.
- Wagner, M. (2015). The environmental kuznets curve, cointegration and nonlinearity. *Journal of Applied Econometrics*, 30(6):948–967.
- Wang, H., Ang, B., and Su, B. (2017). A multi-region structural decomposition analysis of global co2 emission intensity. *Ecological Economics*, 142:163–176.
- Wang, W., Phillips, P. C., and Su, L. (2018). Homogeneity pursuit in panel data models: Theory and application. *Journal of Applied Econometrics*, 33(6):797–815.
- Wang, W., Zhang, X., and Paap, R. (2019). To pool or not to pool: What is a good strategy for parameter estimation and forecasting in panel regressions? *Journal of Applied Econometrics*, 34(5):724–745.
- Wang, Y., Phillips, P. C., and Su, L. (2024). Panel data models with time-varying latent group structures. *Journal of Econometrics*, 240(1):105685.



## A Proof of the Results in Section 3

### A.1 Technical Lemmas

**Lemma A.1.** Lemma A.1 establishes some basic properties of B-splines that are used in several of the following proofs. Let  $b_m(v) > 0$ ,  $m = -d, \dots, M^*$ , denote a basis function of degree  $d > 0$  (order  $d + 1$ ), defined on the sequence of knots  $\mathbb{V}$  as introduced in Appendix B. (i) Then,  $\|\mathbf{b}(v)\|_2 = \left[ \sum_{j=-d}^{M^*} b_m(v)^2 \right]^{1/2} \leq \left[ \sum_{j=-d}^{M^*} b_m(v) \right]^{1/2} = 1$ . (ii)  $\int_0^1 b_m(v) dv = O(M^{-1})$  and  $\int_0^1 \|\mathbf{b}(v)\|_2 dv = \int_0^1 \left[ \sum_{j=-d}^{M^*} b_m(v)^2 \right]^{1/2} dv \leq \int_0^1 \left[ \sum_{j=-d}^{M^*} b_m(v) \right]^{1/2} dv = 1$ . (iii) There exist two constants  $0 < \underline{c}_b \leq \bar{c}_b < \infty$  such that

$$\underline{c}_b \leq \mu_{\min} \left( M \int_0^1 \mathbf{b}(v) \mathbf{b}(v)' dv \right) \leq \mu_{\max} \left( M \int_0^1 \mathbf{b}(v) \mathbf{b}(v)' dv \right) \leq \bar{c}_b.$$

(iv) Given Assumption 1(vi) and  $\beta_i^0(v) \notin \mathbb{B}_{\mathbb{V}, M}$ , there exists a coefficient matrix  $\mathbf{\Pi}_i^0 \in \mathbb{R}^{M \times p}$  such that  $\sup_{v \in [0,1]} \|\beta_i^0(v) - \mathbf{\Pi}_i^0 \mathbf{b}(v)\|_2 = O(M^{-\theta})$ , where  $\theta \geq 1$ .

**Lemma A.2.** Define  $\hat{\mathbf{Q}}_{i, \tilde{z}\tilde{z}} = T^{-1} \sum_{t=1}^T \tilde{\mathbf{z}}_{it} \tilde{\mathbf{z}}'_{it}$  and  $\hat{\mathbf{Q}}_{i, \tilde{z}\tilde{z}} = \sum_{i \in G_k^0} T^{-1} \sum_{t=1}^T \tilde{\mathbf{z}}_{it} \tilde{\mathbf{z}}'_{it}$ . Given Assumptions 1(i)-(ii), 1(iv), and 1(vi), there exist two constants  $0 < \underline{c}_{\tilde{z}\tilde{z}} \leq \bar{c}_{\tilde{z}\tilde{z}} < \infty$  such that (i)

$$\Pr \left( \underline{c}_{\tilde{z}\tilde{z}} \leq \min_i \mu_{\min}(M \hat{\mathbf{Q}}_{i, \tilde{z}\tilde{z}}) \leq \max_i \mu_{\max}(M \hat{\mathbf{Q}}_{i, \tilde{z}\tilde{z}}) \leq \bar{c}_{\tilde{z}\tilde{z}} \right) = 1 - o(N^{-1})$$

and (ii)

$$\Pr \left( \underline{c}_{\tilde{z}\tilde{z}} \leq \min_i \mu_{\min}(N_k^{-1} M \hat{\mathbf{Q}}_{i, \tilde{z}\tilde{z}}) \leq \max_i \mu_{\max}(N_k^{-1} M \hat{\mathbf{Q}}_{i, \tilde{z}\tilde{z}}) \leq \bar{c}_{\tilde{z}\tilde{z}} \right) = 1 - o(N^{-1}).$$

Lemma A.2 is used in Lemmas A.3, A.4, A.6 and Theorems 3.1, 3.3, and 3.5.

**Lemma A.3.** Define  $\hat{\mathbf{q}}_{i, \tilde{z}\tilde{u}} = T^{-1} \sum_{t=1}^T \tilde{\mathbf{z}}_{it} \tilde{u}_{it}$ , with the composite error  $\tilde{u}_{it} = \tilde{\eta}_{it} + \tilde{\epsilon}_{it}$ . Given Assumption 1, (i)  $\|\hat{\mathbf{q}}_{i, \tilde{z}\tilde{u}}\|_2 = O_p(T^{-1/2} M^{-\theta-1/2})$  and (ii)  $N^{-1} \sum_{i=1}^N \|\hat{\mathbf{q}}_{i, \tilde{z}\tilde{u}}\|_2^2 = O_p(T^{-1} + M^{-2\theta-1})$ . Lemma A.3 is used in Lemma A.4, Theorems 3.1(i), and 3.3.

**Lemma A.4.** Recall the preliminary estimate  $\hat{\boldsymbol{\pi}} = \arg \min_{\boldsymbol{\pi}} T^{-1} \sum_{i=1}^N \sum_{t=1}^T (\tilde{y}_{it} - \boldsymbol{\pi}'_i \tilde{\mathbf{z}}_{it})^2$ . Given Assumptions 1 and 2(i),  $\|\hat{\boldsymbol{\pi}}_i - \boldsymbol{\pi}_i^0\|_2 = O_p(MT^{-1/2} + M^{-\theta-1/2})$ . Lemma A.4 is used in Lemma A.5.

**Lemma A.5.** Suppose that Assumptions 1 and 2(i)-(ii) hold. Then (i)  $\min_{i,j \in G_k^0} \dot{\omega}_{ij} = \|\hat{\boldsymbol{\pi}}_i - \hat{\boldsymbol{\pi}}_j\|_2^{-\kappa} = O_p((MT^{-1/2} + M^{-\theta+1/2})^{-\kappa})$  and (ii)  $\max_{i \in G_k^0, j \notin G_k^0} \dot{\omega}_{ij} = O_p(J_{\min}^{-\kappa})$ . Lemma A.5 is employed in Theorems 3.1, 3.3, and 3.5.

**Lemma A.6.** Suppose that Assumption 1 is satisfied. Let  $\mathbf{b}_c = \mathbf{c} \otimes \mathbf{b}(v)$  for some nonrandom  $p \times 1$  vector  $\mathbf{c}$  with  $\|\mathbf{c}\|_2 = 1$ . (i)  $\|\mathbf{b}_c\|_2 = 1$ . (ii)  $s_{c, \hat{G}_k} = O_p(1)$ , with  $s_{c, \hat{G}_k}^2 = M(N_k T)^{-1} \mathbf{b}'_c \left( MN_k^{-1} \hat{\mathbf{Q}}_{G_k^0, \tilde{z}\tilde{z}} \right)^{-1} \sum_{i \in G_k^0} \left( \tilde{\mathbf{Z}}'_i E(\boldsymbol{\epsilon}_i \boldsymbol{\epsilon}'_i \tilde{\mathbf{Z}}_i) \right) \left( MN_k^{-1} \hat{\mathbf{Q}}_{G_k^0, \tilde{z}\tilde{z}} \right)^{-1} \mathbf{b}_c$ , and the individual terms as defined in Theorem 3.5. Lemma A.6 is used in Theorem 3.5(ii).

**Lemma A.7.** Suppose that Assumptions 1-4 hold. Let  $\bar{\mathbb{G}}_K = \{\bar{\mathcal{G}}_K = \{\bar{G}_k\}_{k=1}^K : \#i, j \in \bar{G}_K \text{ where } i \in G_l^0, j \notin G_l^0, 1 \leq l \leq K_0\}$  with  $K_0 < K \leq K_{\max} \leq N$ .<sup>7</sup> Then,  $\max_{K_0 < K \leq K_{\max}} \sup_{\bar{\mathcal{G}}_K \in \bar{\mathbb{G}}_K} |\hat{\sigma}_{\bar{\mathcal{G}}_K}^2 - \hat{\sigma}_{\bar{\mathcal{G}}_0}^2| = O_p(T^{-1}M)$ . The MSE  $\sigma_{\bar{\mathcal{G}}_K}^2$  is defined as in Theorem 3.6. Lemma A.7 is employed in Theorem 3.6.

## A.2 Proof of Theorems and Corollaries

### A.2.1 Theorem 3.1

Suppose that Assumptions 1 and 2(i)-(iii) hold. Theorem 3.1(i) derives the pointwise convergence rate  $\|\hat{\boldsymbol{\pi}}_i - \boldsymbol{\pi}_i^0\|_2 = O_p(MT^{-1/2} + M^{-\theta+1/2})$  and 3.1(ii) the  $L_2$  rate  $N^{-1} \sum_{i=1}^N \|\hat{\boldsymbol{\pi}}_i - \boldsymbol{\pi}_i^0\|_2^2 = O_p(M^2T^{-1} + M^{-2\theta+1})$ .

*Proof:*

**Theorem 3.1(i)** Define  $\mathbf{a}_i = \boldsymbol{\pi}_i - \boldsymbol{\pi}_i^0$ . Recall the criterion function  $\mathcal{F}_{NT,i}^*(\boldsymbol{\pi}_i) = T^{-1} \sum_{t=1}^T [\tilde{y}_{it} - \tilde{\mathbf{z}}'_{it} \boldsymbol{\pi}_i]^2$  and  $\mathcal{F}_{NT,i}(\boldsymbol{\pi}_i, \lambda) = \mathcal{F}_{NT,i}^*(\boldsymbol{\pi}_i) + \lambda N^{-1} \sum_{j=1, j \neq i}^N \dot{\omega}_{ij} \|\boldsymbol{\pi}_i - \boldsymbol{\pi}_j\|_2$  (2.6). Recognize that

$$\begin{aligned}
\mathcal{F}_{NT,i}^*(\boldsymbol{\pi}_i) - \mathcal{F}_{NT,i}^*(\boldsymbol{\pi}_i^0) &= \frac{1}{T} \sum_{t=1}^T [\tilde{y}_{it} - \tilde{\mathbf{z}}'_{it} \boldsymbol{\pi}_i]^2 - \frac{1}{T} \sum_{t=1}^T [\tilde{y}_{it} - \tilde{\mathbf{z}}'_{it} \boldsymbol{\pi}_i^0]^2 \\
&= \frac{1}{T} \sum_{t=1}^T [\tilde{y}_{it} - \tilde{\mathbf{z}}'_{it} (\mathbf{a}_i + \boldsymbol{\pi}_i^0)]^2 - \frac{1}{T} \sum_{t=1}^T \tilde{u}_{it}^2 = \frac{1}{T} \sum_{t=1}^T [\tilde{u}_{it} - \tilde{\mathbf{z}}'_{it} \mathbf{a}_i]^2 - \frac{1}{T} \sum_{t=1}^T \tilde{u}_{it}^2 \\
&= \frac{1}{T} \sum_{t=1}^T \tilde{u}_{it}^2 - \frac{1}{T} \sum_{t=1}^T [2\tilde{u}_{it} \tilde{\mathbf{z}}'_{it} \mathbf{a}_i] + \frac{1}{T} \sum_{t=1}^T [\tilde{\mathbf{z}}'_{it} \mathbf{a}_i]^2 - \frac{1}{T} \sum_{t=1}^T \tilde{u}_{it}^2 \\
&= -2\mathbf{a}'_i \frac{1}{T} \sum_{t=1}^T (\tilde{\mathbf{z}}_{it} \tilde{u}_{it}) + \mathbf{a}'_i \frac{1}{T} \sum_{t=1}^T (\tilde{\mathbf{z}}_{it} \tilde{\mathbf{z}}'_{it}) \mathbf{a}_i \\
&= -2\mathbf{a}'_i \hat{\mathbf{q}}_{i, \tilde{z}\tilde{u}} + \mathbf{a}'_i \hat{\mathbf{Q}}_{i, \tilde{z}\tilde{z}} \mathbf{a}_i.
\end{aligned} \tag{A.1}$$

Notice that  $\mathcal{F}_{NT,i}(\hat{\boldsymbol{\pi}}_i, \lambda) \leq \mathcal{F}_{NT,i}(\boldsymbol{\pi}_i^0, \lambda)$  holds trivially since  $\hat{\boldsymbol{\pi}}_i$  estimates  $\boldsymbol{\pi}_i^0$  by minimizing  $\mathcal{F}_{NT,i}(\boldsymbol{\pi}_i, \lambda)$ .

Using the above decomposition (A.1),

$$\begin{aligned}
0 &\geq \mathcal{F}_{NT,i}(\hat{\boldsymbol{\pi}}_i, \lambda) - \mathcal{F}_{NT,i}(\boldsymbol{\pi}_i^0, \lambda) \\
&= -2\hat{\mathbf{a}}'_i \hat{\mathbf{q}}_{i, \tilde{z}\tilde{u}} + \hat{\mathbf{a}}'_i \hat{\mathbf{Q}}_{i, \tilde{z}\tilde{z}} \hat{\mathbf{a}}_i + \frac{\lambda}{N} \sum_{j=1, j \neq i}^N \dot{\omega}_{ij} (\|\hat{\boldsymbol{\pi}}_i - \hat{\boldsymbol{\pi}}_j\|_2 - \|\boldsymbol{\pi}_i^0 - \boldsymbol{\pi}_j^0\|_2).
\end{aligned} \tag{A.2}$$

<sup>7</sup> $\bar{\mathbb{G}}_K$  denotes the set of all  $K > K_0$  partitions over  $N$  such that there exists excess groups, where no two heterogeneous individuals are pooled together. Subsequently,  $\mathcal{G}^0$  can be retrieved just by merging certain groups of each  $\bar{\mathcal{G}}_K \in \bar{\mathbb{G}}_K$ .

Let  $i \in G_k^0$ . Focusing on the penalty term in (A.2),

$$\begin{aligned} & \frac{\lambda}{N} \sum_{j=1, j \neq i}^N \dot{\omega}_{ij} (\|\hat{\boldsymbol{\pi}}_i - \hat{\boldsymbol{\pi}}_j\|_2 - \|\boldsymbol{\pi}_i^0 - \boldsymbol{\pi}_j^0\|_2) \\ & \geq \frac{\lambda}{N} \sum_{j=1, j \neq i}^N \dot{\omega}_{ij} \|\hat{\boldsymbol{\pi}}_i - \hat{\boldsymbol{\pi}}_j - \boldsymbol{\pi}_i^0 + \boldsymbol{\pi}_j^0\|_2 \\ & \geq \frac{\lambda}{N} \sum_{j \notin G_k^0} \dot{\omega}_{ij} \|\hat{\boldsymbol{a}}_i - \hat{\boldsymbol{a}}_j\|_2. \end{aligned}$$

The first inequality holds due to the triangle inequality and the second inequality since all individuals of group  $k$  are discarded. Multiplying with -1 and employing the triangle inequality again gives

$$\frac{\lambda}{N} \sum_{j \notin G_k^0} \dot{\omega}_{ij} \|\hat{\boldsymbol{a}}_i - \hat{\boldsymbol{a}}_j\|_2 \geq -\frac{\lambda}{N} \sum_{j \notin G_k^0} \dot{\omega}_{ij} \|\hat{\boldsymbol{a}}_i + \hat{\boldsymbol{a}}_j\|_2 \geq -\frac{\lambda}{N} \sum_{j \notin G_k^0} \dot{\omega}_{ij} (\|\hat{\boldsymbol{a}}_i\|_2 + \|\hat{\boldsymbol{a}}_j\|_2). \quad (\text{A.3})$$

Plugging (A.3) back into (A.2) and averaging across all individuals results in

$$\begin{aligned} 0 & \geq \frac{1}{N} \sum_{i=1}^N [-2\hat{\boldsymbol{a}}_i' \hat{\boldsymbol{q}}_{i, \bar{z}\bar{u}}] + \frac{1}{N} \sum_{i=1}^N [\hat{\boldsymbol{a}}_i' \hat{\boldsymbol{Q}}_{i, \bar{z}\bar{z}} \hat{\boldsymbol{a}}_i] \\ & \quad - \frac{\lambda}{N^2} \sum_{k=1}^K \sum_{i \in G_k^0} \sum_{j \notin G_k^0} [\dot{\omega}_{ij} (\|\hat{\boldsymbol{a}}_i\|_2 + \|\hat{\boldsymbol{a}}_j\|_2)] \\ & \geq \frac{1}{N} \sum_{i=1}^N [-2\hat{\boldsymbol{a}}_i' \hat{\boldsymbol{q}}_{i, \bar{z}\bar{u}}] + \frac{1}{N} \sum_{i=1}^N [\hat{\boldsymbol{a}}_i' \hat{\boldsymbol{Q}}_{i, \bar{z}\bar{z}} \hat{\boldsymbol{a}}_i] \\ & \quad - \frac{\lambda}{N^2} \left( \max_{i \in G_k^0, j \notin G_k^0} \dot{\omega}_{ij} \right) \sum_{k=1}^K \sum_{i \in G_k^0} \sum_{j \notin G_k^0} [\|\hat{\boldsymbol{a}}_i\|_2 + \|\hat{\boldsymbol{a}}_j\|_2] \\ & \geq \frac{1}{N} \sum_{i=1}^N [-2\hat{\boldsymbol{a}}_i' \hat{\boldsymbol{q}}_{i, \bar{z}\bar{u}}] + \frac{1}{N} \sum_{i=1}^N [\hat{\boldsymbol{a}}_i' \hat{\boldsymbol{Q}}_{i, \bar{z}\bar{z}} \hat{\boldsymbol{a}}_i] - \frac{2\lambda}{N} \left( \max_{i \in G_k^0, j \notin G_k^0} \dot{\omega}_{ij} \right) \sum_{i=1}^N \|\hat{\boldsymbol{a}}_i\|_2. \end{aligned} \quad (\text{A.4})$$

The second inequality in (A.4) holds by taking the maximum adaptive penalty. In the following, we show the derivation of the third inequality in (A.4) explicitly. Focusing on the third term of the second inequality in (A.4),

$$\begin{aligned} & \frac{\lambda}{N^2} \left( \max_{i \in G_k^0, j \notin G_k^0} \dot{\omega}_{ij} \right) \sum_{k=1}^K \sum_{i \in G_k^0} \sum_{j \notin G_k^0} (\|\hat{\boldsymbol{a}}_i\|_2 + \|\hat{\boldsymbol{a}}_j\|_2) \\ & = \frac{\lambda}{N^2} \left( \max_{i \in G_k^0, j \notin G_k^0} \dot{\omega}_{ij} \right) \left[ \sum_{k=1}^K \sum_{i \in G_k^0} \sum_{j \notin G_k^0} (\|\hat{\boldsymbol{a}}_i\|_2) + \sum_{k=1}^K \sum_{i \in G_k^0} \sum_{j \notin G_k^0} (\|\hat{\boldsymbol{a}}_j\|_2) \right] \\ & \leq \frac{\lambda}{N^2} \left( \max_{i \in G_k^0, j \notin G_k^0} \dot{\omega}_{ij} \right) \left[ \sum_{i=1}^N (\|\hat{\boldsymbol{a}}_i\|_2 (N-1)) + \sum_{j=1}^N (\|\hat{\boldsymbol{a}}_j\|_2 (N-1)) \right] \\ & = \frac{\lambda}{N^2} \left( \max_{i \in G_k^0, j \notin G_k^0} \dot{\omega}_{ij} \right) 2(N-1) \sum_{i=1}^N \|\hat{\boldsymbol{a}}_i\|_2 \\ & \leq \frac{2\lambda}{N} \left( \max_{i \in G_k^0, j \notin G_k^0} \dot{\omega}_{ij} \right) \sum_{i=1}^N \|\hat{\boldsymbol{a}}_i\|_2, \end{aligned}$$

where one is the smallest possible group cardinality, which gives a maximum of  $N - 1$  summands in the third sum of  $\sum_{k=1}^K \sum_{i \in G_k^0} \sum_{j \notin G_k^0}$ .

Returning to (A.4),

$$\begin{aligned} 0 &\geq \frac{1}{N} \sum_{i=1}^N [-2\hat{\mathbf{a}}_i' \hat{\mathbf{q}}_{i,\bar{z}\bar{u}}] + \frac{1}{N} \sum_{i=1}^N [\hat{\mathbf{a}}_i' \hat{\mathbf{Q}}_{i,\bar{z}\bar{z}} \hat{\mathbf{a}}_i] - \frac{2\lambda}{N} \left( \max_{i \in G_k^0, j \notin G_k^0} \dot{\omega}_{ij} \right) \sum_{i=1}^N \|\hat{\mathbf{a}}_i\|_2 \\ &\geq \frac{1}{N} \sum_{i=1}^N [-2\|\hat{\mathbf{a}}_i\|_2 \|\hat{\mathbf{q}}_{i,\bar{z}\bar{u}}\|_2 + \|\hat{\mathbf{a}}_i\|_2^2 M^{-1} \underline{c}_{\bar{z}\bar{z}} - 2\lambda O_p(J_{\min}^{-\kappa}) \|\hat{\mathbf{a}}_i\|_2]. \end{aligned} \quad (\text{A.5})$$

The inequality in (A.5) holds due to (i) the sub-multiplicative property regarding the first summand, (ii) using Lemma A.2(i) to substitute  $M\hat{\mathbf{Q}}_{i,\bar{z}\bar{z}}$  with  $\underline{c}_{\bar{z}\bar{z}}$  in the second summand, and (iii) recognizing  $\max_{i \in G_k^0, j \notin G_k^0} \dot{\omega}_{ij} = O_p(J_{\min}^{-\kappa})$  as provided by Lemma A.5(ii) in the third summand.

Lemma A.3(i) yields  $\|\hat{\mathbf{q}}_{i,\bar{z}\bar{u}}\|_2 = O_p(T^{-1/2} + M^{-\theta-1/2})$ . In addition, Assumption 2(iii) states that  $\lambda O_p(J_{\min}^{-\kappa}) = O_p(T^{-1/2} + M^{-\theta-1/2})$ . Plugging these rates into (A.5), rearranging, and expanding with  $O_p(MT^{-1/2} + M^{-\theta+1/2})^{-2}$  yields

$$\begin{aligned} 0 &\geq \frac{1}{N} \sum_{i=1}^N \left[ -2\|\hat{\mathbf{a}}_i\|_2 O_p(T^{-1/2} + M^{-\theta-1/2}) + \|\hat{\mathbf{a}}_i\|_2^2 M^{-1} \underline{c}_{\bar{z}\bar{z}} - 2O_p(T^{-1/2} + M^{-\theta-1/2}) \|\hat{\mathbf{a}}_i\|_2 \right] \\ &= \frac{1}{N} \sum_{i=1}^N \left[ \|\hat{\mathbf{a}}_i\|_2^2 - \frac{4}{\underline{c}_{\bar{z}\bar{z}}} O_p(MT^{-1/2} + M^{-\theta+1/2}) \|\hat{\mathbf{a}}_i\|_2 \right] \\ &= \frac{1}{N} \sum_{i=1}^N \left[ O_p(MT^{-1/2} + M^{-\theta+1/2})^{-2} \|\hat{\mathbf{a}}_i\|_2^2 - \frac{4}{\underline{c}_{\bar{z}\bar{z}}} \|\hat{\mathbf{a}}_i\|_2 O_p(MT^{-1/2} + M^{-\theta+1/2})^{-1} \right]. \end{aligned} \quad (\text{A.6})$$

For a sufficiently large  $\|\hat{\mathbf{a}}_i\|_2$ ,  $\|\hat{\mathbf{a}}_i\|_2 \ll \|\hat{\mathbf{a}}_i\|_2^2$ , in which case  $\mathcal{F}_{NT,i}(\hat{\boldsymbol{\pi}}_i, \lambda)$  dominates  $\mathcal{F}_{NT,i}(\boldsymbol{\pi}_i^0, \lambda)$  and (A.6) cannot be negative. Since  $\mathcal{F}_{NT,i}(\boldsymbol{\pi}_i^0, \lambda)$  cannot be minimized and  $\mathcal{F}_{NT,i}(\hat{\boldsymbol{\pi}}_i, \lambda) \leq \mathcal{F}_{NT,i}(\boldsymbol{\pi}_i^0, \lambda)$  must hold,  $(MT^{-1/2} + M^{-\theta+1/2})^{-1} \|\hat{\mathbf{a}}_i\|_2$  is stochastically bounded and  $\|\hat{\mathbf{a}}_i\|_2 = \|\hat{\boldsymbol{\pi}}_i - \boldsymbol{\pi}_i^0\|_2 = O_p(MT^{-1/2} + M^{-\theta+1/2})$ . Assumption 2(i) ensures that  $MT^{-1/2}$  is not explosive and  $-\theta + 1/2 < 0$  holds by Assumption 1(vi). ■

**Theorem 3.1(ii)** Expanding upon the intermediary result in (A.4) gives

$$\begin{aligned} 0 &\geq \mathcal{F}_{NT,i}(\hat{\boldsymbol{\pi}}_i, \lambda) - \mathcal{F}_{NT,i}(\boldsymbol{\pi}_i^0, \lambda) \\ &\geq \frac{1}{N} \sum_{i=1}^N [-2\hat{\mathbf{a}}_i' \hat{\mathbf{q}}_{i,\bar{z}\bar{u}}] + \frac{1}{N} \sum_{i=1}^N [\hat{\mathbf{a}}_i' \hat{\mathbf{Q}}_{i,\bar{z}\bar{z}} \hat{\mathbf{a}}_i] - \frac{2\lambda}{N} \left( \max_{i \in G_k^0, j \notin G_k^0} \dot{\omega}_{ij} \right) \sum_{i=1}^N \|\hat{\mathbf{a}}_i\|_2 \\ &\geq -2 \left[ \frac{1}{N} \sum_{i=1}^N \|\hat{\mathbf{a}}_i\|_2^2 \right]^{1/2} \left[ \frac{1}{N} \sum_{i=1}^N \|\hat{\mathbf{q}}_{i,\bar{z}\bar{u}}\|_2^2 \right]^{1/2} + M^{-1} \underline{c}_{\bar{z}\bar{z}} \frac{1}{N} \sum_{i=1}^N [\|\hat{\mathbf{a}}_i\|_2^2] - \frac{2}{\sqrt{N}} \lambda O_p(J_{\min}^{-\kappa}) \left[ \frac{1}{N} \sum_{i=1}^N \|\hat{\mathbf{a}}_i\|_2^2 \right]^{1/2}, \end{aligned}$$

where the last inequality holds because of (i) the Cauchy-Schwarz inequality in the first summand, (ii) by employing the lower bound  $\underline{c}_{\bar{z}\bar{z}}$  of the minimum eigenvalue of the predictor variance-covariance matrix in the second summand according to Lemma A.2(i), and (iii) by the Cauchy-Schwarz inequality for vector spaces

in the third summand. Moreover, again, recognize that  $\lambda O_p(J_{\min}^{-\kappa}) = O_p(T^{-1/2} + M^{-\theta-1/2})$  by Assumption 2(iii) and  $N^{-1} \sum_{i=1}^N \|\hat{\mathbf{q}}_{i,\bar{z}\bar{u}}\|_2^2 = O_p(T^{-1} + M^{-2\theta-1})$  by Lemma A.3(ii). Putting these pieces together,

$$0 \geq -2 \left[ \frac{1}{N} \sum_{i=1}^N \|\hat{\mathbf{a}}_i\|_2^2 \right]^{1/2} \left[ O_p(T^{-1} + TM^{-2\theta-1}) \right]^{1/2} + M^{-1} \underline{c}_{\bar{z}\bar{z}} \frac{1}{N} \sum_{i=1}^N [\|\hat{\mathbf{a}}_i\|_2^2] \\ - \frac{2}{\sqrt{N}} O_p(T^{-1/2} + M^{-\theta-1/2}) \left[ \frac{1}{N} \sum_{i=1}^N \|\hat{\mathbf{a}}_i\|_2^2 \right]^{1/2},$$

and rearranging yields

$$\frac{M}{\underline{c}_{\bar{z}\bar{z}}} \left[ 2 [O_p(T^{-1} + M^{-2\theta-1})]^{1/2} + \frac{2}{\sqrt{N}} [O_p(T^{-1} + M^{-2\theta-1})]^{1/2} \right] \left[ \frac{1}{N} \sum_{i=1}^N \|\hat{\mathbf{a}}_i\|_2^2 \right]^{1/2} \geq \frac{1}{N} \sum_{i=1}^N \|\hat{\mathbf{a}}_i\|_2^2 \\ \frac{2}{\underline{c}_{\bar{z}\bar{z}}} \left[ O_p(M^2 T^{-1} + M^{-2\theta+1}) \frac{1}{N} \sum_{i=1}^N \|\hat{\mathbf{a}}_i\|_2^2 \right]^{1/2} \geq \frac{1}{N} \sum_{i=1}^N \|\hat{\mathbf{a}}_i\|_2^2,$$

where by the same argument as in Theorem 3.1(i),  $N^{-1} \sum_{i=1}^N \|\hat{\mathbf{a}}_i\|_2^2 = N^{-1} \sum_{i=1}^N \|\hat{\boldsymbol{\pi}}_i - \boldsymbol{\pi}_i^0\|_2^2 = O_p(M^2 T^{-1} + M^{-2\theta+1})$  holds to warrant  $\mathcal{F}_{NT,i}(\hat{\boldsymbol{\pi}}_i, \lambda) \leq \mathcal{F}_{NT,i}(\boldsymbol{\pi}_i^0, \lambda)$ . ■

### A.2.2 Corollary 3.2

Suppose that Assumptions A.1 and A.2(i)-(iii) hold. Following Su et al. (2019, Corollary 4.1), Corollaries 3.2(i)-(ii) extend the pointwise and  $L_2$  rates of the PSE derived in Theorem 3.1 to the estimator of the  $p$  regression curves  $\hat{\boldsymbol{\beta}}_i(v)$ .

*Proof:*

(i) Recall that  $\hat{\boldsymbol{\beta}}_i(v) = \hat{\boldsymbol{\Pi}}_i' \mathbf{b}(v) = (\hat{\boldsymbol{\Pi}}_i - \boldsymbol{\Pi}_i^0)' \mathbf{b}(v) + \boldsymbol{\Pi}_i^{0'} \mathbf{b}(v)$ . Using this decomposition,

$$\left\| \hat{\boldsymbol{\beta}}_i(v) - \boldsymbol{\beta}_i^0(v) \right\|_2 = \left\| (\hat{\boldsymbol{\Pi}}_i - \boldsymbol{\Pi}_i^0)' \mathbf{b}(v) + \boldsymbol{\Pi}_i^{0'} \mathbf{b}(v) - \boldsymbol{\beta}_i^0(v) \right\|_2 \\ \leq \left\| (\hat{\boldsymbol{\Pi}}_i - \boldsymbol{\Pi}_i^0)' \mathbf{b}(v) \right\|_2 + \left\| \boldsymbol{\Pi}_i^{0'} \mathbf{b}(v) - \boldsymbol{\beta}_i^0(v) \right\|_2 = \|\mathbf{d}_{1i}\|_2 + \|\mathbf{d}_{2i}\|_2, \quad (\text{A.7})$$

where the inequality holds because of the triangle property. Focusing on the first summand and taking the supremum over the unit interval results in

$$\sup_{v \in [0,1]} \|\mathbf{d}_{1i}\|_2 = \sup_{v \in [0,1]} \left\| (\hat{\boldsymbol{\Pi}}_i - \boldsymbol{\Pi}_i^0)' \mathbf{b}(v) \right\|_2 \leq \left\| \hat{\boldsymbol{\Pi}}_i - \boldsymbol{\Pi}_i^0 \right\|_F \sup_{v \in [0,1]} \|\mathbf{b}(v)\|_2 \leq \left\| \hat{\boldsymbol{\Pi}}_i - \boldsymbol{\Pi}_i^0 \right\|_F,$$

where the first inequality holds because of the Cauchy-Schwarz inequality and the second inequality since  $\|\mathbf{b}(v)\|_2 \leq 1$  as shown in Lemma A.1(i). Moreover,  $\left\| \hat{\boldsymbol{\Pi}}_i - \boldsymbol{\Pi}_i^0 \right\|_F = \left\| \hat{\boldsymbol{\pi}}_i - \boldsymbol{\pi}_i^0 \right\|_2 = O_p(MT^{-1/2} + M^{-\theta+1/2})$  by Theorem 3.1(i) and  $\sup_{v \in [0,1]} \|\mathbf{d}_{2i}\|_2 = \sup_{v \in [0,1]} \left\| \boldsymbol{\Pi}_i^{0'} \mathbf{b}(v) - \boldsymbol{\beta}_i^0(v) \right\|_2 = O(M^{-\theta})$  according to Lemma A.1(iv). As a consequence,  $\sup_{v \in [0,1]} \left\| \hat{\boldsymbol{\beta}}_i(v) - \boldsymbol{\beta}_i^0(v) \right\|_2 = O_p(MT^{-1/2} + M^{-\theta+1/2}) + O(M^{-\theta}) = O_p(MT^{-1/2} + M^{-\theta+1/2})$ . ■

(ii) Employing the same decomposition as in (A.7),  $\int_0^1 \|\hat{\beta}_i(v) - \beta_i^0(v)\|_2^2 dv = \int_0^1 \|\mathbf{d}_{1i} + \mathbf{d}_{2i}\|_2^2 dv$ . By the parallelogram law  $\int_0^1 \|\mathbf{d}_{1i} + \mathbf{d}_{2i}\|_2^2 dv \leq 2 \int_0^1 \|\mathbf{d}_{1i}\|_2^2 dv + 2 \int_0^1 \|\mathbf{d}_{2i}\|_2^2 dv$ .

Again, analyzing both summands on their own,

$$\begin{aligned} \int_0^1 \|\mathbf{d}_{1i}\|_2^2 dv &= \int_0^1 \left\| (\hat{\Pi}_i - \Pi_i^0)' \mathbf{b}(v) \right\|_2^2 dv = \text{tr} \left[ (\hat{\Pi}_i - \Pi_i^0)' \int_0^1 \mathbf{b}(v) \mathbf{b}(v)' dv (\hat{\Pi}_i - \Pi_i^0) \right] \\ &= O(M^{-1}) \left\| \hat{\Pi}_i - \Pi_i^0 \right\|_F^2 = O(M^{-1}) O_p(M^2 T^{-1} + M^{-2\theta+1}) = O_p(MT^{-1} + M^{-2\theta}), \end{aligned}$$

since  $\int_0^1 \mathbf{b}(v) \mathbf{b}(v)' dv = O(M^{-1})$  by Lemma A.1(iii) and  $\|\hat{\pi}_i - \pi_i^0\|_2 = O_p(MT^{-1/2} + M^{-\theta+1/2})$  by Theorem 3.1(i).

Following Lemma A.1(iv),  $\int_0^1 \|\mathbf{d}_{2i}\|_2^2 dv \leq \int_0^1 \sup_{v \in [0,1]} \|\Pi_i^{0'} \mathbf{b}(v) - \beta_i^0(v)\|_2^2 dv = O(M^{-2\theta})$ . Subsequently,  $\int_0^1 \left\| \hat{\beta}_i(v) - \beta_i^0(v) \right\|_2^2 dv \leq O_p(MT^{-1} + M^{-2\theta}) + O(M^{-2\theta}) = O_p(MT^{-1} + M^{-2\theta})$ . ■

### A.2.3 Theorem 3.3

Suppose that Assumptions 1 and 2 hold. Following Mehrabani (2023, Theorem 3.2), Theorem 3.3 shows the classification consistency of the PSE estimator: As  $(N, T) \rightarrow \infty$ ,  $\|\hat{\pi}_i - \hat{\pi}_j\|_2 = 0$  for all  $i, j \in G_k^0$  w.p.a.1.

*Proof:*

Define the  $Mp \times 1$  vector  $\mathbf{a}_{ij} = \pi_i - \pi_j = (a_{ij,1}, \dots, a_{ij,Mp})'$  and suppose there exists an  $i \in G_k^0$  such that  $\|a_{ij}\|_2 \neq 0$  for any  $j \in G_k^0$ . Let  $|a_{ij,r}| = \max_{l=1, \dots, Mp} |a_{ij,l}|$  and reorder  $\mathbf{a}_{ij}$  such that  $r = Mp$ . As a consequence, each  $|a_{ij,l}| \in [0, |a_{ij,Mp}|)$ ,  $l = 1, \dots, Mp$ . Hence  $\|\mathbf{a}_{ij}\|_2 = \left[ \sum_{l=1}^{Mp} a_{ij,l}^2 \right]^{1/2} \leq [Mpa_{ij,Mp}^2]^{1/2} = (Mp)^{1/2} |a_{ij,Mp}|$  and  $(Mp)^{-1/2} \leq |a_{ij,Mp}| / \|\mathbf{a}_{ij}\|_2 \leq 1$ .

Recall the criterion function

$$\begin{aligned} \mathcal{F}_{NT,i}(\pi_i, \lambda) &= \frac{1}{T} \sum_{t=1}^T (\tilde{y}_{it} - \tilde{z}'_{it} \pi_i)^2 + \frac{\lambda}{N} \sum_{j=1, j \neq i}^N \dot{\omega}_{ij} \|\pi_i - \pi_j\|_2 \\ &= \frac{1}{T} \sum_{t=1}^T (\tilde{y}_{it}^2 - 2\tilde{y}_{it} \tilde{z}'_{it} \pi_i + \tilde{z}'_{it} \pi_i \pi_i' \tilde{z}_{it}) \\ &\quad + \frac{\lambda}{N} \sum_{j=1, j \neq i}^N \dot{\omega}_{ij} \left[ \sum_{l=1}^{Mp} (\pi_{il}^2 - 2\pi_{il} \pi_{jl} + \pi_{jl}^2) \right]^{1/2}. \end{aligned} \tag{A.8}$$

Differentiating (A.8) with respect to the scalar  $\pi_{i,Mp}$  yields the first order condition (FOC)

$$\begin{aligned}
\frac{\partial \mathcal{F}_{NT,i}}{\partial \pi_{i,Mp}} &\stackrel{!}{=} 0 \\
&= -\frac{2}{T} \sum_{t=1}^T \tilde{y}_{it} \tilde{z}_{it,Mp} + \frac{2}{T} \sum_{t=1}^T \tilde{z}'_{it} \hat{\boldsymbol{\pi}}_i \tilde{z}_{it,Mp} \\
&\quad + \frac{\lambda}{N} \sum_{j=1, j \neq i}^N \dot{\omega}_{ij} \left\{ \frac{1}{2} \left[ \sum_{l=1}^{Mp} (\hat{\pi}_{il}^2 - 2\hat{\pi}_{il} \hat{\pi}_{jl} + \hat{\pi}_{jl}^2) \right]^{-1/2} (2\hat{\pi}_{i,Mp} - 2\hat{\pi}_{j,Mp}) \right\} \\
&= -\frac{2}{T} \sum_{t=1}^T \tilde{z}_{it,Mp} (\tilde{y}_{it} - \tilde{z}'_{it} \hat{\boldsymbol{\pi}}_i) + \frac{\lambda}{N} \sum_{j=1, j \neq i}^N \dot{\omega}_{ij} \frac{\hat{\pi}_{i,Mp} - \hat{\pi}_{j,Mp}}{\|\boldsymbol{\pi}_i - \boldsymbol{\pi}_j\|_2}.
\end{aligned} \tag{A.9}$$

Now, (i) expand (A.9) with  $(T^{-1/2} + M^{-\theta-1/2})^{-1}$ , (ii) recognize  $\hat{\boldsymbol{\pi}}_i = \boldsymbol{\pi}_i^0 + (\hat{\boldsymbol{\pi}}_i - \boldsymbol{\pi}_i^0)$ , (iii) rewrite the penalty term to discriminate between  $j \in G_k^0$  and  $j \notin G_k^0$ , and (iv) define  $e_{ij,Mp} = (\hat{\pi}_{i,Mp} - \hat{\pi}_{j,Mp}) / \|\hat{\boldsymbol{\pi}}_i - \hat{\boldsymbol{\pi}}_j\|_2$ . This results in

$$\begin{aligned}
0 &= -2(T^{-1/2} + M^{-\theta-1/2})^{-1} \frac{1}{T} \sum_{t=1}^T \tilde{z}_{it,Mp} (\tilde{y}_{it} - \tilde{z}'_{it} \boldsymbol{\pi}_i^0 - \tilde{z}'_{it} (\hat{\boldsymbol{\pi}}_i - \boldsymbol{\pi}_i^0)) \\
&\quad + (T^{-1/2} + M^{-\theta-1/2})^{-1} \frac{\lambda}{N} \sum_{j \in G_k^0, j \neq i} \dot{\omega}_{ij} e_{ij,Mp} + (T^{-1/2} + M^{-\theta-1/2})^{-1} \frac{\lambda}{N} \sum_{j \notin G_k^0, j \neq i} \dot{\omega}_{ij} e_{ij,Mp} \\
&= -2(T^{-1/2} + M^{-\theta-1/2})^{-1} \frac{1}{T} \sum_{t=1}^T \tilde{z}_{it,Mp} \tilde{u}_{it} + 2(T^{-1/2} + M^{-\theta-1/2})^{-1} \frac{1}{T} \sum_{t=1}^T \tilde{z}_{it,Mp} \tilde{z}'_{it} (\hat{\boldsymbol{\pi}}_i - \boldsymbol{\pi}_i^0) \\
&\quad + (T^{-1/2} + M^{-\theta-1/2})^{-1} \frac{\lambda}{N} \sum_{j \in G_k^0, j \neq i} \dot{\omega}_{ij} e_{ij,Mp} + (T^{-1/2} + M^{-\theta-1/2})^{-1} \frac{\lambda}{N} \sum_{j \notin G_k^0} \dot{\omega}_{ij} e_{ij,Mp},
\end{aligned} \tag{A.10}$$

(A.10) is made up of four summands, say  $0 = d_{1i} + d_{2i} + d_{3i} + d_{4i}$ . Studying each summand in isolation,

- $d_{1i} = -2(T^{-1/2} + M^{-\theta-1/2})^{-1} T^{-1} \sum_{t=1}^T \tilde{z}_{it,Mp} \tilde{u}_{it}$ . Note that  $\|\hat{\boldsymbol{q}}_{i,\tilde{z}\tilde{u}}\|_2 = O_p(T^{-1/2} + M^{-\theta-1/2})$  by Lemma A.2(i). Therefore, it is straightforward to see that  $d_{1i}$  is  $O_p(1)$ .
- $d_{2i} = 2(T^{-1/2} + M^{-\theta-1/2})^{-1} T^{-1} \sum_{t=1}^T \tilde{z}_{it,Mp} \tilde{z}'_{it} (\hat{\boldsymbol{\pi}}_i - \boldsymbol{\pi}_i^0)$ . Since  $\|\hat{\boldsymbol{q}}_{i,\tilde{z}M\tilde{p}\tilde{z}}(\hat{\boldsymbol{\pi}}_i - \boldsymbol{\pi}_i^0)\|_2 \leq \|\hat{\boldsymbol{q}}_{i,\tilde{z}M\tilde{p}\tilde{z}}\|_2 \|\hat{\boldsymbol{\pi}}_i - \boldsymbol{\pi}_i^0\|_2 = O_p(M^{-1}) O_p(MT^{-1/2} + M^{-\theta+1/2}) = O_p(T^{-1/2} + M^{-\theta-1/2})$  by Lemma A.3(i) and Theorem 3.1(i), where  $T^{-1} \sum_{t=1}^T \tilde{z}_{it,Mp} \tilde{z}'_{it} = \hat{\boldsymbol{q}}_{i,\tilde{z}M\tilde{p}\tilde{z}}$ , the rate of  $d_{2i}$  follows as  $O_p(1)$ .
- $d_{3i} = (T^{-1/2} + M^{-\theta-1/2})^{-1} \lambda N^{-1} \sum_{j \in G_k^0, j \neq i} \dot{\omega}_{ij} e_{ij,Mp}$ . The lower bound  $(Mp)^{-1/2} \leq |e_{ij,Mp}|$  gives the inequality  $|d_{3i}| \geq (T^{-1/2} + M^{-\theta-1/2})^{-1} \lambda N^{-1} (Mp)^{-1/2} \sum_{j \in G_k^0, j \neq i} \dot{\omega}_{ij}$ . Moreover, recall that Lemma A.5(i) states  $\min_{i,j \in G_k^0} \dot{\omega}_{ij} = O_p((MT^{-1/2} + M^{-\theta+1/2})^{-\kappa})$  and that  $\sum_{j \in G_k^0, j \neq i}$  sums over  $N_k - 1$  elements. As a consequence,  $\sum_{j \in G_k^0, j \neq i} \dot{\omega}_{ij} \geq (N_k - 1) \min_{i,j \in G_k^0} \dot{\omega}_{ij} = (N_k - 1) O_p((MT^{-1/2} + M^{-\theta+1/2})^{-\kappa})$ . Combining all these elements yields  $p^{1/2} |d_{3i}| \geq (T^{-1/2} + M^{-\theta-1/2})^{-1} \lambda N^{-1} M^{-1/2} (N_k - 1) O_p((MT^{-1/2} + M^{-\theta+1/2})^{-\kappa})$ . Note that by Assumption 1(v),  $(N_k - 1)N^{-1} = \tau_k - 1/N \geq 0$ , where  $\tau_k = N_k/N$ . Rearranging and using the bound on  $\tau_k$  yields  $p^{1/2} |d_{3i}| \geq O_p((MT^{-1/2} + M^{-\theta+1/2})^{-\kappa-1} M^{1/2} \lambda \tau_k)$ , which, under Assumption 2(iv), diverges to infinity in the limit.
- $d_{4i} = (T^{-1/2} + M^{-\theta-1/2})^{-1} \lambda N^{-1} \sum_{j \notin G_k^0} \dot{\omega}_{ij} e_{ij,Mp}$ . Recall that by Lemma A.5(ii),  $\max_{i \in G_k^0} \dot{\omega}_{ij} =$

$O_p(J_{\min}^{-\kappa})$ . Furthermore, as shown above,  $1 \geq |a_{ij, Mp}| / \|\mathbf{a}_{ij}\|_2 = |e_{ij, p}|$  and subsequently  $\sum_{j \notin G_k^0} |e_{ij, Mp}| \leq N - N_k$  since  $\sum_{j \notin G_k^0}$  sums over  $N - N_k$  elements. Lastly,  $|d_{4i}| \leq (T^{-1/2} + M^{-\theta-1/2})^{-1} \lambda O_p(J_{\min}^{-\kappa}) N^{-1} (N - N_k) = O_p(1)$  by Assumptions 1(iv) and 2(iii).

Since  $|d_{3i}| \gg |d_{1i} + d_{2i} + d_{3i}|$  cannot hold for large  $(N, T)$ ,  $\|\hat{\boldsymbol{\pi}}_i - \boldsymbol{\pi}_i^0\|_2$  must not be differentiable w.p.a.1 for all  $i, j \in G_k^0$  for  $k = 1, \dots, K^0$  and  $(T^{-1/2} + M^{-\theta-1/2})^{-1} \lambda \dot{\omega}_{ij} e_{ij} = O_p(1)$  in (A.10). This translates to  $\Pr(\|\hat{\boldsymbol{\pi}}_i - \hat{\boldsymbol{\pi}}_j\|_2 = 0) \rightarrow 1 \forall i, j \in G_k^0$  as  $(N, T) \rightarrow \infty$ . ■

#### A.2.4 Corollary 3.4

Suppose that Assumptions 1 and 2 hold. Corollary 3.4 is based on Theorem 3.3 and is composed of two parts. Part 1 shows that the correct total number of groups will be estimated asymptotically. Part 2 demonstrates that the estimated grouping converges to the true latent group structure in the limit.

*Proof:*

(i) Theorem 3.3 gives  $\Pr(\|\hat{\boldsymbol{\pi}}_i - \boldsymbol{\pi}_i^0\|_2 = 0) \rightarrow 1 \forall i, j \in G_k^0$  as  $(N, T) \rightarrow \infty$ . As a consequence, it also holds that  $\lim_{(N, T) \rightarrow \infty} \Pr(\hat{K} = K_0) = 1$  since  $\hat{K}$  is the number of unique subvectors of  $\hat{\boldsymbol{\pi}} = (\hat{\boldsymbol{\pi}}_1', \dots, \hat{\boldsymbol{\pi}}_N)'$ . ■

(ii) Suppose there exist two heterogeneous units  $i \in G_k^0, j \notin G_k^0$  that nonetheless exhibit  $\|\hat{\boldsymbol{\pi}}_i - \hat{\boldsymbol{\pi}}_j\|_2 = 0$ . Expanding  $\hat{\boldsymbol{\pi}}_i - \hat{\boldsymbol{\pi}}_j$  by  $\pm \boldsymbol{\pi}_i^0$  and recognizing  $\|\hat{\boldsymbol{\pi}}_i - \boldsymbol{\pi}_i^0\|_2 = O_p(MT^{-1/2} + M^{-\theta+1/2})$  following Theorem 3.1(i), we obtain

$$0 = \hat{\boldsymbol{\pi}}_i - \hat{\boldsymbol{\pi}}_j = (\boldsymbol{\pi}_i^0 + (\hat{\boldsymbol{\pi}}_i - \boldsymbol{\pi}_i^0)) - (\boldsymbol{\pi}_j^0 + (\hat{\boldsymbol{\pi}}_j - \boldsymbol{\pi}_j^0)) = \boldsymbol{\pi}_i^0 - \boldsymbol{\pi}_j^0 + O_p(MT^{-1/2} + M^{-\theta+1/2}). \quad (\text{A.11})$$

(A.11) makes it easy to see that if  $\|\hat{\boldsymbol{\pi}}_i - \hat{\boldsymbol{\pi}}_j\|_2 = 0$ , then  $\|\boldsymbol{\pi}_i^0 - \boldsymbol{\pi}_j^0\|_2 = O_p(MT^{-1/2} + M^{-\theta+1/2})$ . Recall that  $\|\boldsymbol{\pi}_i^0 - \boldsymbol{\pi}_j^0\|_2 \geq J_{\min}$  by construction. However, Assumption 2(ii) states that  $(MT^{-1/2} + M^{-\theta+1/2})^{-1} J_{\min} \rightarrow \infty$ , in which case (A.11) cannot hold. In consequence,  $\|\hat{\boldsymbol{\pi}}_i - \hat{\boldsymbol{\pi}}_j\|_2 \neq 0$  for all  $i \in G_k^0, j \notin G_k^0$  and  $\lim_{(N, T) \rightarrow \infty} \Pr(\hat{\mathcal{G}}_{K_0} = \mathcal{G}_{K_0}^0) = 1$ . ■

#### A.2.5 Theorem 3.5

Given that Assumptions 1-4 are satisfied, Theorem 3.5 derives the limiting distribution of the *PSE* estimator  $\hat{\boldsymbol{\alpha}}(v) = (\hat{\boldsymbol{\alpha}}_1(v)', \dots, \hat{\boldsymbol{\alpha}}_{\hat{K}}(v)')$  and the *post-Lasso* estimator  $\hat{\boldsymbol{\alpha}}_{\hat{\mathcal{G}}_{\hat{K}}}^p(v) = (\hat{\boldsymbol{\alpha}}_{\hat{\mathcal{G}}_1}^p(v)', \dots, \hat{\boldsymbol{\alpha}}_{\hat{\mathcal{G}}_{\hat{K}}}^p(v)')$ . For this purpose, Theorem 3.5(i) shows that both estimators coincide in the limit. Theorem 3.5(ii) obtains the final asymptotic distribution (see Qian and Su (2016a, Theorem 3.5), Mehrabani (2023, Theorem 3.5), and Su et al. (2019, Theorem 4.5) for similar derivations).

*Proof:*



**Theorem 3.5(i)** Note the decomposition  $\|\hat{\alpha}_k(v) - \hat{\alpha}_{\hat{G}_k}^p(v)\|_2 = \|(\hat{\Xi}_k - \hat{\Xi}_{\hat{G}_k}^p)' \mathbf{b}(v)\|_2 \leq \|\hat{\Xi}_k - \hat{\Xi}_{\hat{G}_k}^p\|_F \|\mathbf{b}(v)\|_2$ . Since  $\|\mathbf{b}(v)\|_2 = 1$  by Lemma A.1(i), it suffices to show that  $(N_k T)^{1/2} M^{-1/2} \|\hat{\Xi}_k - \hat{\Xi}_{\hat{G}_k}^p\|_F = o_p(1)$  in order to prove that the *PSE* and *post-Lasso* feature an identical limiting distribution.<sup>8</sup>

Recall the FOC from Theorem 3.3 (A.9)

$$\frac{\partial \mathcal{F}_{NT,i}}{\partial \boldsymbol{\pi}_i} = 0 = -\frac{2}{T} \sum_{t=1}^T \tilde{\mathbf{z}}_{it} (\tilde{y}_{it} - \tilde{\mathbf{z}}'_{it} \hat{\boldsymbol{\pi}}_i) + \frac{\lambda}{N} \sum_{j=1, j \neq i}^N \dot{\omega}_{ij} (\hat{\boldsymbol{\pi}}_i - \hat{\boldsymbol{\pi}}_j) \|\hat{\boldsymbol{\pi}}_i - \hat{\boldsymbol{\pi}}_j\|_2^{-1}.$$

Write  $\hat{\boldsymbol{\pi}}_i = \hat{\boldsymbol{\xi}}_k$  for any  $i \in \hat{G}_k$  and sum over all  $i \in \hat{G}_k$  to obtain

$$\begin{aligned} 0 &= -\frac{2}{T} \sum_{i \in \hat{G}_k} \sum_{t=1}^T \tilde{\mathbf{z}}_{it} [\tilde{y}_{it} - \tilde{\mathbf{z}}'_{it} \hat{\boldsymbol{\xi}}_k] + \frac{\lambda}{N} \sum_{i \in \hat{G}_k} \sum_{j=1, j \neq i}^N \dot{\omega}_{ij} (\hat{\boldsymbol{\pi}}_i - \hat{\boldsymbol{\pi}}_j) \|\hat{\boldsymbol{\pi}}_i - \hat{\boldsymbol{\pi}}_j\|_2^{-1} \\ &= -\frac{2}{T} \sum_{i \in \hat{G}_k} \sum_{t=1}^T [\tilde{\mathbf{z}}_{it} \tilde{y}_{it} - \tilde{\mathbf{z}}_{it} \tilde{\mathbf{z}}'_{it} \hat{\boldsymbol{\xi}}_k] + \hat{\mathbf{r}}_{\hat{G}_k} \\ &= -2 \left[ \hat{\mathbf{q}}_{\hat{G}_k, \tilde{\mathbf{z}}\tilde{\mathbf{y}}} - \hat{\mathbf{Q}}_{\hat{G}_k, \tilde{\mathbf{z}}\tilde{\mathbf{z}}} \hat{\boldsymbol{\xi}}_k \right] + \hat{\mathbf{r}}_{\hat{G}_k}, \end{aligned} \tag{A.12}$$

where  $\hat{\mathbf{r}}_{\hat{G}_k} = \lambda N^{-1} \sum_{i \in \hat{G}_k} \sum_{j=1, j \neq i}^N \dot{\omega}_{ij} \hat{\mathbf{e}}_{ij}$ ,  $\hat{\mathbf{e}}_{ij} = (\hat{\boldsymbol{\pi}}_i - \hat{\boldsymbol{\pi}}_j) \|\hat{\boldsymbol{\pi}}_i - \hat{\boldsymbol{\pi}}_j\|_2^{-1}$ ,  $\hat{\mathbf{q}}_{\hat{G}_k, \tilde{\mathbf{z}}\tilde{\mathbf{y}}} = \sum_{i \in \hat{G}_k} T^{-1} \sum_{t=1}^T \tilde{\mathbf{z}}_{it} \tilde{y}_{it}$ , and  $\hat{\mathbf{Q}}_{\hat{G}_k, \tilde{\mathbf{z}}\tilde{\mathbf{z}}} = \sum_{i \in \hat{G}_k} T^{-1} \sum_{t=1}^T \tilde{\mathbf{z}}_{it} \tilde{\mathbf{z}}'_{it}$ .

Solving (A.12) for  $\hat{\boldsymbol{\xi}}_k$  gives

$$\hat{\boldsymbol{\xi}}_k = \hat{\mathbf{Q}}_{\hat{G}_k, \tilde{\mathbf{z}}\tilde{\mathbf{z}}}^{-1} \hat{\mathbf{q}}_{\hat{G}_k, \tilde{\mathbf{z}}\tilde{\mathbf{y}}} - 1/2 \hat{\mathbf{Q}}_{\hat{G}_k, \tilde{\mathbf{z}}\tilde{\mathbf{z}}}^{-1} \hat{\mathbf{r}}_{\hat{G}_k} = \hat{\boldsymbol{\xi}}_{\hat{G}_k}^p - 1/2 \hat{\mathbf{Q}}_{\hat{G}_k, \tilde{\mathbf{z}}\tilde{\mathbf{z}}}^{-1} \hat{\mathbf{r}}_{\hat{G}_k}.$$

It is straightforward to see that the *PSE* estimator  $\hat{\boldsymbol{\xi}}_k$  and the *post-Lasso*  $\hat{\boldsymbol{\xi}}_{\hat{G}_k}^p$  are asymptotically equivalent if  $\hat{\mathbf{Q}}_{\hat{G}_k, \tilde{\mathbf{z}}\tilde{\mathbf{z}}}^{-1} \hat{\mathbf{r}}_{\hat{G}_k} = o_p(1)$ . We employ Corollary 3.4 and make use of the oracle property to demonstrate this result. Subsequently, one can infer the limiting behavior of  $\hat{\mathbf{Q}}_{\hat{G}_k, \tilde{\mathbf{z}}\tilde{\mathbf{z}}}^{-1} \hat{\mathbf{r}}_{\hat{G}_k}$  by studying  $\hat{\mathbf{Q}}_{G_k^0, \tilde{\mathbf{z}}\tilde{\mathbf{z}}}^{-1} \hat{\mathbf{r}}_{G_k^0}$ . Scaling by  $\sqrt{N_k T/M}$  and taking the squared  $L_2$  norm yields

$$\begin{aligned} \left\| \sqrt{\frac{N_k T}{M}} \hat{\mathbf{Q}}_{\hat{G}_k, \tilde{\mathbf{z}}\tilde{\mathbf{z}}}^{-1} \hat{\mathbf{r}}_{\hat{G}_k} \right\|_2^2 &= \left\| \left( \frac{M}{N_k} \hat{\mathbf{Q}}_{\hat{G}_k, \tilde{\mathbf{z}}\tilde{\mathbf{z}}} \right)^{-1} \sqrt{\frac{TM}{N_k}} \hat{\mathbf{r}}_{\hat{G}_k} \right\|_2^2 \\ &\leq \left[ \mu_{\min} \left( \frac{M}{N_k} \hat{\mathbf{Q}}_{\hat{G}_k, \tilde{\mathbf{z}}\tilde{\mathbf{z}}} \right) \right]^{-2} \left\| \sqrt{\frac{TM}{N_k}} \hat{\mathbf{r}}_{\hat{G}_k} \right\|_2^2, \end{aligned} \tag{A.13}$$

<sup>8</sup>The  $\sqrt{N_k T/M}$  scaling is required for the *post-Lasso* estimator to converge in distribution. See Theorem 3.5(ii).

where  $\underline{c}_{\tilde{z}\tilde{z}} \leq \mu_{\min} \left( MN_k^{-1} \hat{\mathbf{Q}}_{G_k^0, \tilde{z}\tilde{z}} \right)$  by Lemma A.2(ii). Focusing on the norm in (A.13),

$$\begin{aligned}
\left\| \sqrt{\frac{TM}{N_k}} \hat{\mathbf{r}}_{G_k^0} \right\|_2^2 &= \frac{TM}{N_k} \frac{\lambda^2}{N^2} \left\| \sum_{i \in G_k^0} \sum_{j \notin G_k^0} \dot{\omega}_{ij} \hat{\mathbf{e}}_{ij} \right\|_2^2 \\
&\leq \frac{TM}{N_k} \frac{\lambda^2}{N^2} \left( \sum_{i \in G_k^0} \sum_{j \notin G_k^0} |\dot{\omega}_{ij}| \|\hat{\mathbf{e}}_{ij}\|_2 \right)^2 \\
&\leq \frac{TM}{N_k} \frac{\lambda^2}{N^2} \left( \max_{i \in G_k^0, j \notin G_k^0} |\dot{\omega}_{ij}| \right)^2 \left( \sum_{i \in G_k^0} \sum_{j \notin G_k^0} \|\hat{\mathbf{e}}_{ij}\|_2 \right)^2 \\
&\leq TM \lambda^2 \left( \max_{i \in G_k^0, j \notin G_k^0} |\dot{\omega}_{ij}| \right)^2 \frac{N_k^2 (N - N_k)^2}{N^2 N_k} \\
&\leq TM \lambda^2 \left( \max_{i \in G_k^0, j \notin G_k^0} |\dot{\omega}_{ij}| \right)^2 N_k,
\end{aligned} \tag{A.14}$$

where the first inequality by the Cauchy-Schwarz inequality; the second inequality holds by taking the maximum adaptive weight; the third inequality holds by recognizing that  $\|\hat{\mathbf{e}}_{ij}\|_2 \leq 1$  by the Triangle inequality; the fourth inequality holds by taking  $N^{-2} N_k (N - N_k)^2 = N_k (1 - 2\tau_k + \tau_k^2) \leq N_k$  using Assumption 1(v), where  $\tau_k = N_k/N$ . Furthermore, note that  $\max_{i \in G_k^0, j \notin G_k^0} (|\dot{\omega}_{ij}|^2) = O_p(J_{\min}^{-2\kappa})$  by Lemma A.5(ii). Plugging these pieces into (A.14), it becomes apparent that

$$\left\| \sqrt{\frac{TM}{N_k}} \hat{\mathbf{r}}_{G_k^0} \right\|_2^2 \leq TM \lambda^2 O_p(J_{\min}^{-2\kappa}) N_k = O_p(\sqrt{N_k TM} \lambda J_{\min}^{-\kappa})^2.$$

Assumption 3 gives  $O_p(\sqrt{N_k TM} \lambda J_{\min}^{-\kappa}) = o_p(1)$ . In consequence, the whole term (A.13) becomes negligible in the limit and  $\|\hat{\boldsymbol{\alpha}}_k(v) - \hat{\boldsymbol{\alpha}}_{\hat{G}_k}^p(v)\|_2 = o_p(1)$ . ■

**Theorem 3.5(ii)** We make use of the decomposition

$$\begin{aligned}
\sqrt{\frac{N_k T}{M}} \left[ \hat{\boldsymbol{\alpha}}_{\hat{G}_k}^p(v) - \boldsymbol{\alpha}_k^0(v) \right] &= \sqrt{\frac{N_k T}{M}} (\hat{\boldsymbol{\Xi}}_{\hat{G}_k}^p - \boldsymbol{\Xi}_k^0)' \mathbf{b}(v) + \sqrt{\frac{N_k T}{M}} (\boldsymbol{\Xi}_k^{0'} \mathbf{b}(v) - \boldsymbol{\alpha}_k^0(v)) \\
&= \mathbf{d}_{1, \hat{G}_k} + \mathbf{d}_{2, \hat{G}_k},
\end{aligned} \tag{A.15}$$

where  $\boldsymbol{\alpha}_k^0(v) = \boldsymbol{\Xi}_k^{0'} \mathbf{b}(v) + (\boldsymbol{\alpha}_k^0(v) - \boldsymbol{\Xi}_k^{0'} \mathbf{b}(v))$ .

It is easy to show that  $\mathbf{d}_{2, \hat{G}_k} / s_{c, \hat{G}_k} = \sqrt{N_k T / M} O(M^{-\theta}) O_p(1) = o_p(1)$ , since  $\|\boldsymbol{\alpha}_k^0(v) - \boldsymbol{\Xi}_k^{0'} \mathbf{b}(v)\|_2 = O(M^{-\theta})$  by Lemma A.1(iv),  $\sqrt{N_k T / M^{2\theta}} = o_p(1)$  according to Assumption 4(ii), and  $s_{c, \hat{G}_k} = O_p(1)$  by Lemma A.6(ii).<sup>9</sup> As a result, the second summand is negligible for the remainder of the proof and it is sufficient to study  $\mathbf{d}_{1, \hat{G}_k}$  only.

Regarding  $\mathbf{d}_{1, \hat{G}_k}$ , consider  $\mathbf{d}'_{1, \hat{G}_k} \mathbf{c}$  for some nonrandom  $p \times 1$  vector  $\mathbf{c}$  with  $\|\mathbf{c}\|_2 = 1$ . Define  $\mathbf{b}_c = \mathbf{c} \otimes \mathbf{b}(v)$ . Recognize that  $\text{vec}(\mathbf{b}'(v) (\hat{\boldsymbol{\Xi}}_{\hat{G}_k}^p - \boldsymbol{\Xi}_k^0) \mathbf{c}) = (\mathbf{c}' \otimes \mathbf{b}(v)) \text{vec}(\hat{\boldsymbol{\Xi}}_{\hat{G}_k}^p - \boldsymbol{\Xi}_k^0)$  (see Bernstein, 2009, p. 249). In addition, let  $\hat{\mathbf{q}}_{\hat{G}_k, \tilde{z}a} = \sum_{i \in \hat{G}_k} T^{-1} \sum_{t=1}^T \tilde{\mathbf{z}}_{it} a_{it}$  for  $a = \{\tilde{y}, \tilde{u}, \tilde{\epsilon}\}$ . Recall that the error term  $\tilde{u}_{it}$  can be

<sup>9</sup> $s_{c, \hat{G}_k}$  is a scaling factor that is introduced at a later stage.

decomposed into an idiosyncratic  $\tilde{\epsilon}_{it}$  and a sieve  $\tilde{\eta}_{it}$  component  $\tilde{u}_{it} = \tilde{\eta}_{it} + \tilde{\epsilon}_{it}$  (see, e.g., (2.5)). Then,

$$\begin{aligned}
\mathbf{d}'_{1, \hat{G}_k} \mathbf{c} &= \sqrt{\frac{N_k T}{M}} \mathbf{b}'(v) (\hat{\Xi}_{\hat{G}_k}^p - \Xi_k^0) \mathbf{c} = \sqrt{\frac{N_k T}{M}} \mathbf{b}'_c (\hat{\xi}_{\hat{G}_k}^p - \xi_k^0) = \sqrt{\frac{N_k T}{M}} \mathbf{b}'_c \left[ \hat{\mathcal{Q}}_{\hat{G}_k, \tilde{z}\tilde{z}}^{-1} \hat{\mathbf{q}}_{\hat{G}_k, \tilde{z}\tilde{y}} - \xi_k^0 \right] \\
&= \sqrt{\frac{N_k T}{M}} \mathbf{b}'_c \hat{\mathcal{Q}}_{\hat{G}_k, \tilde{z}\tilde{z}}^{-1} \left[ \hat{\mathbf{q}}_{\hat{G}_k, \tilde{z}\tilde{y}} - \hat{\mathcal{Q}}_{\hat{G}_k, \tilde{z}\tilde{z}} \xi_k^0 \right] \\
&= \sqrt{\frac{N_k T}{M}} \mathbf{b}'_c \hat{\mathcal{Q}}_{\hat{G}_k, \tilde{z}\tilde{z}}^{-1} \left[ \hat{\mathbf{q}}_{\hat{G}_k, \tilde{z}\tilde{u}} + \sum_{i \in \hat{G}_k} \frac{1}{T} \sum_{t=1}^T z_{it} z'_{it} (\boldsymbol{\pi}_i^0 - \xi_k^0) \right] \\
&= \sqrt{\frac{N_k T}{M}} \mathbf{b}'_c \hat{\mathcal{Q}}_{\hat{G}_k, \tilde{z}\tilde{z}}^{-1} \hat{\mathbf{q}}_{\hat{G}_k, \tilde{z}\tilde{\epsilon}} + \sqrt{\frac{N_k T}{M}} \mathbf{b}'_c \hat{\mathcal{Q}}_{\hat{G}_k, \tilde{z}\tilde{z}}^{-1} \hat{\mathbf{q}}_{\hat{G}_k, \tilde{z}\tilde{\eta}} \\
&\quad + \sqrt{\frac{N_k}{TM}} \mathbf{b}'_c \hat{\mathcal{Q}}_{\hat{G}_k, \tilde{z}\tilde{z}}^{-1} \sum_{i \in \hat{G}_k} \sum_{t=1}^T z_{it} z'_{it} (\boldsymbol{\pi}_i^0 - \xi_k^0).
\end{aligned} \tag{A.16}$$

Exploiting the oracle property by Corollary 3.4, we study  $\mathbf{d}_{1, \hat{G}_k}$  by analyzing  $\mathbf{d}_{1, G_k^0}$ . Subsequently,

$$\begin{aligned}
\mathbf{d}'_{1, G_k^0} \mathbf{c} &= \sqrt{\frac{N_k T}{M}} \mathbf{b}'_c \hat{\mathcal{Q}}_{G_k^0, \tilde{z}\tilde{z}}^{-1} \hat{\mathbf{q}}_{G_k^0, \tilde{z}\tilde{\epsilon}} + \sqrt{\frac{N_k T}{M}} \mathbf{b}'_c \hat{\mathcal{Q}}_{G_k^0, \tilde{z}\tilde{z}}^{-1} \hat{\mathbf{q}}_{G_k^0, \tilde{z}\tilde{\eta}} \\
&= d_{11, G_k^0} + d_{12, G_k^0},
\end{aligned} \tag{A.17}$$

where the last summand in (A.16) equals zero since  $\boldsymbol{\pi}_i^0 = \xi_k^0$  for  $i \in G_k^0$ .

We show that  $d_{12, G_k^0}$  vanishes in the limit before studying the asymptotic behavior of  $d_{11, G_k^0}$ . But first, note two preliminary results that are used later.

$$\begin{aligned}
\frac{1}{N_k T} \sum_{i \in G_k^0} \sum_{t=1}^T \tilde{\eta}_{it}^2 &= \frac{1}{N_k T} \sum_{i \in G_k^0} \sum_{t=1}^T \left( \left[ \beta_i^0 \left( \frac{t}{T} \right) - \boldsymbol{\Pi}_i^{0'} \mathbf{b} \left( \frac{t}{T} \right) \right]' \tilde{\mathbf{x}}_{it} \right)^2 \\
&\leq \left[ \sup_{v \in [0,1]} \|\boldsymbol{\alpha}_k^0(v) - \Xi_k^{0'} \mathbf{b}(v)\|_2 \right]^2 \frac{1}{N_k T} \sum_{i \in G_k^0} \sum_{t=1}^T \tilde{\mathbf{x}}_{it} \tilde{\mathbf{x}}'_{it} \\
&\leq O_p(M^{-\theta})^2 \bar{c}_{xx} (1 + o_p(1)) = O_p(M^{-2\theta}),
\end{aligned} \tag{A.18}$$

where the rates are given by Lemma A.1(iv) and Assumption 1(iv). In addition,

$$\begin{aligned}
&\frac{M}{N_k T} \sum_{i \in G_k^0} \sum_{t=1}^T \left[ \mathbf{b}'_c \left( M N_k^{-1} \hat{\mathcal{Q}}_{G_k^0, \tilde{z}\tilde{z}} \right)^{-1} \tilde{\mathbf{z}}_{it} \right]^2 \\
&= \frac{M}{N_k T} \sum_{i \in G_k^0} \sum_{t=1}^T \left[ \mathbf{b}'_c \left( M N_k^{-1} \hat{\mathcal{Q}}_{G_k^0, \tilde{z}\tilde{z}} \right)^{-1} \tilde{\mathbf{z}}_{it} \tilde{\mathbf{z}}'_{it} \left( M N_k^{-1} \hat{\mathcal{Q}}_{G_k^0, \tilde{z}\tilde{z}} \right)^{-1} \mathbf{b}_c \right] \\
&= \frac{M}{N_k T} \sum_{i \in G_k^0} \sum_{t=1}^T \left[ \boldsymbol{\varpi}' \tilde{\mathbf{z}}_{it} \tilde{\mathbf{z}}'_{it} \boldsymbol{\varpi} \right] \\
&= \frac{M}{N_k T} \sum_{i \in G_k^0} \sum_{t=1}^T \left[ \mathbf{g}'_{\boldsymbol{\varpi}} \left( \frac{t}{T} \right) \tilde{\mathbf{x}}_{it} \tilde{\mathbf{x}}'_{it} \mathbf{g}_{\boldsymbol{\varpi}} \left( \frac{t}{T} \right) \right],
\end{aligned} \tag{A.19}$$

where  $\mathbf{g}_{\boldsymbol{\varpi}}(v)$  is a  $p \times 1$  vector of spline functions  $\mathbf{g}_{\boldsymbol{\varpi}}(v) = (g_1(v, \boldsymbol{\varpi}_1), \dots, g_p(v, \boldsymbol{\varpi}_p))'$ , with  $g_l(v, \boldsymbol{\varpi}_l) = \boldsymbol{\varpi}'_l \mathbf{b}(v)$ , and  $\boldsymbol{\varpi}_l = (\boldsymbol{\varpi}_{l1}, \dots, \boldsymbol{\varpi}_{lM})'$ . The  $M \times p$  matrix  $\mathbf{W}$  is defined as  $\boldsymbol{\varpi} = \text{vec}(\mathbf{W}) = \mathbf{b}'_c \left( M N_k^{-1} \hat{\mathcal{Q}}_{G_k^0, \tilde{z}\tilde{z}} \right)^{-1}$

with  $\mathbf{W} = (\boldsymbol{\varpi}_1, \dots, \boldsymbol{\varpi}_p)$ . Additionally,  $\mathbf{g}_\varpi(v) = \mathbf{W}'\mathbf{b}(v)$ . The last inequality in (A.19) holds due to the decomposition  $\boldsymbol{\varpi}'\tilde{\mathbf{z}}_{it} = \boldsymbol{\varpi}'(\tilde{\mathbf{x}}_{it} \otimes \mathbf{b}(t/T)) = \mathbf{b}(t/T)'\mathbf{W}\tilde{\mathbf{x}}_{it} = \mathbf{g}'_\varpi(t/T)\tilde{\mathbf{x}}_{it}$ .

We rewrite (A.19) as

$$\begin{aligned}
& \frac{M}{N_k T} \sum_{i \in G_k^0} \sum_{t=1}^T \mathbf{g}'_\varpi \left( \frac{t}{T} \right) \tilde{\mathbf{x}}_{it} \tilde{\mathbf{x}}'_{it} \mathbf{g}_\varpi \left( \frac{t}{T} \right) \\
&= \frac{M}{N_k T} \sum_{i \in G_k^0} \sum_{t=1}^T \mathbf{g}'_\varpi \left( \frac{t}{T} \right) E(\tilde{\mathbf{x}}_{it} \tilde{\mathbf{x}}'_{it}) \mathbf{g}_\varpi \left( \frac{t}{T} \right) (1 + o_p(1)) \\
&\leq \frac{M \bar{c}_{\tilde{x}\tilde{x}}}{T} \sum_{t=1}^T \mathbf{g}'_\varpi \left( \frac{t}{T} \right) \mathbf{g}_\varpi \left( \frac{t}{T} \right) = \frac{M \bar{c}_{\tilde{x}\tilde{x}}}{T} \sum_{t=1}^T \boldsymbol{\varpi}' \mathbf{b} \left( \frac{t}{T} \right) \mathbf{b} \left( \frac{t}{T} \right)' \boldsymbol{\varpi} \\
&= \bar{c}_{\tilde{x}\tilde{x}} \|\boldsymbol{\varpi}\|_2^2 \frac{1}{T} \sum_{t=1}^T M \mathbf{b} \left( \frac{t}{T} \right) \mathbf{b} \left( \frac{t}{T} \right)' .
\end{aligned} \tag{A.20}$$

The first equality holds since  $T^{-1} \sum_{t=1}^T \tilde{\mathbf{x}}_{it} \tilde{\mathbf{x}}'_{it} = T^{-1} \sum_{t=1}^T E(\tilde{\mathbf{x}}_{it} \tilde{\mathbf{x}}'_{it}) (1 + o_p(1))$  by Huang et al. (2004, Lemma A.2). The first inequality uses the fact that  $E(\tilde{\mathbf{x}}_{it} \tilde{\mathbf{x}}'_{it}) = E(\mathbf{x}_{it} \mathbf{x}'_{it}) - E(\mathbf{x}_{it})E(\mathbf{x}'_{it}) \leq E(\mathbf{x}_{it} \mathbf{x}'_{it}) \leq \bar{c}_{\tilde{x}\tilde{x}}$  by Assumption 1(iv) and consequently  $(N_k T)^{-1} \sum_{i \in G_k^0} \sum_{t=1}^T E(\tilde{\mathbf{x}}_{it} \tilde{\mathbf{x}}'_{it}) \leq \bar{c}_{\tilde{x}\tilde{x}}$ . Recall that by property of the Riemann sum and Lemma A.1(iii),  $\lim_{T \rightarrow \infty} T^{-1} \sum_{t=1}^T M \mathbf{b}(t/T) \mathbf{b}(t/T)' = \int_0^1 M \mathbf{b}(v) \mathbf{b}(v)' dv = O(1)$ . Moreover,  $\|\mathbf{W}\|_F = O_p(1)$  since  $\text{vec}(\mathbf{W}) = \mathbf{b}'_c \left( M N_k^{-1} \hat{\mathbf{Q}}_{G_k^0, \tilde{z}\tilde{z}} \right)^{-1}$ , with  $\|M N_k^{-1} \hat{\mathbf{Q}}_{G_k^0, \tilde{z}\tilde{z}}\|_F = O_p(1)$  following Lemma A.2(ii) and  $\|\mathbf{b}_c\|_2 = O_p(1)$  following Lemma A.6(i). Plugging these intermediate results into (A.20), the rate of (A.19) (and likewise the rate of (A.20)) becomes apparent as  $\bar{c}_{\tilde{x}\tilde{x}} \text{vec}(\boldsymbol{\varpi})' \text{vec}(\boldsymbol{\varpi}) T^{-1} \sum_{t=1}^T M \mathbf{b}(t/T) \mathbf{b}(t/T)' = O_p(1)$ .

Turning to  $d_{12, G_k^0}$ ,

$$\begin{aligned}
|d_{12, G_k^0}| &= \left| \sqrt{\frac{N_k T}{M}} \mathbf{b}'_c \hat{\mathbf{Q}}_{G_k^0, \tilde{z}\tilde{z}}^{-1} \hat{\mathbf{q}}_{G_k^0, \tilde{z}\tilde{z}} \right| = \left| (N_k T)^{-1/2} M^{1/2} \frac{1}{T} \sum_{i \in G_k^0} \sum_{t=1}^T \mathbf{b}'_c (M N_k^{-1} \hat{\mathbf{Q}}_{G_k^0, \tilde{z}\tilde{z}})^{-1} \tilde{\mathbf{z}}_{it} \tilde{\eta}_{it} \right| \\
&\leq (N_k T)^{-1/2} M^{1/2} \frac{1}{T} \sum_{i \in G_k^0} \sum_{t=1}^T \left| \mathbf{b}'_c (M N_k^{-1} \hat{\mathbf{Q}}_{G_k^0, \tilde{z}\tilde{z}})^{-1} \tilde{\mathbf{z}}_{it} \right| |\tilde{\eta}_{it}| \\
&\leq (N_k T)^{1/2} \left[ \frac{M}{N_k T} \sum_{i \in G_k^0} \sum_{t=1}^T \left| \mathbf{b}'_c (M N_k^{-1} \hat{\mathbf{Q}}_{G_k^0, \tilde{z}\tilde{z}})^{-1} \tilde{\mathbf{z}}_{it} \right|^2 \right]^{1/2} \left[ \frac{1}{N_k T} \sum_{i \in G_k^0} \sum_{t=1}^T |\tilde{\eta}_{it}|^2 \right]^{1/2},
\end{aligned} \tag{A.21}$$

where the first inequality holds by the triangle property and the second because of the Cauchy-Schwarz inequality. (A.19)-(A.20) provide the rate of the first term in squared brackets and (A.18) gives the rate of the second term in squared brackets of (A.21). Consequently, it is apparent that  $|d_{12, G_k^0}| = (N_k T)^{1/2} O_p(1) O_p(M^{-\theta})$  and  $O_p((N_k T)^{1/2} M^{-\theta}) = o_p(1)$  under Assumption 4(ii). Moreover, as  $|s_{c, G_k^0}| = O_p(1)$  by Lemma A.6(ii),  $|d_{12, G_k^0}|/s_{c, G_k^0} = o_p(1)$  and  $d_{12, G_k^0}$  is negligible in the limit.

As a result, it suffices to study the behavior of  $d_{11, G_k^0}$  in (A.17) to derive the limiting distribution of the

post-Lasso estimator. To this end,

$$\begin{aligned}
d_{11,G_k^0} &= \sqrt{\frac{N_k T}{M}} \mathbf{b}'_c \hat{\mathbf{Q}}_{G_k^0, \tilde{z}\tilde{z}}^{-1} \hat{\mathbf{q}}_{G_k^0, \tilde{z}\tilde{z}} = \mathbf{b}'_c \left( \frac{M}{N_k} \hat{\mathbf{Q}}_{G_k^0, \tilde{z}\tilde{z}} \right)^{-1} \sqrt{\frac{M}{N_k T}} \sum_{i \in G_k^0} \sum_{t=1}^T \tilde{\mathbf{z}}_{it} \tilde{\epsilon}_{it} \\
&= \left[ \mathbf{b}'_c \left( \frac{M}{N_k} \hat{\mathbf{Q}}_{G_k^0, \tilde{z}\tilde{z}} \right)^{-1} \frac{M}{N_k T} \sum_{i \in G_k^0} \left( \tilde{\mathbf{Z}}'_i E(\epsilon_i \epsilon'_i) \tilde{\mathbf{Z}}_i \right) \left( \frac{M}{N_k} \hat{\mathbf{Q}}_{G_k^0, \tilde{z}\tilde{z}} \right)^{-1} \mathbf{b}_c \right]^{1/2} \zeta_i \\
&= \sum_{i \in G_k^0} a_i \zeta_i,
\end{aligned}$$

where  $\epsilon_i = (\epsilon_{i1}, \dots, \epsilon_{iT})'$ ,  $\tilde{\mathbf{Z}}_i = (\tilde{z}_{i1}, \dots, \tilde{z}_{iT})'$ , and  $a_i = \left[ \mathbf{b}'_c \left( \frac{M}{N_k} \hat{\mathbf{Q}}_{G_k^0, \tilde{z}\tilde{z}} \right)^{-1} \frac{M}{N_k T} \left( \tilde{\mathbf{Z}}'_i E(\epsilon_i \epsilon'_i) \tilde{\mathbf{Z}}_i \right) \left( \frac{M}{N_k} \hat{\mathbf{Q}}_{G_k^0, \tilde{z}\tilde{z}} \right)^{-1} \mathbf{b}_c \right]^{1/2}$ .  $\zeta_i$  is an independent random variable with variance one and mean  $\mathbf{c}' \mathbf{q}_{G_k^0} = \mathbf{c}' \sqrt{M/(N_k T)} \sum_{i \in G_k^0} \sum_{t=1}^T E(\tilde{\mathbf{z}}_{it} \tilde{\epsilon}_{it})$ , conditional on  $\{\mathbf{z}_i\}_{i=1}^N$ .

Subsequently, we prove

$$\frac{d_{11,G_k^0}}{\sqrt{\sum_{i \in G_k^0} a_i^2}} - \frac{\mathbf{c}' \mathbf{q}_{G_k^0}}{\sqrt{M/(N_k T) \mathbf{c}' \sum_{i \in G_k^0} \left( \tilde{\mathbf{Z}}'_i E(\epsilon_i \epsilon'_i) \tilde{\mathbf{Z}}_i \right) \mathbf{c}}} \xrightarrow{D} N(0, 1),$$

by verifying the Lindeberg condition

$$\frac{\max_{i \in G_k^0} a_i^2}{\sum_{i \in G_k^0} a_i^2} = o_p(1).$$

Considering  $\max_{i \in G_k^0} a_i^2$  first,

$$\begin{aligned}
\max_{i \in G_k^0} a_i^2 &= \max_{i \in G_k^0} \left[ \mathbf{b}'_c \left( \frac{M}{N_k} \hat{\mathbf{Q}}_{G_k^0, \tilde{z}\tilde{z}} \right)^{-1} \frac{M}{N_k T} \left( \tilde{\mathbf{Z}}'_i E(\epsilon_i \epsilon'_i) \tilde{\mathbf{Z}}_i \right) \left( \frac{M}{N_k} \hat{\mathbf{Q}}_{G_k^0, \tilde{z}\tilde{z}} \right)^{-1} \mathbf{b}_c \right] \\
&\leq \max_{i \in G_k^0} \left[ \frac{M}{N_k T} \mu_{\max} \left( \tilde{\mathbf{Z}}'_i E(\epsilon_i \epsilon'_i) \tilde{\mathbf{Z}}_i \right) \mathbf{b}'_c \left( \frac{M}{N_k} \hat{\mathbf{Q}}_{G_k^0, \tilde{z}\tilde{z}} \right)^{-1} \left( \frac{M}{N_k} \hat{\mathbf{Q}}_{G_k^0, \tilde{z}\tilde{z}} \right)^{-1} \mathbf{b}_c \right] \\
&\leq \frac{1}{N_k} \max_{i \in G_k^0} [\mu_{\max}(E(\epsilon_i \epsilon'_i))] \max_{i \in G_k^0} \left[ \mu_{\max} \left( \frac{M}{T} \tilde{\mathbf{Z}}'_i \tilde{\mathbf{Z}}_i \right) \right] \left[ \mu_{\min} \left( \frac{M}{N_k} \hat{\mathbf{Q}}_{G_k^0, \tilde{z}\tilde{z}} \right) \right]^{-2} \|\mathbf{b}_c\|_2^2 \\
&= \frac{1}{N_k} \bar{c}_{\epsilon\epsilon} O_p(1) O_p(1) O_p(1) = o_p(1)
\end{aligned}$$

by Assumptions 1(iv) and 4(i). Note that the inequalities hold by the property of a p.s.d. symmetric matrix  $A$  and a conformable vector  $a$ ,  $a' A a \leq \mu_{\max}(A) a' a$ . Furthermore,  $\mu_{\max}(E(\epsilon_i \epsilon'_i))$  is bounded from above by Assumption 4(i), while  $\mu_{\max}(M T^{-1} \tilde{\mathbf{Z}}'_i \tilde{\mathbf{Z}}_i) = \mu_{\max}(M T^{-1} \sum_{t=1}^T \tilde{z}_{it} \tilde{z}'_{it})$  and  $\mu_{\min}(M N_k^{-1} \hat{\mathbf{Q}}_{G_k^0, \tilde{z}\tilde{z}})$  are bounded by Lemma A.2. In addition,  $\|\mathbf{b}_c\|_2 = 1$  following Lemma A.6.

In conclusion, it is straightforward to see that the whole term in (A.15) converges in distribution

$$\frac{\sqrt{N_k T/M} \mathbf{c}' [\hat{\alpha}_{G_k^0}^p(v) - \alpha_k^0(v)]}{\sqrt{\sum_{i \in G_k^0} a_i^2}} - \frac{\mathbf{c}' \mathbf{q}_{G_k^0}}{\sqrt{M/(N_k T) \mathbf{c}' \sum_{i \in G_k^0} \left( \tilde{\mathbf{Z}}'_i E(\epsilon_i \epsilon'_i) \tilde{\mathbf{Z}}_i \right) \mathbf{c}}} \xrightarrow{D} N(0, 1),$$

for all  $k = 1, \dots, K_0$ . By defining  $\sum_{i \in G_k^0} a_i^2 = \mathbf{c}' \hat{\mathbf{\Omega}}_{G_k^0} \mathbf{c}$  and making use of the Cramér-World Theorem, this

generalizes to

$$\sqrt{\frac{N_k T}{M}} \hat{\Omega}_{G_k^0}^{-1/2} \left[ \hat{\alpha}_{\hat{G}_k}^p(v) - \alpha_k^0(v) \right] - \hat{\mathcal{E}}_{G_k^0}^{-1/2} \mathbf{q}_{G_k^0} \xrightarrow{D} N(0, \mathbf{I}_p), \text{ for } k = 1, \dots, K_0,$$

where  $\hat{\Omega}_{G_k^0}^{-1/2}$  is the symmetric square root of the inverse of  $\hat{\Omega}_{G_k^0} = \hat{\nu}'_{G_k^0} \hat{\mathcal{E}}_{G_k^0} \hat{\nu}_{G_k^0}$ , with

$$\hat{\mathcal{E}}_{G_k^0} = \frac{M}{N_k T} \sum_{i \in G_k^0} \tilde{\mathbf{Z}}_i' E(\epsilon_i \epsilon_i') \tilde{\mathbf{Z}}_i \text{ and } \hat{\nu}_{G_k^0} = \left( \frac{M}{N_k} \hat{\mathcal{Q}}_{G_k^0, \tilde{z}\tilde{z}} \right)^{-1} (\mathbf{I}_p \otimes \mathbf{b}(v)). \blacksquare$$

### A.2.6 Theorem 3.6

Given that Assumptions 1-6 are satisfied, Theorem 3.6 shows that asymptotically neither an over- nor an under-fitted models is selected:  $\Pr \left( \inf_{\lambda \in \Lambda_{-,NT} \cup \Lambda_{+,NT}} IC(\lambda) > \sup_{\lambda \in \Lambda_{0,NT}} IC(\lambda) \right) \rightarrow 1$  as  $(N, T) \rightarrow \infty$ .

*Proof:*

First, recall that  $IC(\lambda) = \ln(\sigma_{\hat{G}_{\hat{K}_\lambda}}^2) + \rho_{NT} p M \hat{K}_\lambda$ , where  $\rho_{NT}$  is a tuning parameter and  $\sigma_{\hat{G}_{\hat{K}_\lambda}}^2$  reflects the MSE  $\sigma_{\hat{G}_{\hat{K}_\lambda}}^2 = (NT)^{-1} \sum_{k=1}^{\hat{K}_\lambda} \sum_{i \in \hat{G}_{k,\lambda}} \sum_{t=1}^T \left( \tilde{y}_{it} - \hat{\alpha}_{\hat{G}_{k,\lambda}}^p(t/T) \tilde{\mathbf{x}}_{it} \right)^2$ .

Let  $\Lambda = [0, \lambda_{\max}]$  be an interval in  $\mathbb{R}^+$ . Define three subsets  $\Lambda_0$ ,  $\Lambda_-$  and  $\Lambda_+$ , such that

$$\Lambda_0 = \{\lambda \in \Lambda : \hat{K}_\lambda = K_0\}, \Lambda_- = \{\lambda \in \Lambda : \hat{K}_\lambda < K_0\}, \Lambda_+ = \{\lambda \in \Lambda : \hat{K}_\lambda > K_0\}.$$

Moreover, all  $\lambda \in \Lambda_0$  comply with the regularity conditions in Assumption 2, which allows the use of the oracle property by Corollary 3.3. In addition, since the *post-Lasso* estimator converges to the true estimator by Theorem 3.5,  $\sigma_{\hat{G}_{\hat{K}_\lambda}}^2 = \sigma_{\hat{G}_0}^2$  w.p.a.1. Therefore, let  $\inf_{\lambda \in \Lambda_{0,NT}} IC(\lambda) = IC(\lambda_0)$  and

$$IC(\lambda_0) = \ln(\sigma_{\hat{G}_0}^2) + \rho_{NT} p M \hat{K}_\lambda \xrightarrow{P} \ln(\sigma_0^2),$$

where  $\sigma_0^2$  is the irreducible MSE  $\sigma_0^2 = \text{plim}_{(N,T) \rightarrow \infty} (NT)^{-1} \sum_{i=1}^N \sum_{t=1}^T \tilde{\epsilon}_{it}$  and Assumption 6(i) gives  $\rho_{NT} p M K_0 \rightarrow 0$  as  $(N, T) \rightarrow \infty$ .

The proof of Theorem 3.6 works by showing that  $IC(\lambda)$  converges in probability to some value strictly larger than  $IC(\lambda_0)$ ,  $\forall \lambda \in \Lambda_- \cup \Lambda_+$ .

**Case 1: Underfitting**  $\lambda \in \Lambda_-$  such that  $\hat{K}_\lambda < K_0$ .

Let  $\mathbb{G}$  denote the set of all possible partitions over  $N$ . Note that

$$\begin{aligned}\sigma_{\hat{\mathcal{G}}_{\hat{K},\lambda}}^2 &= (NT)^{-1} \sum_{k=1}^{\hat{K}_\lambda} \sum_{i \in \hat{G}_{k,\lambda}} \sum_{t=1}^T \left( \tilde{y}_{it} - \hat{\xi}_{\hat{G}_{k,\lambda}}^{p'} \tilde{z}_{it} \right)^2 \\ &\geq \min_{1 \leq K < K_0} \inf_{\mathcal{G}_K \in \mathbb{G}} \sum_{k=1}^K \sum_{i \in G_k} \sum_{t=1}^T \left( \tilde{y}_{it} - \hat{\xi}_{G_k}^{p'} \tilde{z}_{it} \right)^2 \\ &= \min_{1 \leq K < K_0} \inf_{\mathcal{G}_K \in \mathbb{G}} \hat{\sigma}_{\mathcal{G}(K)}^2.\end{aligned}$$

Assumption A.5 states,  $\lim_{(N,T) \rightarrow \infty} \min_{1 \leq K < K_0} \inf_{\mathcal{G}_K \in \mathbb{G}} \hat{\sigma}_{\mathcal{G}_K}^2 \xrightarrow{p} \underline{\sigma}^2 > \sigma_0^2$ . Therefore, applying Slutsky,

$$\inf_{\lambda \in \Lambda_-} IC(\lambda) \geq \min_{1 \leq K < K_0} \inf_{\mathcal{G}_K \in \mathbb{G}} \ln(\sigma_{\mathcal{G}_K}^2) + \rho_{NT} p M K \xrightarrow{p} \ln(\underline{\sigma}^2) > \ln(\sigma_0^2)$$

and in consequence  $\Pr(\inf_{\lambda \in \Lambda_-} IC(\lambda) \geq IC(\lambda_0)) \rightarrow 1$ .

**Case 2: Overfitting**  $\lambda \in \Lambda_+$  such that  $\hat{K}_\lambda > K_0$ .

Define the set  $\bar{\mathbb{G}}_K = \{\bar{\mathcal{G}}_K = \{\bar{G}_k\}_{k=1}^K : \nexists i, j \in \bar{G}_k \text{ where } i \in G_l^0, j \notin G_l^0, 1 \leq l \leq K_0\}$  with  $K > K_0$ . That is, each  $\bar{\mathcal{G}}_K \in \bar{\mathbb{G}}_K$  denotes a partition of  $K > K_0$  over  $N$  where no heterogeneous cross-sectional units are pooled together in any group. Recognize that such an over-fitted model yields a weakly lower *MSE*  $\hat{\sigma}_{\bar{\mathcal{G}}_K}^2 \leq \hat{\sigma}_{\mathcal{G}^0}^2$ .

Let

$$\begin{aligned}&\Pr\left(\inf_{\lambda \in \Lambda_+} IC(\lambda) > IC(\lambda_0)\right) \\ &\geq \Pr\left(\min_{K_0 < K \leq N} \inf_{\bar{\mathcal{G}}_K \in \bar{\mathbb{G}}_K} \left(\ln(\hat{\sigma}_{\bar{\mathcal{G}}_K}^2) + \rho_{NT} p M K\right) > \ln(\sigma_{\mathcal{G}^0}^2) + \rho_{NT} p M K_0\right) \\ &\geq \Pr\left(\min_{K_0 < K \leq N} \inf_{\bar{\mathcal{G}}_K \in \bar{\mathbb{G}}_K} \left(\ln(\hat{\sigma}_{\bar{\mathcal{G}}_K}^2) + \rho_{NT} p M K\right) > \ln(\sigma_{\mathcal{G}^0}^2) + \rho_{NT} p M K_0\right) \\ &= \Pr\left(\min_{K_0 < K \leq N} \inf_{\bar{\mathcal{G}}_K \in \bar{\mathbb{G}}_K} \left[\ln(\hat{\sigma}_{\bar{\mathcal{G}}_K}^2 / \sigma_{\mathcal{G}^0}^2) + \rho_{NT} p M (K - K_0)\right] > 0\right) \\ &= \Pr\left(\min_{K_0 < K \leq N} \inf_{\bar{\mathcal{G}}_K \in \bar{\mathbb{G}}_K} \left[(\hat{\sigma}_{\bar{\mathcal{G}}_K}^2 - \sigma_{\mathcal{G}^0}^2) / \sigma_{\mathcal{G}^0}^2 + o_p(1) + \rho_{NT} p M (K - K_0)\right] > 0\right).\end{aligned}$$

Employing Lemma A.7,  $TM^{-1}(\hat{\sigma}_{\bar{\mathcal{G}}_K}^2 - \sigma_{\mathcal{G}^0}^2) = O_p(1)$  and  $\sigma_{\mathcal{G}^0}^2 \rightarrow \sigma_0^2$  as shown above. Therefore, after expanding by  $TM^{-1}$  and using the fact that  $T\rho_{NT} \rightarrow \infty$  by Assumption 6(ii),

$$\Pr\left(\min_{K_0 < K \leq N} \inf_{\bar{\mathcal{G}}_K \in \bar{\mathbb{G}}_K} [O_p(1) + o_p(1) + T\rho_{NT} p (K - K_0)] > 0\right) \rightarrow 1,$$

as  $(N, T) \rightarrow \infty$ . ■

### A.3 Proof of Technical Lemmas

#### A.3.1 Lemma A.1

**Lemma A.1(i)**  $b_m(v) > 0$ ,  $m = -d, \dots, M^*$ , is a basis function of degree  $d$  (order  $d + 1$ ) and defined on the interval  $[v_m, v_{m+d+1})$  (De Boor, 2001, ch. 9, eq. 21). Moreover, by property of B-splines, all spline basis functions sum up to one for each  $v$ :  $\sum_{m=-d}^{M^*} b_m(v) = 1$  (De Boor, 2001, ch. 9, eq. 37). From here it follows that  $\|\mathbf{b}(v)\|_2 = \left[ \sum_{j=-d}^{M^*} b_m(v)^2 \right]^{1/2} \leq \left[ \sum_{j=-d}^{M^*} b_m(v) \right]^{1/2} = 1$ .

**Lemma A.1(ii)** As stated above,  $b_m(v)$  is uniformly bounded on the unit interval and  $\sum_{m=-d}^{M^*} b_m(v) = 1$ . As a consequence,  $\int_0^1 b_m(v) dv = O(M^{-1})$  and

$$\int_0^1 \|\mathbf{b}(v)\|_2 dv = \int_0^1 \left[ \sum_{m=-d}^{M^*} b_m(v)^2 \right]^{1/2} dv \leq \int_0^1 \left[ \sum_{m=-d}^{M^*} b_m(v) \right]^{1/2} dv = 1.$$

**Lemma A.1(iii)** As shown in De Boor (2001, ch. 11, eq. 8), there exist two constants  $0 < \underline{c}_b \leq \bar{c}_b < \infty$  such that  $\underline{c}_b \|\mathbf{c}\|_2^2 \leq M \int (\mathbf{c}'\mathbf{b}(v))^2 dv \leq \bar{c}_b \|\mathbf{c}\|_2^2$  for all nonrandom  $\mathbf{c} \in \mathbb{R}^M$ . Using the Cramér–World device,  $M \int_0^1 \mathbf{b}(v)\mathbf{b}(v)' dv = O(1)$  and the minimum and maximum eigenvalues are bounded  $\underline{c}_b \leq \mu_{\min} \left( M \int_0^1 \mathbf{b}(v)\mathbf{b}(v)' dv \right) \leq \mu_{\max} \left( M \int_0^1 \mathbf{b}(v)\mathbf{b}(v)' dv \right) \leq \bar{c}_b$ .

**Lemma A.1(iv)** The proof is analogous to De Boor (2001, ch. 12, Theorem 6).

#### A.3.2 Lemma A.2

Consistent with Su et al. (2019, Lemma A.3), the proof exploits the inherent property that B-splines are bounded.

**Lemma A.2(i)** Recall that  $\hat{\mathbf{Q}}_{i,\tilde{z}\tilde{z}} = T^{-1} \sum_{t=1}^T \tilde{z}_{it} \tilde{z}'_{it}$  and  $\hat{\mathbf{Q}}_{i,\tilde{z}\tilde{z}} = \sum_{i \in G_k^0} T^{-1} \sum_{t=1}^T \tilde{z}_{it} \tilde{z}'_{it}$ . Define the  $M \times p$  matrix  $\mathbf{W} = (\boldsymbol{\varpi}_1, \dots, \boldsymbol{\varpi}_p)$  with  $\boldsymbol{\varpi} = \text{vec}(\mathbf{W})$ ,  $\boldsymbol{\varpi}_l = (\varpi_{l,1}, \dots, \varpi_{l,M})'$ , and  $\|\boldsymbol{\varpi}\|_2 \leq c_\varpi < \infty$  for some positive constant  $c_\varpi$ . Let  $\mathbb{B}_{\mathbb{V},M}$  denote a linear space as defined in Subsection 2.2. The vector  $\mathbf{g}_\varpi(v) = \mathbf{W}'\mathbf{b}(v)$  collects spline basis functions  $\mathbf{g}_\varpi(v) = (g_1(v, \boldsymbol{\varpi}_1), \dots, g_p(v, \boldsymbol{\varpi}_p))'$ , where  $g_l(v, \boldsymbol{\varpi}_l) = \boldsymbol{\varpi}'_l \mathbf{b}(v) \in \mathbb{B}_{\mathbb{V},M}$  for  $l = 1, \dots, p$  and  $\mathbf{g}_\varpi(v) \in \mathbb{B}_{\mathbb{V},M}^{\otimes p}$ . Recognize that  $\hat{\mathbf{Q}}_{i,\tilde{z}\tilde{z}} = T^{-1} \sum_{t=1}^T \mathbf{z}_{it} \mathbf{z}'_{it} - T^{-1} \sum_{t=1}^T \mathbf{z}_{it} T^{-1} \sum_{t=1}^T \mathbf{z}'_{it} = \mathbf{A}_{1i} - \mathbf{A}_{2i}$ .

**Case 1:  $\mathbf{x}_{it}$  does not contain an intercept.**

Consider  $\boldsymbol{\varpi}' \mathbf{A}_{1i} \boldsymbol{\varpi}$ ,

$$\begin{aligned} \boldsymbol{\varpi}' \frac{1}{T} \sum_{t=1}^T \mathbf{z}_{it} \mathbf{z}'_{it} \boldsymbol{\varpi} &= \boldsymbol{\varpi}' \frac{1}{T} \sum_{t=1}^T \left[ \mathbf{x}_{it} \otimes \mathbf{b} \left( \frac{t}{T} \right) \right] \left[ \mathbf{x}_{it} \otimes \mathbf{b} \left( \frac{t}{T} \right) \right]' \boldsymbol{\varpi} \\ &= \frac{1}{T} \sum_{t=1}^T \left[ \mathbf{b} \left( \frac{t}{T} \right)' \mathbf{W} \mathbf{x}_{it} \right]^2 = \frac{1}{T} \sum_{t=1}^T \left[ \mathbf{g}_\varpi \left( \frac{t}{T} \right)' \mathbf{x}_{it} \right]^2 = \frac{1}{T} \sum_{t=1}^T \mathbf{g}_\varpi \left( \frac{t}{T} \right)' \mathbf{x}_{it} \mathbf{x}'_{it} \mathbf{g}_\varpi \left( \frac{t}{T} \right), \end{aligned} \tag{A.22}$$



since  $(\mathbf{x}_{it} \otimes \mathbf{b}(v))\text{vec}(\mathbf{W})' = \text{vec}(\mathbf{b}'(v)\mathbf{W}\mathbf{x}_{it})$  by property of the Kronecker product (see [Bernstein, 2009](#), p. 249).

Note that the maximum eigenvalue of  $E(\mathbf{x}_{it}\mathbf{x}'_{it})$  is bounded away from infinity by Assumption 1(iv). Furthermore, as shown in Lemma [Huang et al. \(2004, A.2\)](#),

$$\frac{1}{T} \sum_{t=1}^T \mathbf{g}_\varpi \left( \frac{t}{T} \right)' \mathbf{x}_{it}\mathbf{x}'_{it}\mathbf{g}_\varpi \left( \frac{t}{T} \right) = \frac{1}{T} \sum_{t=1}^T \mathbf{g}_\varpi \left( \frac{t}{T} \right)' E(\mathbf{x}_{it}\mathbf{x}'_{it})\mathbf{g}_\varpi \left( \frac{t}{T} \right) (1 + o_p(1)) \quad (\text{A.23})$$

for strong mixing processes and

$$\frac{1}{T} \sum_{t=1}^T \mathbf{g}_\varpi \left( \frac{t}{T} \right)' E(\mathbf{x}_{it}\mathbf{x}'_{it})\mathbf{g}_\varpi \left( \frac{t}{T} \right) (1 + o_p(1)) \leq \bar{c}_{xx} \frac{1}{T} \sum_{t=1}^T \mathbf{g}_\varpi \left( \frac{t}{T} \right)' \mathbf{g}_\varpi \left( \frac{t}{T} \right) (1 + o_p(1)), \quad (\text{A.24})$$

where  $T^{-1} \sum_{t=1}^T \mathbf{g}_\varpi(t/T)' \mathbf{g}_\varpi(t/T) = \int_0^1 \mathbf{g}_\varpi(v)' \mathbf{g}_\varpi(v) dv [1 + O(T^{-1})]$  by property of the Riemann sum and  $\int_0^1 \mathbf{g}_\varpi(v)' \mathbf{g}_\varpi(v) dv = \sum_{l=1}^p \varpi_l \int_0^1 \mathbf{b}(v)\mathbf{b}(v)' dv \varpi_l = O_p(M^{-1})$  by Lemma [A.1\(iii\)](#), since  $\|\varpi\|_2^2 < \infty$ . As a consequence, after plugging into [\(A.22\)](#) it is apparent that the whole term in [\(A.22\)](#)  $\varpi' \mathbf{A}_{1i} \varpi \leq O(M^{-1}) [1 + O(T^{-1})] (1 + o(1)) = O(M^{-1})$ . Since  $\mu_{\max}(\mathbf{B} - \mathbf{C}) \leq \mu_{\max}(\mathbf{B}) + \mu_{\max}(-\mathbf{C}) = \mu_{\max}(\mathbf{B}) - \mu_{\min}(\mathbf{C}) \leq \mu_{\max}(\mathbf{B})$  for two generic real matrices  $\mathbf{B}, \mathbf{C}$ ,  $\mu_{\max}(\hat{\mathbf{Q}}_{i,\bar{z}\bar{z}}) \leq \mu_{\max}(\mathbf{A}_{1i})$  and  $\mu_{\max}(M\hat{\mathbf{Q}}_{i,\bar{z}\bar{z}})$  is bounded away from infinity in probability, uniformly in  $\varpi$ . This result also applies uniformly across the cross-section to  $\max_i \mu_{\max}(M\hat{\mathbf{Q}}_{i,\bar{z}\bar{z}})$  with probability  $1 - o(N^{-1})$ .

To study the behavior of the minimum eigenvalue of  $\hat{\mathbf{Q}}_{i,\bar{z}\bar{z}}$ , one must also consider  $\mathbf{A}_{2i}$ . For this purpose, take

$$\begin{aligned} \varpi' \mathbf{A}_{2i} \varpi &= \varpi' \frac{1}{T} \sum_{t=1}^T \mathbf{z}_{it} \frac{1}{T} \sum_{t=1}^T \mathbf{z}'_{it} \varpi \\ &= \varpi' \frac{1}{T} \sum_{t=1}^T \left[ \mathbf{x}_{it} \otimes \mathbf{b} \left( \frac{t}{T} \right) \right] \frac{1}{T} \sum_{t=1}^T \left[ \mathbf{x}_{it} \otimes \mathbf{b} \left( \frac{t}{T} \right) \right]' \varpi \\ &= \left[ \frac{1}{T} \sum_{t=1}^T \mathbf{b} \left( \frac{t}{T} \right)' \varpi \mathbf{x}_{it} \right]^2 = \left[ \frac{1}{T} \sum_{t=1}^T \mathbf{g}_\varpi \left( \frac{t}{T} \right)' \mathbf{x}_{it} \right]^2 \\ &= E \left[ \frac{1}{T} \sum_{t=1}^T \mathbf{g}_\varpi \left( \frac{t}{T} \right)' \mathbf{x}_{it} \right]^2 (1 + o_p(1)), \end{aligned} \quad (\text{A.25})$$

where the last equality holds again by Lemma [Huang et al. \(2004, A.2\)](#). Using [\(A.25\)](#) and the result in [\(A.23\)](#),

$$\begin{aligned} \varpi' (\mathbf{A}_{1i} - \mathbf{A}_{2i}) \varpi &= \varpi' \left( \hat{\mathbf{Q}}_{i,\bar{z}\bar{z}} - T^{-1} \sum_{t=1}^T \mathbf{z}_{it} T^{-1} \sum_{t=1}^T \mathbf{z}'_{it} \right) \varpi \\ &= \frac{1}{T} \sum_{t=1}^T E \left[ \left( \mathbf{g}_\varpi \left( \frac{t}{T} \right)' \mathbf{x}_{it} \right)^2 \right] - E \left[ \frac{1}{T} \sum_{t=1}^T \mathbf{g}_\varpi \left( \frac{t}{T} \right)' \mathbf{x}_{it} \right]^2 + o(N^{-1}), \end{aligned} \quad (\text{A.26})$$

uniformly in  $\varpi$  and  $i$ .

In order to show that the minimum eigenvalue of  $M\hat{\mathbf{Q}}_{i,\bar{z}\bar{z}}$  is bounded away from 0, define

$$\boldsymbol{\mu}_i(v) = \begin{cases} \mathbf{0}_{p \times 1} & \text{if } v = 0 \\ E(\mathbf{x}_{it}) & \text{if } v \in (\frac{t-1}{T}, \frac{t}{T}] \end{cases} \quad \text{and } \boldsymbol{\Sigma}_i(v) = \begin{cases} \mathbf{0}_{p \times p} & \text{if } v = 0 \\ E(\mathbf{x}_{it}\mathbf{x}'_{it}) & \text{if } v \in (\frac{t-1}{T}, \frac{t}{T}], \end{cases}$$

for  $v \in [0, 1]$ . Note that  $\bar{\boldsymbol{\Sigma}}_i(t/T) = \boldsymbol{\Sigma}_i(t/T) - \boldsymbol{\mu}_i(t/T)\boldsymbol{\mu}_i(t/T)' = \text{Var}(\mathbf{x}_{it})$ . Rewrite  $T^{-1} \sum_{t=1}^T E \left[ (\mathbf{g}_{\varpi}(t/T)' \mathbf{x}_{it})^2 \right] - E \left[ T^{-1} \sum_{t=1}^T \mathbf{g}_{\varpi}(t/T)' \mathbf{x}_{it} \right]^2$  in (A.26) to

$$\begin{aligned} & \frac{1}{T} \sum_{t=1}^T \left[ \mathbf{g}_{\varpi} \left( \frac{t}{T} \right)' \boldsymbol{\Sigma}_i \left( \frac{t}{T} \right) \mathbf{g}_{\varpi} \left( \frac{t}{T} \right) \right] - \left[ \frac{1}{T} \sum_{t=1}^T \mathbf{g}_{\varpi} \left( \frac{t}{T} \right)' \boldsymbol{\mu}_i \left( \frac{t}{T} \right) \right]^2 \\ &= \int_0^1 \mathbf{g}_{\varpi}(v)' \boldsymbol{\Sigma}_i(v) \mathbf{g}_{\varpi}(v) dv [1 + O(T^{-1})] - \left[ \int_0^1 \mathbf{g}_{\varpi}(v)' \boldsymbol{\mu}_i(v) dv [1 + O(T^{-1})] \right]^2 \\ &\geq \int_0^1 \mathbf{g}_{\varpi}(v)' \boldsymbol{\Sigma}_i(v) \mathbf{g}_{\varpi}(v) dv [1 + O(T^{-1})] - \int_0^1 \mathbf{g}_{\varpi}(v)' \boldsymbol{\mu}_i(v) \boldsymbol{\mu}_i(v)' \mathbf{g}_{\varpi}(v) dv [1 + O(T^{-1})] \\ &= \left[ \int_0^1 \mathbf{g}_{\varpi}(v)' \boldsymbol{\Sigma}_i(v) \mathbf{g}_{\varpi}(v) dv - \int_0^1 \mathbf{g}_{\varpi}(v)' \boldsymbol{\mu}_i(v) \boldsymbol{\mu}_i(v)' \mathbf{g}_{\varpi}(v) dv \right] \\ &\quad - O(T^{-1}) \left[ \int_0^1 \mathbf{g}_{\varpi}(v)' \boldsymbol{\Sigma}_i(v) \mathbf{g}_{\varpi}(v) dv - \int_0^1 \mathbf{g}_{\varpi}(v)' \boldsymbol{\mu}_i(v) \boldsymbol{\mu}_i(v)' \mathbf{g}_{\varpi}(v) dv \right] \\ &= d_{1i} - d_{2i}, \end{aligned}$$

where the inequality holds because of Jensen's inequality. Studying  $d_{1i}$  first,

$$\begin{aligned} d_{1i} &= \int_0^1 \mathbf{g}_{\varpi}(v)' \boldsymbol{\Sigma}_i(v) \mathbf{g}_{\varpi}(v) dv - \int_0^1 \mathbf{g}_{\varpi}(v)' \boldsymbol{\mu}_i(v) \boldsymbol{\mu}_i(v)' \mathbf{g}_{\varpi}(v) dv \\ &= \int_0^1 \mathbf{g}_{\varpi}(v)' \bar{\boldsymbol{\Sigma}}_i(v) \mathbf{g}_{\varpi}(v) dv \geq \underline{c}_{zz} \sum_{l=1}^p \int_0^1 g_l(v, \varpi_l)' g_l(v, \varpi_l) dv \\ &= \underline{c}_{zz} \sum_{l=1}^p \varpi'_{il} \int_0^1 \mathbf{b}(v) \mathbf{b}(v)' dv \varpi_{il} = \|\boldsymbol{\varpi}\|_2^2 O(M^{-1}) = O(M^{-1}), \end{aligned}$$

where  $\underline{c}_{zz} \leq \text{Var}(\mathbf{x}_{it}) = \bar{\boldsymbol{\Sigma}}_i(t/T)$  by Assumption 1(iv).

Since  $D_{2i} = O(T^{-1})D_{1i} = O((MT)^{-1})$ , the minimum eigenvalue  $\min_i \mu_{\min}(M\hat{\mathbf{Q}}_{i,\bar{z}\bar{z}})$  is bounded away from 0 uniformly in  $\mathbf{W}$  and  $i$  with probability  $1 - o(N^{-1})$ .

**Case 2:**  $\mathbf{x}_{it} = \mathbf{1}$ . Then (A.22) collapses to

$$\boldsymbol{\varpi}' \frac{1}{T} \sum_{t=1}^T z_{it} z'_{it} \boldsymbol{\varpi} = \boldsymbol{\varpi}' \frac{1}{T} \sum_{t=1}^T \mathbf{b} \left( \frac{t}{T} \right) \mathbf{b} \left( \frac{t}{T} \right)' \boldsymbol{\varpi} \quad (\text{A.27})$$

and (A.26) becomes

$$\begin{aligned} & \boldsymbol{\varpi}' \left( \hat{\mathbf{Q}}_{i,zz} - \frac{1}{T} \sum_{t=1}^T \mathbf{z}_{it} \frac{1}{T} \sum_{t=1}^T \mathbf{z}'_{it} \right) \boldsymbol{\varpi} \\ &= \boldsymbol{\varpi}' \left( \frac{1}{T} \sum_{t=1}^T \mathbf{b} \left( \frac{t}{T} \right) \mathbf{b} \left( \frac{t}{T} \right)' - \frac{1}{T} \sum_{t=1}^T \mathbf{b} \left( \frac{t}{T} \right) \frac{1}{T} \sum_{t=1}^T \mathbf{b} \left( \frac{t}{T} \right)' \right) \boldsymbol{\varpi}. \end{aligned} \quad (\text{A.28})$$

It suffices to apply the basic properties of B-splines in order to study the minimum and maximum eigenvalues of  $\hat{\mathbf{Q}}_{i,zz}$ . To this end, Lemma A.1(iii) shows that  $M \int_0^1 \mathbf{b}(t/T) \mathbf{b}(t/T)' dv$  has bounded minimum and maximum eigenvalues, where  $T^{-1} \sum_{t=1}^T \mathbf{b}(t/T) \mathbf{b}(t/T)' = \int_0^1 \mathbf{b}(t/T) \mathbf{b}(t/T)' dv [1 + O(T^{-1})]$  by the Riemann sum and  $\|\mathbf{W}\|_F < \infty$  in (A.27). Furthermore,  $T^{-1} \sum_{t=1}^T \mathbf{b}(t/T) \mathbf{b}(t/T)' - T^{-1} \sum_{t=1}^T \mathbf{b}(t/T) T^{-1} \sum_{t=1}^T \mathbf{b}(t/T)'$  in (A.28) can be considered as a vector product of standardized spline basis functions. Subsequently, the properties of B-splines, including the ones stated in Theorem 1(iii) carry over. As a consequence, the results obtained under Case 1 hold by Theorem 1(iii).

**Case 3:  $\mathbf{x}_{it}$  contains an intercept and stochastic regressors.** Reorder  $\mathbf{x}_{it}$  so that  $\mathbf{x}_{it} = (1, \mathbf{x}_{it}^{(2)})'$  and  $\mathbf{x}_{it}^{(2)}$  is a  $(p-1) \times 1$  vector of random variables. This instance presents a mix of the two previously considered cases, where Case 1 applies to  $\mathbf{x}_{it}^{(2)}$  and Case 2 concerns the intercept in  $\mathbf{x}_{it}$ . Therefore, the results with respect to the minimum and maximum eigenvalues of  $\hat{\mathbf{Q}}_{i,zz}$  also hold for  $\mathbf{x}_{it} = (1, \mathbf{x}_{it}^{(2)})'$ . I refer to Su et al. (2019, Lemma A.3(i)) for more details. ■

**Lemma A.2(ii)** Consider  $\hat{\mathbf{Q}}_{i,zz} = \sum_{i \in G_k^0} \hat{\mathbf{Q}}_{i,zz}$ . Since cross-sectional individuals are weakly dependent as given in Assumption 1(i), it holds that

$$\Pr \left( \underline{c}_{zz} \leq \mu_{\min} \left( \frac{M}{N_k} \hat{\mathbf{Q}}_{i,zz} \right) < \mu_{\max} \left( \frac{M}{N_k} \hat{\mathbf{Q}}_{i,zz} \right) \leq \bar{c}_{zz} \right) = 1 - o(N^{-1})$$

for  $i = 1, \dots, N$  and two constants  $0 < \underline{c}_{zz} \leq \bar{c}_{zz} < \infty$ , as shown in Lemma A.2(i). ■

### A.3.3 Lemma A.3

Recall  $\hat{\mathbf{q}}_{i,\tilde{z}\tilde{u}} = T^{-1} \sum_{t=1}^T \tilde{\mathbf{z}}_{it} \tilde{u}_{it}$ , where  $\tilde{u}_{it} = \tilde{\eta}_{it} + \tilde{\epsilon}_{it}$ . Following Su et al. (2019, Lemma A.4), the proof of Lemma A.3 is constructed by decomposing the error  $u_{it}$  into the idiosyncratic and the sieve elements and analyzing both separately.

**Lemma A.3(i)** Define the sieve-bias as  $a_{it} = \beta_i^0(t/T) - \mathbf{\Pi}_i^{0'} \mathbf{b}(t/T)$  and  $\eta_{it} = \mathbf{x}'_{it} a_{it}$ . Recognize the identity  $u_{it} = \epsilon_{it} + [\beta_i^{0'}(t/T) \mathbf{x}_{it} - \boldsymbol{\pi}_i^{0'} \mathbf{z}_{it}] = \epsilon_{it} + \mathbf{x}'_{it} [\beta_i^0(t/T) - \mathbf{\Pi}_i^{0'} \mathbf{b}(t/T)] = \epsilon_{it} + \eta_{it}$ . Likewise,  $\tilde{u}_{it} = \tilde{\eta}_{it} + \tilde{\epsilon}_{it}$ ,  $\hat{\mathbf{q}}_{i,\tilde{z}\tilde{u}} = \hat{\mathbf{q}}_{i,\tilde{z}\tilde{\eta}} + \hat{\mathbf{q}}_{i,\tilde{z}\tilde{\epsilon}}$ , and  $\|\hat{\mathbf{q}}_{i,\tilde{z}\tilde{u}}\|_2 \leq \|\hat{\mathbf{q}}_{i,\tilde{z}\tilde{\eta}}\|_2 + \|\hat{\mathbf{q}}_{i,\tilde{z}\tilde{\epsilon}}\|_2$  by the Triangle inequality, where  $\hat{\mathbf{q}}_{i,\tilde{z}a} = T^{-1} \sum_{t=1}^T \mathbf{z}_{it} a_{it}$  for  $a_{it} = \{\tilde{\eta}_{it}, \tilde{\epsilon}_{it}\}$ . First we derive the rate of  $\|\hat{\mathbf{q}}_{i,\tilde{z}\tilde{\eta}}\|_2$ , then the rate of  $\|\hat{\mathbf{q}}_{i,\tilde{z}\tilde{\epsilon}}\|_2$ .

By the triangle inequality and the sub-multiplicative property

$$\|\hat{\mathbf{q}}_{i,\bar{z}\bar{\eta}}\|_2 = \left\| T^{-1} \sum_{t=1}^T \mathbf{z}_{it} \eta_{it} - T^{-1} \sum_{t=1}^T \mathbf{z}_{it} T^{-1} \sum_{t=1}^T \eta_{it} \right\|_2 \leq \left\| T^{-1} \sum_{t=1}^T \mathbf{z}_{it} \eta_{it} \right\|_2 + \left\| T^{-1} \sum_{t=1}^T \mathbf{z}_{it} \right\|_2 \left| T^{-1} \sum_{t=1}^T \eta_{it} \right|. \quad (\text{A.29})$$

Studying all these elements in isolation, consider

$$\left| \frac{1}{T} \sum_{t=1}^T \eta_{it} \right|^2 = \left| \frac{1}{T} \sum_{t=1}^T \mathbf{x}'_{it} a_{it} \right|^2 \leq \left\| \frac{1}{T} \sum_{t=1}^T \mathbf{x}_{it} \mathbf{x}'_{it} \right\|_F \left\| \frac{1}{T} \sum_{t=1}^T a_{it} a'_{it} \right\|_F, \quad (\text{A.30})$$

where the inequality holds because of the Chauchy-Schwarz property. Assumption 1(iv) ensures that

$\left\| T^{-1} \sum_{t=1}^T \mathbf{x}_{it} \mathbf{x}'_{it} \right\|_2 \leq \bar{c}_{xx}$  in probability. Furthermore, Lemma A.1(iv) gives  $\sup_{v \in [0,1]} \|\boldsymbol{\beta}_i^0(t/T) - \boldsymbol{\Pi}_i^{0'} \mathbf{b}(t/T)\|_2 = O(M^{-\theta})$ . As a consequence,

$$\begin{aligned} \left\| \frac{1}{T} \sum_{t=1}^T a_{it} a'_{it} \right\|_F &= \left\| \left[ \boldsymbol{\beta}_i^0 \left( \frac{t}{T} \right) - \boldsymbol{\Pi}_i^{0'} \mathbf{b} \left( \frac{t}{T} \right) \right] \left[ \boldsymbol{\beta}_i^0 \left( \frac{t}{T} \right) - \boldsymbol{\Pi}_i^{0'} \mathbf{b} \left( \frac{t}{T} \right) \right]' \right\|_F \\ &\leq \left[ \sup_{v \in [0,1]} \|\boldsymbol{\beta}_i^0(v) - \boldsymbol{\Pi}_i^{0'} \mathbf{b}(v)\|_2 \right]^2 = O(M^{-2\theta}), \end{aligned} \quad (\text{A.31})$$

and  $\left| T^{-1} \sum_{t=1}^T \eta_{it} \right|^2 = \bar{c}_{xx} O_p(M^{-2\theta})$ , from which follows  $\left| T^{-1} \sum_{t=1}^T \eta_{it} \right| = O_p(M^{-\theta})$ .

Define the real  $M \times p$  matrix  $\mathbf{W}$  with  $\text{vec}(\mathbf{W}) = \boldsymbol{\varpi}$  and  $\|\boldsymbol{\varpi}\|_2 < \infty$ . Then

$$\begin{aligned} \boldsymbol{\varpi}' \left\| \frac{1}{T} \sum_{t=1}^T \mathbf{z}_{it} \right\|_2^2 \boldsymbol{\varpi} &= \left| \boldsymbol{\varpi}' \frac{1}{T} \sum_{t=1}^T \left[ \mathbf{x}_{it} \otimes \mathbf{b} \left( \frac{t}{T} \right) \right] \right|^2 \\ &= \left| \frac{1}{T} \sum_{t=1}^T \mathbf{b} \left( \frac{t}{T} \right)' \mathbf{W} \mathbf{x}_{it} \right|^2 \leq \left\| \frac{1}{T} \sum_{t=1}^T \mathbf{W}' \mathbf{b} \left( \frac{t}{T} \right) \mathbf{b} \left( \frac{t}{T} \right)' \mathbf{W} \right\|_F \left\| \frac{1}{T} \sum_{t=1}^T \mathbf{x}_{it} \mathbf{x}'_{it} \right\|_F, \end{aligned}$$

where by Assumption 1(iv)  $\left\| T^{-1} \sum_{t=1}^T \mathbf{x}_{it} \mathbf{x}'_{it} \right\|_F \leq \bar{c}_{xx}$  in probability. In addition, using the B-spline property in Lemma A.1(iii)

$$\begin{aligned} \left\| \frac{1}{T} \sum_{t=1}^T \mathbf{W}' \mathbf{b} \left( \frac{t}{T} \right) \mathbf{b} \left( \frac{t}{T} \right)' \mathbf{W} \right\|_F &= \left\| \mathbf{W}' \int_0^1 \mathbf{b}(v) \mathbf{b}(v)' dv \mathbf{W} (1 + O(T^{-1})) \right\|_F \\ &\leq \|\mathbf{W}\|_F^2 O(M^{-1})(1 + O(T^{-1})) = O(M^{-1}), \end{aligned} \quad (\text{A.32})$$

since  $\|\mathbf{W}\|_F^2$  is bounded. Subsequently,  $\left\| T^{-1} \sum_{t=1}^T \mathbf{z}_{it} \right\|_2 = O_p(M^{-1/2})$ .

Lastly, making use of the Cauchy-Schwarz inequality,

$$\|\hat{\mathbf{q}}_{i,z\eta}\|_2^2 = \left\| \frac{1}{T} \sum_{t=1}^T \mathbf{z}_{it} \eta_{it} \right\|_2^2 \leq \left\| \frac{1}{T} \sum_{t=1}^T \mathbf{z}_{it} \mathbf{z}'_{it} \right\|_F \left| \frac{1}{T} \sum_{t=1}^T \eta_{it}^2 \right|, \quad (\text{A.33})$$

where  $\left\| T^{-1} \sum_{t=1}^T \mathbf{z}_{it} \mathbf{z}'_{it} \right\|_F = O_p(M^{-1})$  by Lemma A.2(i) and

$$\begin{aligned} E \left| \frac{1}{T} \sum_{t=1}^T \eta_{it}^2 \right| &= E \left| \frac{1}{T} \sum_{t=1}^T (\mathbf{x}'_{it} a_{it})^2 \right| = \left[ \sup_{v \in [0,1]} \|\alpha_k^0(v) - \mathbf{\Pi}_i^{0'} \mathbf{b}(v)\|_2 \right]^2 \frac{1}{T} \sum_{t=1}^T E \|\mathbf{x}_{it}\|_2^2 \\ &\leq O(M^{-2\theta}) \bar{c}_x^{2/q} = O(M^{-2\theta}), \end{aligned} \quad (\text{A.34})$$

where  $\sup_{v \in [0,1]} \|\alpha_k^0(v) - \mathbf{\Pi}_i^{0'} \mathbf{b}(v)\|_2 = O(M^{-\theta})$  by Lemma A.1(iv) and  $E \|\mathbf{x}_{it}\|_2^2 \leq \bar{c}_x^{2/q}$  by Assumption 1(iii). As a consequence,  $\left| \frac{1}{T} \sum_{t=1}^T \eta_{it}^2 \right| = O_p(M^{-2\theta})$  by Chebyshev's inequality and  $\|\hat{\mathbf{q}}_{i,z\eta}\|_2^2 = O_p(M^{-1})O_p(M^{-2\theta})$  with  $\|\hat{\mathbf{q}}_{i,z\eta}\|_2 = O_p(M^{-\theta-1/2})$ .

Plugging the results of (A.31), (A.32), (A.33), and (A.34) into (A.29) yields

$$\|\hat{\mathbf{q}}_{i,z\bar{\eta}}\|_2 \leq \|\hat{\mathbf{q}}_{i,z\eta}\|_2 + \left\| T^{-1} \sum_{t=1}^T \mathbf{z}_{it} \right\|_2 \left\| T^{-1} \sum_{t=1}^T \eta_{it} \right\| = O_p(M^{-\theta-1/2}) + O_p(M^{-1/2})O_p(M^{-\theta}) = O_p(M^{-\theta-1/2}). \quad (\text{A.35})$$

Turning to  $\hat{\mathbf{q}}_{i,z\bar{\epsilon}}$ , note that  $\hat{\mathbf{q}}_{i,z\bar{\epsilon}} = \hat{\mathbf{q}}_{i,z\epsilon} - T^{-1} \sum_{t=1}^T \mathbf{z}_{it} T^{-1} \sum_{t=1}^T \epsilon_{it}$ . Studying  $\hat{\mathbf{q}}_{i,z\epsilon}$  first,

$$\begin{aligned} E \|\hat{\mathbf{q}}_{i,z\epsilon}\|_2^2 &= E \left\| \frac{1}{T} \sum_{t=1}^T \mathbf{z}_{it} \epsilon_{it} \right\|_2^2 = E \left\| \frac{1}{T} \sum_{t=1}^T \left[ \mathbf{x}_{it} \otimes \mathbf{b} \left( \frac{t}{T} \right) \right] \epsilon_{it} \right\|_2^2 = E \left\| \frac{1}{T} \sum_{t=1}^T (\mathbf{x}_{it} \epsilon_{it}) \otimes \mathbf{b} \left( \frac{t}{T} \right) \right\|_2^2 \\ &= \frac{1}{T^2} \sum_{t=1}^T \sum_{s=1}^T E (\mathbf{x}'_{it} \mathbf{x}_{is} \epsilon_{it} \epsilon_{is}) \mathbf{b} \left( \frac{t}{T} \right)' \mathbf{b} \left( \frac{s}{T} \right) \\ &= \frac{1}{T^2} \sum_{t=1}^T E (\mathbf{x}'_{it} \mathbf{x}_{it} \epsilon_{it}^2) \left\| \mathbf{b} \left( \frac{t}{T} \right) \right\|_2^2 \\ &\quad + \frac{2}{T^2} \sum_{t=1}^{T-1} \sum_{s=1}^T E (\mathbf{x}'_{it} \mathbf{x}_{is} \epsilon_{it} \epsilon_{is}) \mathbf{b} \left( \frac{t}{T} \right)' \mathbf{b} \left( \frac{s}{T} \right) = d_{1i} + d_{2i}. \end{aligned}$$

Employing Assumption 1(iii) gives  $E (\mathbf{x}'_{it} \mathbf{x}_{it} \epsilon_{it}^2) \leq E (\|\mathbf{x}_{it}\|_2^2 \|\epsilon_{it}\|_2^2) \leq (\bar{c}_x \bar{c}_\epsilon)^{2/q}$ . In addition,  $T^{-1} \sum_{t=1}^T \|\mathbf{b}(t/T)\|_2^2 = \int_0^1 \|\mathbf{b}(v)\|_2^2 dv (1 + O(T^{-1})) \leq (1 + O(T^{-1}))$  by Lemma A.1(ii) and the Riemann sum. Therefore,

$$d_{1i} \leq T^{-1} (\bar{c}_x \bar{c}_\epsilon)^{2/q} (1 + O(T^{-1})) = O(T^{-1}).$$

Similarly,

$$\begin{aligned} |d_{2i}| &= \left| \frac{2}{T^2} \sum_{t=1}^{T-1} \sum_{s=1}^T E (\mathbf{x}'_{it} \mathbf{x}_{is} \epsilon_{it} \epsilon_{is}) \mathbf{b} \left( \frac{t}{T} \right)' \mathbf{b} \left( \frac{s}{T} \right) \right| \\ &\leq \frac{2}{T^2} \sum_{l=1}^p \sum_{t=1}^{T-1} \sum_{s=t+1}^T \left| E (x_{it,l} \epsilon_{it} x_{is,l} \epsilon_{is}) \mathbf{b} \left( \frac{t}{T} \right) \right| \\ &\leq \frac{16}{T^2} \sum_{l=1}^p \max_{i,t} \left\{ E |x_{it,l} \epsilon_{it}|^{2/q} \right\}^{4/q} \sum_{t=1}^{T-1} \sum_{j=1}^{\infty} \phi(j)^{q-4/q}, \end{aligned}$$

where the last inequality holds by the Davydov inequality for strong mixing processes in combination with the moment conditions in Assumption 1(iii), qualified by the strong mixing condition on  $\{(\mathbf{x}_{it}^{(2)}, \epsilon_{it}, t = 1, \dots, T)\}$

in Assumption 1(ii). Subsequently,

$$\begin{aligned} & \frac{16}{T^2} \sum_{l=1}^p \max_{i,t} \left\{ E |x_{it,l} \epsilon_{it}|^{2/q} \right\}^{4/q} \sum_{t=1}^{T-1} \sum_{j=1}^{\infty} \phi(j)^{q-4/q} \\ & \leq \frac{16}{T} \sum_{l=1}^p \max_{i,t} \{ E |x_{it,l} \epsilon_{it}| \}^{6/q} c_\phi = O_p(T^{-1}). \end{aligned}$$

As a result,  $E \|\hat{\mathbf{q}}_{i,z\epsilon}\|_2^2 = O(T^{-1})$  and, using Chebyshev's inequality,  $\|\hat{\mathbf{q}}_{i,z\epsilon}\|_2 = O_p(T^{-1/2})$ . Furthermore,  $\|T^{-1} \sum_{t=1}^T \mathbf{z}_{it}\|_2 = O_p(M^{-1/2})$  as shown in (A.32) and  $|T^{-1} \sum_{t=1}^T \epsilon_{it}| = O_p(T^{-1/2})$  by Assumption 1(ii). Using these intermediary steps, the triangle inequality, and the sub-multiplicative property,

$$\|\hat{\mathbf{q}}_{i,\bar{z}\bar{\epsilon}}\|_2 \leq \|\hat{\mathbf{q}}_{i,z\epsilon}\|_2 + \|T^{-1} \sum_{t=1}^T \mathbf{z}_{it}\|_2 |T^{-1} \sum_{t=1}^T \epsilon_{it}| = O_p(T^{-1/2}) + O_p(M^{-1/2})O_p(T^{-1/2}) = O_p(T^{-1/2}). \quad (\text{A.36})$$

Combining the results in (A.35) and (A.36) yields

$$\|\hat{\mathbf{q}}_{i,\bar{z}\bar{u}}\|_2 = \|\hat{\mathbf{q}}_{i,\bar{z}\bar{\epsilon}} + \hat{\mathbf{q}}_{i,\bar{z}\bar{\eta}}\|_2 \leq \|\hat{\mathbf{q}}_{i,\bar{z}\bar{\epsilon}}\|_2 + \|\hat{\mathbf{q}}_{i,\bar{z}\bar{\eta}}\|_2 = O_p(T^{-1/2}) + O_p(M^{-\theta-1/2}) = O_p(T^{-1/2} + M^{-\theta-1/2})$$

by the triangle inequality. ■

**Lemma A.3(ii)** Since the cross-sectional dependence is bounded according to Assumption 1(i), it follows readily that

$$\frac{1}{N} \sum_{i=1}^N \|\hat{\mathbf{q}}_{i,\bar{z}\bar{\epsilon}}\|_2^2 = O_p(T^{-1} + M^{-2\theta-1}),$$

using Lemma A.3(i). ■

#### A.3.4 Lemma A.4

Consider the un-penalized criterion function  $\mathcal{F}_{NT,i}^*(\boldsymbol{\pi}_i) = T^{-1} \sum_{t=1}^T [\tilde{y}_{it} - \tilde{\mathbf{z}}'_{it} \boldsymbol{\pi}_i]^2$ . Define  $\mathbf{a}_i = \boldsymbol{\pi}_i - \boldsymbol{\pi}_i^0$  and recognize that  $\mathcal{F}_{NT,i}^*(\boldsymbol{\pi}_i) - \mathcal{F}_{NT,i}^*(\boldsymbol{\pi}_i^0) = -2\mathbf{a}'_i \hat{\mathbf{q}}_{i,\bar{z}\bar{u}} + \mathbf{a}'_i \hat{\mathbf{Q}}_{i,\bar{z}\bar{z}} \mathbf{a}_i$  as shown in (A.1). The inequality  $\mathcal{F}_{NT,i}^*(\hat{\boldsymbol{\pi}}_i, \lambda) \leq \mathcal{F}_{NT,i}^*(\boldsymbol{\pi}_i^0, \lambda)$  holds trivially since  $\hat{\boldsymbol{\pi}}_i = \arg \min_{\boldsymbol{\pi}_i} \mathcal{F}_{NT,i}^*(\boldsymbol{\pi}_i, \lambda)$ . Plugging the decomposition into this inequality gives

$$\begin{aligned} 0 & \geq \mathcal{F}_{NT,i}^*(\hat{\boldsymbol{\pi}}_i, \lambda) - \mathcal{F}_{NT,i}^*(\boldsymbol{\pi}_i^0, \lambda) = -2\mathbf{a}'_i \hat{\mathbf{q}}_{i,\bar{z}\bar{u}} + \mathbf{a}'_i \hat{\mathbf{Q}}_{i,\bar{z}\bar{z}} \mathbf{a}_i \\ & \geq -2\|\mathbf{a}_i\|_2 \|\hat{\mathbf{q}}_{i,\bar{z}\bar{u}}\|_2 + \|\mathbf{a}_i\|_2^2 M^{-1} \underline{c}_{\bar{z}\bar{z}} = 2\|\mathbf{a}_i\|_2 O_p(T^{-1/2} + M^{-\theta-1/2}) + \|\mathbf{a}_i\|_2^2 M^{-1} \underline{c}_{\bar{z}\bar{z}}, \end{aligned}$$

where Lemma A.3(i) provides the rate of  $\|\hat{\mathbf{q}}_{i,\bar{z}\bar{u}}\|_2$  and the predictor variance-covariance matrix is substituted with its lower bound  $\underline{c}_{\bar{z}\bar{z}}$  according to Lemma A.2(i), similar to the argument in Theorem 3.1.

Averaging over all  $i = 1, \dots, N$  and rearranging yields

$$\frac{2}{\underline{c}_{\bar{z}\bar{z}}} O_p(MT^{-1/2} + M^{-\theta+1/2}) \frac{1}{N} \sum_{i=1}^N \|\mathbf{a}_i\|_2 \geq \sum_{i=1}^N \|\mathbf{a}_i\|_2^2. \quad (\text{A.37})$$

As in Theorem 3.1,  $\|\hat{\mathbf{a}}_i\|_2 = \|\hat{\boldsymbol{\pi}}_i - \boldsymbol{\pi}_i^0\|_2 = O_p(T^{-1/2}M + M^{-\theta+1/2})$  to ensure that the inequality in (A.37) holds for an arbitrarily large  $\|\hat{\mathbf{a}}_i\|_2$ . Assumption 2(i) ensures that  $T^{-1/2}M$  is not explosive and  $-\theta + 1/2 < 0$  by Assumption 1(vi). ■

### A.3.5 Lemma A.5

Recall that  $\hat{\boldsymbol{\pi}} = (\hat{\boldsymbol{\pi}}_1', \dots, \hat{\boldsymbol{\pi}}_N')$  represents an initial least squares estimate, which, given Lemma A.4, is  $(MT^{-1/2} + M^{-\theta+1/2})^{-1}$  consistent. Define  $\hat{\boldsymbol{\pi}}_i - \boldsymbol{\pi}_i^0 = (MT^{-1/2} + M^{-\theta+1/2})\dot{\mathbf{v}}_i$  and recognize that  $\|\dot{\mathbf{v}}_i\|_2 = O_p(1)$ . Along the lines of Qian and Su (2016a, Lemma B.2), rewrite

$$\begin{aligned}\dot{\omega}_{ij} &= \|\hat{\boldsymbol{\pi}}_i - \hat{\boldsymbol{\pi}}_j\|_2^{-\kappa} = \left\| \left[ (MT^{-1/2} + M^{-\theta+1/2})\dot{\mathbf{v}}_i + \boldsymbol{\pi}_i^0 \right] - \left[ (MT^{-1/2} + M^{-\theta+1/2})\dot{\mathbf{v}}_j + \boldsymbol{\pi}_j^0 \right] \right\|_2^{-\kappa} \\ &= \left\| \boldsymbol{\pi}_i^0 - \boldsymbol{\pi}_j^0 + (MT^{-1/2} + M^{-\theta+1/2})(\dot{\mathbf{v}}_i - \dot{\mathbf{v}}_j) \right\|_2^{-\kappa} = \left\| \boldsymbol{\pi}_i^0 - \boldsymbol{\pi}_j^0 + (MT^{-1/2} + M^{-\theta+1/2}) \right\|_2^{-\kappa}.\end{aligned}$$

**Lemma A.5(i)** Let  $i, j \in G_k^0$  and subsequently  $\boldsymbol{\pi}_i^0 = \boldsymbol{\pi}_j^0 = \boldsymbol{\xi}_k^0$ . Considering the minimum adaptive weight,

$$\begin{aligned}\min_{i, j \in G_k^0} \dot{\omega}_{ij} &= \min_{i, j \in G_k^0} \left\| \boldsymbol{\pi}_i^0 - \boldsymbol{\pi}_j^0 + O_p(MT^{-1/2} + M^{-\theta+1/2}) \right\|_2^{-\kappa} \\ &= \min_{i, j \in G_k^0} \left\| O_p(MT^{-1/2} + M^{-\theta+1/2}) \right\|_2^{-\kappa} = O_p((MT^{-1/2} + M^{-\theta+1/2})^{-\kappa}). \blacksquare\end{aligned}$$

**Lemma A.5(ii)** Let  $i \in G_k^0, j \notin G_k^0$  and as a result  $\boldsymbol{\pi}_i^0 \neq \boldsymbol{\pi}_j^0$ . Now, analyzing the maximum weight,

$$\begin{aligned}\max_{i \in G_k^0, j \notin G_k^0} \dot{\omega}_{ij} &= \max_{i \in G_k^0, j \notin G_k^0} \left\| \boldsymbol{\pi}_i^0 - \boldsymbol{\pi}_j^0 + O_p(MT^{-1/2} + M^{-\theta+1/2}) \right\|_2^{-\kappa} \\ &= \left\| \min_{i \in G_k^0, j \notin G_k^0} (\boldsymbol{\pi}_i^0 - \boldsymbol{\pi}_j^0) + O_p(MT^{-1/2} + M^{-\theta+1/2}) \right\|_2^{-\kappa} \\ &= O_p(J_{\min}^{-\kappa}),\end{aligned}$$

where  $J_{\min} = \min_{i \in G_k^0, j \notin G_k^0} \|\boldsymbol{\pi}_i^0 - \boldsymbol{\pi}_j^0\|_2$  and Assumption 2(ii) ensures that  $J_{\min}$  dominates an  $O_p(MT^{-1/2} + M^{-\theta+1/2})$  term in the limit. ■

### A.3.6 Lemma A.6

**Lemma A.6(i)** Recognize that  $\|\mathbf{b}_c\|_2 = \|\mathbf{c} \otimes \mathbf{b}(v)\|_2 = \|\mathbf{c}\|_2 \|\mathbf{b}(v)\|_2$  by property of the Kronecker product and a nonrandom  $p \times 1$  vector  $\mathbf{c}$  with  $\|\mathbf{c}\|_2 = 1$  (see Theorem 3.5(ii)) and, following Lemma A.1(i),  $\|\mathbf{b}(v)\|_2 = 1$ . Subsequently,  $\|\mathbf{b}_c\|_2 = O_p(1)$ . ■

**Lemma A.6(ii)** Consider

$$\begin{aligned}
s_{c, \hat{G}_k}^2 &= \frac{M}{N_k T} \mathbf{b}'_c \left( MN_k^{-1} \hat{\mathbf{Q}}_{G_k^0, \bar{z}\bar{z}} \right)^{-1} \sum_{i \in G_k^0} \left[ \tilde{\mathbf{Z}}'_i E(\boldsymbol{\epsilon}_i \boldsymbol{\epsilon}'_i) \tilde{\mathbf{Z}}_i \right] \left( MN_k^{-1} \hat{\mathbf{Q}}_{G_k^0, \bar{z}\bar{z}} \right)^{-1} \mathbf{b}_c \\
&\leq \|\mathbf{b}_c\|_2^2 \left[ \mu_{\min} \left( MN_k^{-1} \hat{\mathbf{Q}}_{G_k^0, \bar{z}\bar{z}} \right) \right]^{-2} \frac{M}{N_k T} \sum_{i \in G_k^0} \left[ \tilde{\mathbf{Z}}'_i E(\boldsymbol{\epsilon}_i \boldsymbol{\epsilon}'_i) \tilde{\mathbf{Z}}_i \right] \\
&\leq \|\mathbf{b}_c\|_2^2 \left[ \mu_{\min} \left( MN_k^{-1} \hat{\mathbf{Q}}_{G_k^0, \bar{z}\bar{z}} \right) \right]^{-2} \max_{i \in G_k^0} [\mu_{\max}(E(\boldsymbol{\epsilon}_i \boldsymbol{\epsilon}'_i))] \mu_{\max} \left( \frac{M}{N_k} \hat{\mathbf{Q}}_{G_k^0, \bar{z}\bar{z}} \right) \\
&\leq \frac{\|\mathbf{b}_c\|_2^2 \bar{c}_{\epsilon\epsilon} \bar{c}_{\bar{z}\bar{z}}}{\underline{c}_{\bar{z}\bar{z}}^2},
\end{aligned}$$

by the Triangle property and  $\mathbf{a}'\mathbf{A}\mathbf{a} \geq \mu_{\min}(\mathbf{A})\mathbf{a}'\mathbf{a}$  for a conformable vector  $\mathbf{a}$  and matrix  $\mathbf{A}$ . Furthermore, notice that  $\|\mathbf{b}_c\|_2^2 = O_p(1)$  as shown in Lemma A.6(i),  $\max_{1 \leq i \leq N} \mu_{\max} \left( MN_k^{-1} \hat{\mathbf{Q}}_{G_k^0, \bar{z}\bar{z}} \right) \leq \bar{c}_{\bar{z}\bar{z}}$  and  $\min_{1 \leq i \leq N} \mu_{\min} \left( MN_k^{-1} \hat{\mathbf{Q}}_{G_k^0, \bar{z}\bar{z}} \right) \geq \underline{c}_{\bar{z}\bar{z}}$  by Lemma A.2(ii), and  $\max_{i \in G_k^0} \mu_{\max}(E(\boldsymbol{\epsilon}_i \boldsymbol{\epsilon}'_i)) \leq \bar{c}_{\epsilon\epsilon}$  by Assumption 4(i). In consequence,  $s_{c, \hat{G}_k}^2 = O_p(1)$  (see Su et al., 2019, Lemma A.8). ■

### A.3.7 Lemma A.7

The proof of (A.41) works by demonstrating that the *MSE* of an over-fitted model and the *MSE* of a model with the true grouping structure both converge towards the non-reducible residual error variance in the limit. The different converge rates give the result in (A.41).

$$\begin{aligned}
\hat{\sigma}_{\mathcal{G}^0}^2 &= \frac{1}{NT} \sum_{k=1}^{K_0} \sum_{i \in G_k^0} \sum_{t=1}^T \hat{u}_{it}^2 = \frac{1}{NT} \sum_{k=1}^{K_0} \sum_{i \in G_k^0} \sum_{t=1}^T \left[ \tilde{y}_{it} - \hat{\boldsymbol{\alpha}}_{G_k^0}^{p'} \left( \frac{t}{T} \right) \tilde{\mathbf{x}}_{it} \right]^2 \\
&= \frac{1}{NT} \sum_{k=1}^{K_0} \sum_{i \in G_k^0} \sum_{t=1}^T \left[ \tilde{\epsilon}_{it} - \left( \hat{\boldsymbol{\alpha}}_{G_k^0}^p \left( \frac{t}{T} \right) - \boldsymbol{\alpha}_{G_k^0}^0 \left( \frac{t}{T} \right) \right)' \tilde{\mathbf{x}}_{it} \right]^2 \\
&= \frac{1}{NT} \sum_{i=1}^N \sum_{t=1}^T \tilde{\epsilon}_{it}^2 - \frac{1}{NT} \sum_{k=1}^{K_0} \sum_{i \in G_k^0} \sum_{t=1}^T \left[ \left( \hat{\boldsymbol{\alpha}}_{G_k^0}^p \left( \frac{t}{T} \right) - \boldsymbol{\alpha}_{G_k^0}^0 \left( \frac{t}{T} \right) \right)' \tilde{\mathbf{x}}_{it} \tilde{\epsilon}_{it} \right] \\
&\quad + \frac{1}{NT} \sum_{k=1}^{K_0} \sum_{i \in G_k^0} \sum_{t=1}^T \left[ \left( \hat{\boldsymbol{\alpha}}_{G_k^0}^p \left( \frac{t}{T} \right) - \boldsymbol{\alpha}_{G_k^0}^0 \left( \frac{t}{T} \right) \right)' \tilde{\mathbf{x}}_{it} \right]^2
\end{aligned} \tag{A.38}$$

Denote the irreducible sample *MSE* as  $\bar{\sigma}_{NT}^2 = (NT)^{-1} \sum_{i=1}^N \sum_{t=1}^T \tilde{\epsilon}_{it}^2$ . Moreover, given Theorem 3.5(ii),  $\hat{\boldsymbol{\alpha}}_{G_k}^p(t/T)$  is  $((N_{k, \min} T)^{1/2} M^{1/2})$ -consistent, where  $N_{k, \min} = \min_{k=1, \dots, K_0} N_k$ . Due to Assumption 1(ii),  $\|T^{-1} \sum_{t=1}^T \tilde{\mathbf{x}}_{it} \tilde{\epsilon}_{it}\|_2 = O_p(T^{1/2})$ . In addition, note that  $N^{-1} \sum_{k=1}^{K_0} \sum_{i \in G_k^0} \|\hat{\mathbf{q}}_{i, \bar{x}\bar{\epsilon}}\|_2 = N^{1/2} O_p(T^{1/2})$  as a function of weak cross-sectional dependence (see Assumption 1(i)). Plugging these results into (A.38) yields the rates

$$\begin{aligned}
\hat{\sigma}_{\mathcal{G}^0}^2 &= \bar{\sigma}_{NT}^2 + O_p \left( (NT)^{1/2} M^{1/2} \right) O_p((NT)^{1/2}) + O_p \left( (NT)^{-1} M \right) O_p(1) \\
&= \bar{\sigma}_{NT}^2 + O_p \left( (TN)^{-1} M \right).
\end{aligned} \tag{A.39}$$



Define the set  $\bar{\mathcal{G}}_K = \{\bar{\mathcal{G}}_K = \{\bar{G}_k\}_{k=1}^K : \#i, j \in \bar{G}_K \text{ where } i \in G_l^0, j \notin G_l^0, 1 \leq l \leq K_0\}$  with  $K_0 < K \leq K_{\max} = N$ . That is, each  $\bar{\mathcal{G}}_K \in \bar{\mathcal{G}}_K$  denotes a partition of  $K > K_0$  over  $N$  where no heterogeneous cross-sectional units are pooled together in any group. Hence, it is trivial that  $\hat{\sigma}_{\bar{\mathcal{G}}_K}^2 \leq \hat{\sigma}_{\mathcal{G}^0}^2$ . Given the result in (A.39), we can expand this inequality to

$$0 \leq \hat{\sigma}_{\mathcal{G}^0}^2 - \hat{\sigma}_{\bar{\mathcal{G}}_K}^2 = \bar{\sigma}_{NT}^2 - \hat{\sigma}_{\bar{\mathcal{G}}_K}^2 + O_p((NT)^{-1}M). \quad (\text{A.40})$$

Let  $\mathcal{J}_{NT}$  be the largest distance between the estimated and irreducible mean squared error for any of the  $K_0 < K \leq K_{\max}$  groups

$$\mathcal{J}_{NT} = \max_{K_0 < k \leq K} \inf_{\alpha} \left\{ \frac{1}{N_k T} \sum_{i \in \bar{G}_k} \sum_{t=1}^T \left[ \tilde{\epsilon}_{it}^2 - \left( \tilde{y}_{it} - \tilde{\mathbf{x}}'_{it} \alpha_k \left( \frac{t}{T} \right) \right)^2 \right] \right\},$$

such that  $\bar{\sigma}_{NT}^2 - \hat{\sigma}_{\bar{\mathcal{G}}_K}^2 \leq K \mathcal{J}_{NT}$ . Then

$$\check{\alpha}_k \left( \frac{t}{T} \right) = \check{\Xi}'_k B \left( \frac{t}{T} \right) = \arg \min_{\xi_k} \frac{1}{N_k T} \sum_{i \in \bar{G}_k} \sum_{t=1}^T \left[ \tilde{\epsilon}_{it}^2 - \left( \tilde{y}_{it} - \tilde{\mathbf{z}}'_{it} \xi_k \left( \frac{t}{T} \right) \right)^2 \right],$$

with  $\check{\xi}_k = (\sum_{i \in \bar{G}_k} \sum_{t=1}^T \tilde{\mathbf{z}}_{it} \tilde{\mathbf{z}}'_{it})^{-1} \sum_{i \in \bar{G}_k} \sum_{t=1}^T \tilde{\mathbf{z}}_{it} \tilde{y}_{it}$ . Since  $K_0 < K \leq K_{\max} = N$ , the minimum group cardinality is 1 and  $\check{\alpha}_k(t/T)$  is, in line with Theorem 3.5, only  $\sqrt{M/T}$ -consistent. As a consequence,  $\mathcal{J}_{NT} = O_p(T^{-1}M)$ .

Plugging  $\bar{\sigma}_{NT}^2 - \hat{\sigma}_{\bar{\mathcal{G}}_K}^2 \leq K \mathcal{J}_{NT} = O_p(T^{-1}M)$  into (A.40), it becomes apparent that  $0 \leq \hat{\sigma}_{\mathcal{G}^0}^2 - \hat{\sigma}_{\bar{\mathcal{G}}_K}^2 \leq O_p(T^{-1}M) + O_p((NT)^{-1}M) = O_p(T^{-1}M)$ . Then, by construction of  $\mathcal{J}_{NT}$ ,

$$\max_{K_0 < K \leq K_{\max}} \sup_{\bar{\mathcal{G}}_K \in \bar{\mathcal{G}}_K} |\hat{\sigma}_{\bar{\mathcal{G}}_K}^2 - \hat{\sigma}_{\mathcal{G}^0}^2| = O_p(T^{-1}M). \blacksquare \quad (\text{A.41})$$

## B Details on the Sieve Estimation of Time-varying Coefficient Functions

Consider a B-spline with  $M^* > 0$  interior knots that is piece-wise polynomial of degree  $d \geq 1$  (order  $d + 1$ ) on the unit interval. The  $M \times 1$  vector  $\mathbf{b}(v)$  holds the common time-varying basis functions  $\mathbf{b}(v) = (b_{-d}(v), \dots, b_{M^*}(v))'$ , with  $M = M^* + d + 1$  and  $v \in [0, 1]$ . Let  $\mathbb{V}_{\text{int}}$  represent an increasing sequence  $0 < v_1 < \dots < v_{M^*} < 1$ , such that  $\mathbb{V}_{\text{int}}$  gives  $M^*$  equidistant interior knots of the B-spline, which divide the unit interval into  $M^* + 1$  partitions.<sup>10</sup> The total set of knots  $\mathbb{V}$  extends  $\mathbb{V}_{\text{int}}$  to  $0 = v_{-d} = \dots = v_0 <$

<sup>10</sup>We conjecture that the basic results of this paper also hold for free-knot spline functions, where the distance between interior knots may deviate from  $1/(M^* + 1)$ . However, altering the theory in this respect and introducing a data-driven knot placement routine is very involved (see Hansen and Koopberg, 2002; Scarpiniti et al., 2013; Dung and Tjahjowidodo, 2017). A rigorous extension of the theory to free-knot splines is beyond the scope of this paper.

$v_1 < \dots < v_{M^*} < v_{M^*+1} = \dots = v_M = 1$ . The boundary knots  $\{v_m\}_{m=-d}^0 \cup \{v_m\}_{m=M^*+1}^M$  coincide at either zero or one and force the final B-spline to pass through the start and end points exactly using the *de Boor recurrence relation*:

$$b_{m,j}(v) = a_{m,j}(v)b_{m,j-1}(v) + [1 - a_{m+1,j}(v)]b_{m+1,j-1}(v),$$

with  $a_{m,j}(v) = [(v - v_m)/(v_{m+j} - v_m)] \mathbf{1}\{v_{m+j} \neq v_m\}$ ,  $b_{m,0}(v) = \mathbf{1}\{v_m \leq v < v_{m+1}\}$ , and  $b_{m,d}(v) = b_m(v)$  (De Boor, 2001, ch. 9, eq. 14). Hence, each basis function  $b_m(v)$ ,  $m = -d, \dots, M^*$ , defined on the knots  $\{v_m\}_{m=-d}^M$ , is a convex combination of two lower-order basis functions and vanishes outside the interval  $\{V_m\}_{m=-d}^{M^*}$  with

$$V_m = \begin{cases} [v_m, v_{m+d+1}), & \text{for } m = -d, \dots, M^* - d - 1 \\ [v_m, v_{m+d+1}], & \text{for } m = M^* - d, \dots, M^*. \end{cases} \quad (\text{B.1})$$

The space generated by these  $M$  polynomial basis functions is denoted as  $\mathbb{B}_M$  and each function in  $\mathbb{B}_M$  is a B-spline that is piece-wise polynomial of degree  $d$  on each sub-interval  $\{V_m\}_{m=-d}^{M^*}$  and globally  $d - 1$  times continuously differentiable for  $d \geq 1$ . We refer to De Boor (2001) for a textbook treatment of spline functions.

The  $M \times 1$  vector of control points  $\boldsymbol{\pi}_{il}^0$  weights each basis function in  $\mathbf{b}(v)$  and, in turn, constructs a linear combination, the B-spline, that approximates a scalar square-integrable coefficient function  $\beta_{il}^0(v)$

$$\beta_{il}^0(v) \approx \boldsymbol{\pi}_{il}^0 \mathbf{b}(v), \quad l = 1, \dots, p. \quad (\text{B.2})$$

We can replace the approximation sign in (B.2) with an equality if  $\beta_{il}^0(v) \in \mathbb{B}_M$  and  $M$  is known. However, since  $\beta_{il}^0(v)$  may generally not belong to the linear space  $\mathbb{B}_M$ , we allow  $M$  to increase with the sample size and obtain ever closer approximations of the true underlying coefficient function.  $\mathbb{B}_M$  acts as a tractable sieve of the space of square-integrable functions, where increasing  $M$  is akin to moving to an ever denser sieve. Throughout the paper, we assume the generalizing case  $\beta_{il}^0(v) \notin \mathbb{B}_M$ .

Figure 5 illustrates the approximation of a logistic cumulative distribution function (CDF) using a B-spline with  $M^* = 2$  interior knots and polynomial degree  $d = 2$ , resulting in a system of  $M = M^* + d + 1 = 5$  basis functions. The vector of control points  $\boldsymbol{\pi}_{il}^0$  is estimated by regressing realizations of the function of interest, in this example, a logistic CDF, on  $\mathbf{b}(v)$ , using least squares (Huang et al., 2004, sec. 2).

## C Numerical Implementation

We minimize the criterion (2.6) using an iterative *ADMM* algorithm, adapted from (Ma and Huang, 2017, sec. 3.1) and Mehrabani (2023, sec. 5.1). Let  $\mathbf{a}_{ij} = \boldsymbol{\pi}_i - \boldsymbol{\pi}_j$ . Then minimizing

$$\mathcal{F}_{NT}(\boldsymbol{\pi}, \mathbf{a}, \lambda) = \frac{1}{T} \sum_{i=1}^N \sum_{t=1}^T (\tilde{y}_{it} - \tilde{\mathbf{z}}_{it}' \boldsymbol{\pi}_i)^2 + \frac{\lambda}{N} \sum_{i=1}^{N-1} \sum_{j=i+1}^N \dot{\omega}_{ij} \|\mathbf{a}_{ij}\|_2 \quad \text{subject to } \mathbf{a}_{ij} = \boldsymbol{\pi}_i - \boldsymbol{\pi}_j, \quad (\text{C.1})$$

<sup>11</sup>A B-spline can be equivalently expressed as convex combinations of control points, with  $B_{m,0}$  acting as indicators. In this case, recursively constructed convex combinations of control points yield the  $M^*$  polynomial functions, which continuously tie together at the interior knots (see De Boor, 2001, pp. 99).

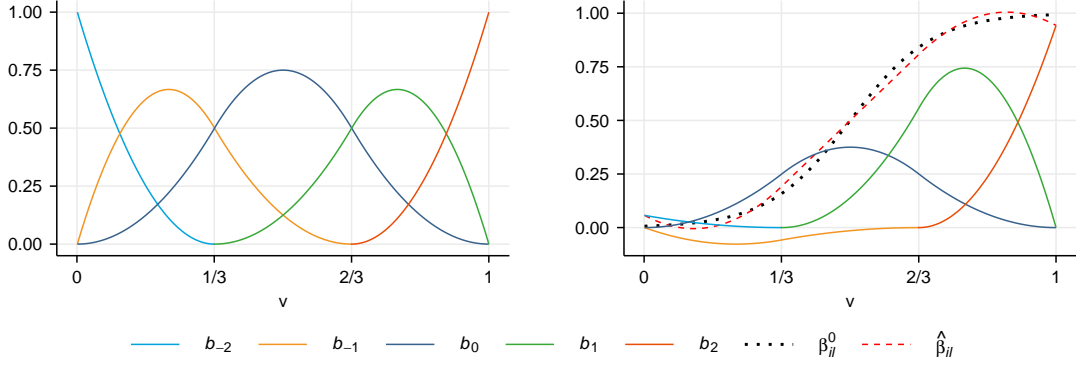


Figure 5: The left panel sketches five polynomial basis functions  $b_m(v)$ ,  $m = -d, \dots, M^*$  for  $d = 2$  and  $M^* = 2$ . The right panel displays the weighted basis functions (solid) and the resulting B-spline (red, dashed), approximating a logistic CDF  $\beta_{il}^0(v)$  (black, dotted).

is equivalent to optimizing the objective in (2.6). We can rewrite this constraint optimization as an Augmented Lagrangian problem

$$\begin{aligned}
\mathcal{L}_{NT,\vartheta}(\boldsymbol{\pi}, \mathbf{a}, \lambda, \mathbf{v}) &= \frac{T}{2} \mathcal{F}_{NT}(\boldsymbol{\pi}, \mathbf{a}, \lambda) + \sum_{i=1}^{N-1} \sum_{j=i+1}^N \mathbf{v}'_{ij} (\boldsymbol{\pi}_i - \boldsymbol{\pi}_j - \mathbf{a}_{ij}) + \frac{\vartheta}{2} \sum_{i=1}^{N-1} \sum_{j=i+1}^N \|\boldsymbol{\pi}_i - \boldsymbol{\pi}_j - \mathbf{a}_{ij}\|_2^2 \\
&= \mathcal{F}_{NT}^*(\boldsymbol{\pi}) + \mathcal{P}_{NT}^*(\mathbf{a}, \lambda) + \sum_{i=1}^{N-1} \sum_{j=i+1}^N \mathbf{v}'_{ij} (\boldsymbol{\pi}_i - \boldsymbol{\pi}_j - \mathbf{a}_{ij}) \\
&\quad + \frac{\vartheta}{2} \sum_{i=1}^{N-1} \sum_{j=i+1}^N \|\boldsymbol{\pi}_i - \boldsymbol{\pi}_j - \mathbf{a}_{ij}\|_2^2,
\end{aligned} \tag{C.2}$$

where  $\mathcal{F}_{NT}^*$  reflects the goodness-of-fit term and  $\mathcal{P}_{NT}^*(\mathbf{a}, \lambda)$  the *time-varying PAGFL* penalty in (C.1).  $\mathbf{v}_{ij}$  denotes the dual variable and  $\vartheta > 0$  the *ADMM* penalty parameter controlling the trade-off between feasibility and optimization.

The *ADMM* algorithm 1 minimizes the objective (C.2) iteratively up to a convergence tolerance  $\varepsilon_{\text{tol}}^{\text{ADMM}}$  and, to arrest problems with an excessive computational burden, a maximum number of iterations  $l_{\text{max}}$ . We recommend setting  $\varepsilon_{\text{tol}}^{\text{ADMM}} = 1 \times 10^{-10}$  and  $l_{\text{max}} = 50,000$ . Clearly,  $\varepsilon_{\text{tol}}^{\text{ADMM}}$  can be decreased and  $l_{\text{max}}$  increased arbitrarily. Define  $\tilde{\mathbf{y}} = (\tilde{\mathbf{y}}'_1, \dots, \tilde{\mathbf{y}}'_N)'$ ,  $\tilde{\mathbf{y}}_i = (\tilde{y}_{i1}, \dots, \tilde{y}_{iT})'$ ; the  $NT \times NMp$  regressor block-matrix  $\tilde{\mathbf{Z}} = \text{diag}(\tilde{\mathbf{Z}}_1, \dots, \tilde{\mathbf{Z}}_N)$  with  $\tilde{\mathbf{Z}}_i = (\tilde{z}_{i1}, \dots, \tilde{z}_{iT})'$ ; the  $NMp \times 1$  coefficient vector  $\boldsymbol{\pi} = (\boldsymbol{\pi}'_1, \dots, \boldsymbol{\pi}'_N)'$ ; the  $MpN(N-1)/2 \times NMp$  differencing matrix  $\boldsymbol{\Delta} = \boldsymbol{\varsigma} \otimes \mathbf{I}_{Mp}$  with  $\boldsymbol{\varsigma} = \{\boldsymbol{\zeta}_i - \boldsymbol{\zeta}_j, 1 \leq i < j \leq N\}'$ , and the  $N \times 1$  indicator vector  $\boldsymbol{\zeta}_i$  with a one as its  $i^{\text{th}}$  element and zeros elsewhere; the  $MpN(N-1)/2 \times 1$  vectors  $\mathbf{a} = \{\mathbf{a}'_{ij}, 1 \leq i < j \leq N\}'$  and  $\mathbf{v} = \{\mathbf{v}'_{ij}, 1 \leq i < j \leq N\}'$ . The primal steps of the *ADMM* are proximal updates of  $\hat{\boldsymbol{\pi}}$  and  $\hat{\mathbf{a}}$  and take the form

$$\begin{aligned}
\boldsymbol{\pi}^{(l+1)} &= \arg \min_{\boldsymbol{\pi}} \left\{ \mathcal{F}_{NT}^*(\boldsymbol{\pi}) + \frac{\vartheta}{2} \left\| \boldsymbol{\Delta} \boldsymbol{\pi} - \mathbf{a}^{(l)} + \vartheta^{-1} \mathbf{v}^{(l)} \right\|_2^2 \right\} \\
\mathbf{a}^{(l+1)} &= \arg \min_{\mathbf{a}} \left\{ \mathcal{P}_{NT}^*(\mathbf{a}, \lambda) + \frac{\vartheta}{2} \left\| \boldsymbol{\Delta} \boldsymbol{\pi}^{(l)} - \mathbf{a} + \vartheta^{-1} \mathbf{v}^{(l)} \right\|_2^2 \right\}.
\end{aligned}$$

---

**Algorithm 1:** *ADMM* algorithm to minimize the *time-varying PAGFL* criterion (2.6).

---

**Result:**  $\hat{\boldsymbol{\pi}}_i = \boldsymbol{\pi}_i^{(l)}$   
 $l \leftarrow 0$ ;  
 $\boldsymbol{\pi}^{(l)} \leftarrow \hat{\boldsymbol{\pi}}$ ;  
 $\mathbf{a}^{(l)} \leftarrow \boldsymbol{\Delta} \hat{\boldsymbol{\pi}}^{(l)}$ ;  
 $\mathbf{v}^{(l)} \leftarrow 0$ ;  
**while**  $\|\boldsymbol{\Delta} \boldsymbol{\pi}^{(l)} - \mathbf{a}^{(l)}\|_2 > \varepsilon_{tol}^{ADMM}$  &  $l < l_{\max}$  **do**  
     $l \leftarrow l + 1$ ;  
    **Primal step 1:**  $\boldsymbol{\pi}^{(l)} \leftarrow \left( \tilde{\mathbf{Z}}' \tilde{\mathbf{Z}} + \vartheta \boldsymbol{\Delta}' \boldsymbol{\Delta} \right)^{-1} \left( \tilde{\mathbf{Z}}' \tilde{\mathbf{y}} + \vartheta \boldsymbol{\Delta}' \mathbf{a}^{(l-1)} - \boldsymbol{\Delta}' \mathbf{v}^{(l-1)} \right)$ ;  
    **Primal step 2:**  $\boldsymbol{\psi}_{ij}^{(l)} \leftarrow \vartheta \boldsymbol{\pi}_i^{(l)} - \vartheta \boldsymbol{\pi}_j^{(l)} - \mathbf{v}_{ij}^{(l-1)}$ ,  
         $\mathbf{a}_{ij}^{(l)} \leftarrow \max \left\{ 1 - \dot{\omega}_{ij} T \lambda / \left( 2N \|\boldsymbol{\psi}_{ij}^{(l)}\| \right), 0 \right\} \boldsymbol{\psi}_{ij}^{(l)}$  for each  $1 \leq i < j \leq N$ ,  
         $\mathbf{a}^{(l)} \leftarrow \left\{ \mathbf{a}_{ij}^{(l)}, 1 \leq i < j \leq N \right\}'$ ;  
    **Dual step:**  $\mathbf{v}^{(l)} \leftarrow \mathbf{v}^{(l-1)} + \vartheta \left( \boldsymbol{\Delta} \boldsymbol{\pi}^{(l)} - \mathbf{a}^{(l)} \right)$ ;  
**end**

---

In particular, we obtain  $\boldsymbol{\pi}^{(l+1)}$  by setting

$$\frac{\partial}{\partial \boldsymbol{\pi}} \left[ \mathcal{F}_{NT}^*(\boldsymbol{\pi}) + \vartheta/2 \left\| \boldsymbol{\Delta} \boldsymbol{\pi} - \mathbf{a}^{(l)} + \vartheta^{-1} \mathbf{v}^{(l)} \right\|_2^2 \right]$$

to zero, where  $\mathcal{F}_{NT}^*(\boldsymbol{\pi}) = 1/2 \|\tilde{\mathbf{y}} - \tilde{\mathbf{Z}} \boldsymbol{\pi}\|_2^2$ . The *time-varying PAGFL* penalty is applied to each pair of cross-sectional units separately. Subsequently,  $\mathbf{a}^{(l+1)}$  must be derived individually for each  $i, j$ . Therefore, we take

$$\mathbf{a}_{ij}^{(l+1)} = \arg \min_{\mathbf{a}_{ij}} \left\{ \frac{T \lambda}{2N} \sum_{i=1}^{N-1} \sum_{j=i+1}^N \dot{\omega}_{ij} \|\mathbf{a}_{ij}\|_2 + \frac{\vartheta}{2} \sum_{i=1}^{N-1} \sum_{j=i+1}^N \|\boldsymbol{\pi}_i^{(l)} - \boldsymbol{\pi}_j^{(l)} - \mathbf{a}_{ij} - \vartheta^{-1} \mathbf{v}_{ij}\|_2^2 \right\},$$

the closed-form solution of which is the typical soft thresholding rule

$$\mathbf{a}_{ij}^{(l+1)} = \max \left\{ 1 - \frac{T \lambda}{2N} \frac{\dot{\omega}_{ij} / \vartheta}{\|\boldsymbol{\pi}_i^{(l)} - \boldsymbol{\pi}_j^{(l)} - \mathbf{a}_{ij} - \vartheta^{-1} \mathbf{v}_{ij}\|_2}, 0 \right\} \left( \boldsymbol{\pi}_i^{(l)} - \boldsymbol{\pi}_j^{(l)} - \mathbf{a}_{ij} - \vartheta^{-1} \mathbf{v}_{ij} \right)$$

which appears in algorithm 1. The Dual step of the *ADMM* algorithm pushes the solutions towards satisfying the constraint  $\boldsymbol{\pi}_i - \boldsymbol{\pi}_j - \mathbf{a}_{ij}$ , moderated by the *ADMM* penalty  $\vartheta$ .

Since the objective function of the *time-varying PAGFL* (2.6) is convex, the Algorithm 1 achieves convergence to the optimal point as  $l \rightarrow \infty$ . Furthermore, given that the primal residual  $\mathbf{r}_1^{(l)} = \boldsymbol{\Delta} \boldsymbol{\pi}^{(l)} - \mathbf{a}^{(l)}$  and dual residual  $\mathbf{r}_2^{(l)} = \vartheta \boldsymbol{\Delta} (\boldsymbol{\pi}^{(l)} - \boldsymbol{\pi}^{(l-1)})$  tend to zero asymptotically  $\lim_{l \rightarrow \infty} \|\mathbf{r}_d^{(l)}\|_2^2 = 0$  for  $d = \{1, 2\}$ , the algorithm is both primal and dual feasible. The proof for primal and dual feasibility is identical to Mehrabani (2023, Supplement, Appendix C) and thus omitted.

In theory, two individuals  $i, j$  are only fused together if  $\|\hat{\boldsymbol{\pi}}_i - \hat{\boldsymbol{\pi}}_j\|_2 = 0$ . However, employing the *ADMM* algorithm, it is not always computationally feasible for normed coefficient vector differences to equal zero exactly. As a consequence, we relax this condition and group two individuals if  $\|\hat{\boldsymbol{\pi}}_i - \hat{\boldsymbol{\pi}}_j\|_2 < \varepsilon_{tol}^G$ , where  $\varepsilon_{tol}^G$  is set to a machine inaccuracy value. The smaller  $\varepsilon_{tol}^G$ , the more *ADMM* algorithm iterations are required to obtain suitable results. As a consequence, there is an efficiency-accuracy trade-off when selecting  $\varepsilon_{tol}^G$ . We find

that  $\varepsilon_{\text{tol}}^{\mathcal{G}} = 0.001$  yields good computational efficiency while still providing sharp between-group distinction. Similarly, it may occur that  $\|\hat{\boldsymbol{\pi}}_i - \hat{\boldsymbol{\pi}}_j\|_2 < \varepsilon_{\text{tol}}^{\mathcal{G}}$  and  $\|\hat{\boldsymbol{\pi}}_i - \hat{\boldsymbol{\pi}}_l\|_2 < \varepsilon_{\text{tol}}^{\mathcal{G}}$ , but  $\|\hat{\boldsymbol{\pi}}_j - \hat{\boldsymbol{\pi}}_l\|_2 \geq \varepsilon_{\text{tol}}^{\mathcal{G}}$ . Since the group structure must be transitive, we nonetheless assign such three individuals,  $i, j$ , and  $l$ , to the same group in our numerical implementation.

Furthermore, splinter groups with only one or a few members may emerge in empirical or simulation settings. This characteristic also has been previously documented for similar models (see [Su et al., 2016](#), [2019](#); [Mehrabani, 2023](#); [Dzemeski and Okui, 2024](#)). Such trivial groups can be precluded by either increasing  $\varepsilon_{\text{tol}}^{\mathcal{G}}$  or by increasing the number of iterations of the *ADMM* algorithm. However, another solution is to specify a lower bound on the group cardinalities, e.g., 5% of  $N$ , and place individuals of groups that fall short of this threshold into remaining groups of sufficient size according to the lowest *MSE*. We impose such a  $N_k/N \geq 5\%$  rule for the simulation study in [Section 4](#) and the empirical illustration in [Section 5](#). Note that in the subsequent simulation study, the preliminary coefficient vector differences  $\|\hat{\boldsymbol{\pi}}_i - \hat{\boldsymbol{\pi}}_j\|_2$  exceed  $\varepsilon_{\text{tol}}^{\mathcal{G}} = 0.001$  in all but a negligible amount of instances. Subsequently, this simple *MSE*-based classifier in combination with  $\varepsilon_{\text{tol}}^{\mathcal{G}}$  leads to next to no groupings and the classification procedure is driven by the penalization routine.

Our companion R-package *PAGFL* ([Haimerl et al., 2025](#)) provides an user-friendly and efficient open-source software implementation of the numerical algorithm presented in this section.

## D Extensions

In the following, we provide details on several extensions to broaden the scope the *time-varying PAGFL*.

### D.1 Panels with Coefficient-specific Groups

Consider a panel data model where each coefficient function follows a distinct group structure. Such a set-up reflects, e.g., the effect of commodity shocks on economies with different energy mixes: a specific country may be equally exposed to fluctuations in oil prices than one set of peers but form a group with a different set of countries regarding the effect of coal prices ([Cashin et al., 2014](#)).

We extend the DGP in [\(2.1\)](#) to allow each of the  $p$  functional coefficients in  $\boldsymbol{\beta}_i^0(t/T)$  to follow an unique unobserved group pattern

$$\beta_{il}^0\left(\frac{t}{T}\right) = \sum_{k=1}^{K_{0l}} \alpha_{kl}^0\left(\frac{t}{T}\right) \mathbf{1}\{i \in G_{kl}^0\}, \quad l = 1, \dots, p. \quad (\text{D.1})$$

Note that not only the group adherence  $G_{kl}^0$  but also the total number of groups  $K_{0l}$  may vary for each of the  $p$  coefficient functions. To identify the coefficient-specific groups in [\(D.1\)](#), we adjust the *time-varying PAGFL* penalty such that the group-Lasso aspect concerns the  $M$  control points associated with each functional coefficient, as opposed to the entire  $M \times p$  matrix  $\boldsymbol{\Pi}_i$ . Let  $\boldsymbol{\pi}_{il}$  denote the  $l^{\text{th}}$  column of  $\boldsymbol{\Pi}_i$  and specify the

criterion

$$\mathcal{F}_{NT}(\pi, \lambda) = \frac{1}{T} \sum_{i=1}^N \sum_{t=1}^T (\tilde{y}_{it} - \boldsymbol{\pi}'_i \tilde{\mathbf{z}}_{it})^2 + \frac{\lambda}{N} \sum_{l=1}^p \sum_{i=1}^{N-1} \sum_{j=i+1}^N \hat{\omega}_{ijl} \|\pi_{il} - \pi_{jl}\|_2,$$

where the adaptive weight is defined as  $\hat{\omega}_{ijl} = \|\hat{\pi}_{il} - \hat{\pi}_{jl}\|_2^{-\kappa}$  and  $\hat{\boldsymbol{\pi}}_i$  is identical to the base-case in Section 2.

Having obtained the  $p$  distinct group structures, the *post-Lasso* estimator follows as

$$\hat{\boldsymbol{\xi}}^p = (\check{\mathbf{Z}}' \check{\mathbf{Z}})^{-1} \check{\mathbf{Z}}' \tilde{\mathbf{y}},$$

where the  $M \times \sum_{l=1}^p \hat{K}_l$  matrix  $\hat{\boldsymbol{\Xi}}^p = (\hat{\boldsymbol{\Xi}}_1^p, \dots, \hat{\boldsymbol{\Xi}}_p^p)$ ,  $\text{vec}(\hat{\boldsymbol{\Xi}}^p) = \hat{\boldsymbol{\xi}}^p$ , stacks coefficient-wise with  $\hat{\boldsymbol{\Xi}}_l^p = (\hat{\boldsymbol{\xi}}_{l1}^p, \dots, \hat{\boldsymbol{\xi}}_{l\hat{K}_l}^p)$  and  $\hat{\boldsymbol{\xi}}_{lk}^p$  holds the  $M$  control points shaping the time-varying function  $l$  of group  $k$ , with  $k = 1, \dots, \hat{K}_l$  and  $l = 1, \dots, p$ . Moreover, let  $\tilde{\mathbf{y}} = (\tilde{\mathbf{y}}_1', \dots, \tilde{\mathbf{y}}_N')'$ ,  $\tilde{\mathbf{y}}_i = (\tilde{y}_{i1}, \dots, \tilde{y}_{iT})'$ , and  $\check{\mathbf{Z}} = (\check{\mathbf{Z}}_1, \dots, \check{\mathbf{Z}}_p)$ , where  $\check{\mathbf{Z}}_l$  is a  $NT \times \hat{K}_l M$  regressor matrix  $\check{\mathbf{Z}}_l = (\mathbf{D}_{l1}, \dots, \mathbf{D}_{l\hat{K}_l})(\mathbf{I}_{\hat{K}_l} \otimes \tilde{\mathbf{z}}_l)$ .  $\mathbf{D}_{kl}$  indicates a  $NT \times NT$  matrix selecting observations pertaining to group  $k$  of the  $l^{\text{th}}$  coefficient function  $\mathbf{D}_{kl} = \text{diag}(\mathbf{d}_{kl}) \otimes \mathbf{I}_T$ , where  $\mathbf{d}_{kl}$  is a vector of length  $N$  with ones for all  $\{i \in \hat{G}_{kl}, 1 \leq i \leq N\}$  and zeros elsewhere.  $\tilde{\mathbf{Z}}_l$  is a  $NT \times M$  matrix that collects all basis functions corresponding to the  $l^{\text{th}}$  coefficient function  $\tilde{\mathbf{Z}}_l = (\tilde{\mathbf{z}}'_{1l}, \dots, \tilde{\mathbf{z}}'_{Nl})'$ ,  $\tilde{\mathbf{z}}_{il} = (\tilde{z}_{i1l}, \dots, \tilde{z}_{iTl})'$ , with  $\tilde{z}_{itl} = (\mathbf{r}_l \tilde{\mathbf{x}}_{it}) \otimes \mathbf{b}(t/T)$  and the  $1 \times p$  selection vector  $\mathbf{r}_l$  featuring a one at position  $l$  and zeros for all remaining elements. The time-varying functional coefficients for individual  $i$  are given by  $\hat{\boldsymbol{\alpha}}_i^p(t/T) = \mathbf{W}_i \hat{\boldsymbol{\Xi}}^p \mathbf{b}(t/T)$ , where  $\mathbf{W}_i$  represents a  $p \times \sum_{l=1}^p \hat{K}_l$  selection matrix  $\mathbf{W}_i = \{(\mathbf{0}'_{1\{l \neq 1\}} \sum_{s=1}^{l-1} \hat{K}_s, \mathbf{w}'_l, \mathbf{0}'_{1\{l \neq p\}} \sum_{s=l+1}^p \hat{K}_s), 1 \leq l \leq p\}'$  and  $\mathbf{w}_l$  is a vector of length  $\hat{K}_l$  with a one on position  $k = \{k : i \in \hat{G}_{kl}, 1 \leq k \leq \hat{K}_l\}$  and zeros elsewhere.

Based on the derivations in Section 3, we conjecture that the preliminary convergence rates also apply when generalizing to coefficient-wise groups. Moreover, the same applies to the limiting distribution of each coefficient function in Theorem 3 after replacing the global  $N_k$  with the coefficient-specific group size  $N_{kl}$  and inserting the coefficient group equivalents of  $\hat{\boldsymbol{\Omega}}_{G_k^0}$ ,  $\hat{\boldsymbol{\mathcal{E}}}_{G_k^0}$ , and  $\mathbf{q}_{G_k^0}$ .

Analogous to defining the group-Lasso over the columns of  $\hat{\boldsymbol{\Pi}}_i$ , it is also straightforward to penalize  $\hat{\boldsymbol{\Pi}}_i$  row-wise. Subsequently, the grouping varies among each of the  $M$  basis functions in  $\mathbf{b}(t/T)$ , and since the basis functions vanish outside their respective interval  $\{V_m\}_{m=-d}^{M^*}$  (cf. B.1), the grouping varies across time. Furthermore, as  $d+1$  basis functions overlap at any point along the domain (see Figure 5, left panel), such a specification produces up to  $\prod_{j=0}^d \hat{K}_{-d+j+\varphi}$  functional coefficient vectors unique to each interval  $[v_\varphi, v_{\varphi+1})$  for  $\varphi = 0, \dots, M^* - 1$  and  $[v_{M^*}, v_{M^*+1}]$ , where  $\hat{K}_{-d+j+\varphi} = \hat{K}_m$  denotes the estimated number of groups of basis function  $m$  and  $v_\varphi$  indicates the respective knot (cf. Appendix B). This significantly complicates the interpretation of the group structure but allows the coefficient functions of different cross-sectional individuals to coincide only for specific periods. Each interior knot reflects a break-point at which the group adherence may change, allowing for a total of  $M^* + 1$  distinct groupings with a potential switch every  $T/(M^* + 1)$  time periods.

Furthermore, models with a mix of group-specific, global, and individual coefficients have found ample empirical use. This setting mirrors models with both group-level, common, and idiosyncratic factors, as

previously studied by [Diebold et al. \(2008\)](#); [Ando and Bai \(2016\)](#); [Freyaldenhoven \(2022\)](#), among others. Such a structure is nested in coefficient-specific groups as introduced in this subsection. Reorder  $\beta_i(t/T)$  such that  $\beta_i(t/T) = (\beta_i^{(1)'}(t/T), \beta_i^{(2)'}(t/T), \beta_i^{(3)'}(t/T))'$ , where only the  $p^{(1)} \times 1$  functional vector  $\beta_i^{(1)}(t/T)$  follows a latent group structure as described in (2.3), that is  $\hat{G}_l$  is identical for all  $l = 1, \dots, p^{(1)}$ . The  $p^{(2)} \times 1$  vector  $\beta_i^{(2)}(t/T)$  is idiosyncratic,  $K_l = N$  for all  $l = 1, \dots, p^{(2)}$ . The  $p^{(3)} \times 1$  vector  $\beta_i^{(3)}(t/T)$  is common across all cross-sectional units such that  $K_l = 1$  for all  $l = 1, \dots, p^{(3)}$ . Then, estimation follows readily from the derivations above. The limiting distributions in Theorem 3.5 now hold for  $\hat{\alpha}_{\hat{G}_k}^{(1)p}(t/T)$  when replacing  $p$  with  $p^{(1)}$  and for  $\hat{\alpha}_i^{(2)p}(t/T)$  when setting  $p = p^{(2)}$  and  $N_k = 1$ . The global coefficients are subject to quicker convergence rates since all  $N$  individuals are pooled. Subsequently,  $\hat{\pi}_i^{(3)}$  converges pointwise with a rate of  $O_p(M(NT)^{-\frac{1}{2}} + M^{-\theta+\frac{1}{2}})$  and in mean-squares with  $O_p(M^2(NT)^{-1} + M^{-2\theta+1})$ . Likewise, to obtain the limiting distributions of the global coefficients in  $\hat{\alpha}_i^{(3)p}(t/T)$ , one only needs to replace  $p$  with  $p^{(3)}$  and substitute  $N_k$  with  $N$  in Theorem 3.5.

## D.2 Panels with Time-Varying and Time-Constant Coefficients

Despite the frequent occurrence of time-variant functional relationships in applied settings, some coefficients may nonetheless remain constant. In order to keep a subset of coefficients time-invariant, reorder  $\beta_i(t/T)$  such that  $\beta_i(t/T) = (\beta_i^{(1)'}(t/T), \beta_i^{(2)'})'$ , where the  $p^{(1)} \times 1$  vector  $\beta_i^{(1)}(t/T)$  varies smoothly over time and the  $p^{(2)} \times 1$  vector  $\beta_i^{(2)}$  is constant. After partitioning  $\mathbf{x}_{it} = (\mathbf{x}_{it}^{(1)'}, \mathbf{x}_{it}^{(2)'})'$  to conform with  $\beta_i(t/T)$ , extend the criterion (2.6) to

$$\begin{aligned} \mathcal{F}_{NT}(\boldsymbol{\pi}^{(1)}, \boldsymbol{\beta}^{(2)}, \lambda) &= \frac{1}{T} \sum_{i=1}^N \sum_{t=1}^T \left( \tilde{y}_{it} - \boldsymbol{\pi}_i^{(1)'} \tilde{\mathbf{z}}_{it}^{(1)} - \boldsymbol{\beta}_i^{(2)'} \tilde{\mathbf{x}}_{it}^{(2)} \right)^2 \\ &\quad + \frac{\lambda}{N} \sum_{i=1}^{N-1} \sum_{j=i+1}^N \dot{\omega}_{ij} \|\boldsymbol{\varpi}_i - \boldsymbol{\varpi}_j\|_2, \end{aligned}$$

where  $\boldsymbol{\beta}^{(2)} = (\beta_1^{(2)'}, \dots, \beta_N^{(2)'})'$  and  $\boldsymbol{\varpi}_i = (\boldsymbol{\pi}_i^{(1)'}, \boldsymbol{\beta}_i^{(2)'})'$ . Furthermore, we now estimate the adaptive penalty weight  $\dot{\omega}_{ij} = \|\hat{\boldsymbol{\varpi}}_i - \hat{\boldsymbol{\varpi}}_j\|_2^{-\kappa}$  as

$$\hat{\boldsymbol{\varpi}}_i = \arg \min_{\boldsymbol{\varpi}_i} \frac{1}{T} \sum_{t=1}^T \left( \tilde{y}_{it} - \boldsymbol{\pi}_i^{(1)'} \tilde{\mathbf{z}}_{it}^{(1)} - \boldsymbol{\beta}_i^{(2)'} \tilde{\mathbf{x}}_{it}^{(2)} \right)^2.$$

The *post-Lasso* estimator is defined as

$$\hat{\boldsymbol{\varpi}}^p = \arg \min_{\boldsymbol{\varpi}} \frac{1}{T} \sum_{t=1}^T \left( \tilde{y}_t - \text{diag}(\tilde{\mathbf{Z}}_{\hat{G}_1 t}^{(1)}, \dots, \tilde{\mathbf{Z}}_{\hat{G}_K t}^{(1)})' \boldsymbol{\xi}^{(1)} - \text{diag}(\tilde{\mathbf{X}}_{\hat{G}_1 t}^{(2)}, \dots, \tilde{\mathbf{X}}_{\hat{G}_K t}^{(2)})' \boldsymbol{\alpha}^{(2)} \right)^2,$$

where  $\tilde{\mathbf{Z}}_{\hat{G}_k t}^{(1)} = \{\tilde{\mathbf{z}}_{it}^{(1)} : i \in \hat{G}_k, 1 \leq i \leq N\}$  and  $\tilde{\mathbf{X}}_{\hat{G}_k t}^{(2)} = \{\tilde{\mathbf{x}}_{it}^{(2)} : i \in \hat{G}_k, 1 \leq i \leq N\}$ ,  $\hat{\boldsymbol{\varpi}}^p = (\hat{\boldsymbol{\varpi}}_{\hat{G}_1}^{p'}, \dots, \hat{\boldsymbol{\varpi}}_{\hat{G}_K}^{p'})'$  are  $Mp^{(1)} \times \hat{K}$  and  $Mp^{(2)} \times \hat{K}$  matrices collecting all observations pertaining to group  $k$ , respectively. Furthermore,  $\hat{\boldsymbol{\varpi}}_{\hat{G}_k}^p = (\hat{\boldsymbol{\xi}}_{\hat{G}_k}^{(1)p'}, \hat{\boldsymbol{\alpha}}_{\hat{G}_k}^{(2)p'})'$ ,  $\hat{\boldsymbol{\xi}}^{(1)p} = (\hat{\boldsymbol{\xi}}_{\hat{G}_1}^{(1)p}, \dots, \hat{\boldsymbol{\xi}}_{\hat{G}_K}^{(1)p})$ ,  $\hat{\boldsymbol{\alpha}}_{\hat{G}_k}^{(2)p} = (\hat{\boldsymbol{\alpha}}_{\hat{G}_1}^{(2)p'}, \dots, \hat{\boldsymbol{\alpha}}_{\hat{G}_K}^{(2)p'})'$ , and  $\hat{\boldsymbol{\alpha}}_{\hat{G}_k}^{(1)p}(t/T) =$

$\hat{\Xi}_{\hat{G}_k}^{(1)p'}$   $\mathbf{b}(t/T)$ . The remaining terms are as introduced in Section 2.1 and above.

It is straightforward to see that the asymptotic properties of  $\boldsymbol{\pi}_i^{(1)}$  remain unchanged from Section 3 when substituting  $p$  with  $p^{(1)}$ . The same holds for  $\hat{\boldsymbol{\beta}}_i^{(2)}$  when taking  $M = 1$ ,  $p = p^{(2)}$ , and treating  $M$  as constant. The limiting distributions in Theorem 3.5 apply, when replacing  $p$  with  $p^{(l)}$ ,  $l = \{1, 2\}$ , respectively, and when fixing  $M = 1$  for the vector of time-invariant coefficients.

### D.3 Unbalanced Panels

Panel datasets with varying numbers of observations among individuals are ubiquitous in empirical applications. We accommodate such unbalanced panels in the *time-varying PAGFL* framework by adjusting the DGP in (2.5) to

$$y_{it} = \gamma_i + \boldsymbol{\pi}_i^{0'} \mathbf{z}_{it} + u_{it}, \quad u_{it} = \epsilon_{it} + \eta_{it}, \quad i = 1, \dots, N, \quad t = t_i, \dots, T_i,$$

where  $t_i$  indicates the individual start of the observational period for each cross-sectional unit,  $T_i$  the end, and  $\mathcal{T}_i = T_i - t_i - 1$  the number of observed time periods per unit. It is straightforward to extend the objective function (2.6) to this scenario by rewriting

$$\mathcal{F}_{NT}(\boldsymbol{\pi}, \lambda) = \frac{1}{T} \sum_{i=1}^N \sum_{t=t_i}^{T_i} (\tilde{y}_{it} - \boldsymbol{\pi}_i' \tilde{\mathbf{z}}_{it})^2 + \frac{\lambda}{N} \sum_{i=1}^{N-1} \sum_{j=i+1}^N \dot{\omega}_{ij} \|\boldsymbol{\pi}_i - \boldsymbol{\pi}_j\|_2,$$

with  $\tilde{a}_{it} = a_{it} - \mathcal{T}_i^{-1} \sum_{t=t_i}^{T_i} a_{it}$  for  $a_{it} = \{y_{it}, \mathbf{z}_{it}\}$ . The remaining notation is left unchanged.

Similarly, the *post-Lasso* is given by

$$\hat{\boldsymbol{\xi}}_{\hat{G}_k}^p = \left( \sum_{i \in \hat{G}_k} \sum_{t=t_i}^{T_i} \tilde{\mathbf{z}}_{it} \tilde{\mathbf{z}}_{it}' \right)^{-1} \sum_{i \in \hat{G}_k} \sum_{t=t_i}^{T_i} \tilde{\mathbf{z}}_{it} \tilde{y}_{it}.$$

In order to study the asymptotic behavior, let  $T_{\min} = \min_i \mathcal{T}_i$  and assume  $T_{\min} \rightarrow \infty$ . When substituting  $T$  with  $T_{\min}$ , all proofs and assumptions carry seamlessly over to unbalanced panel datasets (see Su et al., 2019, sec. 5.2). Notice that this extension also applies to missing observations in the middle of the panel, i.e.  $t = t_i, \dots, t_{i+j}, t_{i+j+l}, \dots, T_i$ , for some integers  $0 < j < T_i - 2$  and  $1 < l < T_i - i - j$ , since nonparametric splines implicitly interpolate missing values. Furthermore, the *post-Lasso* pools homogenous cross-sectional units. In consequence, remaining group members compensate for a missing observation in individual series. These two aspects make our methodology particularly powerful in empirical applications with unbalanced panel datasets.



Table 3:  $\lambda$  tuning parameter candidate values in the simulation studies

DGP 1		Section 4.3		AR(1) errors (E.1)		30% of the sample discarded (E.2)	
N	T	$\underline{\lambda}$	$\bar{\lambda}$	$\underline{\lambda}$	$\bar{\lambda}$	$\underline{\lambda}$	$\bar{\lambda}$
50	50	0.1	50	0.1	20	0.1	10
100	50	0.1	50	0.1	20	0.1	10
50	100	0.1	50	0.1	20	0.1	10
100	100	0.1	50	0.1	20	0.1	10
DGP 2		Section 4.3		AR(1) errors (E.1)		30% of the sample discarded (E.2)	
N	T	$\underline{\lambda}$	$\bar{\lambda}$	$\underline{\lambda}$	$\bar{\lambda}$	$\underline{\lambda}$	$\bar{\lambda}$
50	50	10	35	30	75	15	47
100	50	10	35	25	65	10	30
50	100	1	20	8	25	10	60
100	100	1	20	18	37	10	60
DGP 3		Section 4.3		AR(1) errors (E.1)		30% of the sample discarded (E.2)	
N	T	$\underline{\lambda}$	$\bar{\lambda}$	$\underline{\lambda}$	$\bar{\lambda}$	$\underline{\lambda}$	$\bar{\lambda}$
50	50	0.01	15	0.1	20	0.1	20
100	50	0.01	15	4	20	5	25
50	100	0.01	15	0.1	20	0.1	20
100	100	0.01	15	0.1	8	0.1	9

Notes: Upper and lower limits for the sequences of candidate  $\lambda$  penalty tuning parameter values. The sequences are of length 50 and run from  $\underline{\lambda}$  to  $\bar{\lambda}$ .

## E Additional Simulation Studies and Details

Subsections E.1 and E.2 present the simulation study results when the errors are serially correlated and when 30% of observations are randomly discarded, respectively. Subsection E.3 provides details on the implementation of the *time-varying C-Lasso* benchmark model.

Table 3 reports the tuning parameter candidate values employed in the Monte Carlo experiments.

### E.1 DGPs with Serially Correlated Errors

Tables 4 and 5 report the Monte Carlo simulation study results when the innovations are constructed as  $\epsilon_{it} = 0.3\epsilon_{it-1} + e_{it}$ , where  $e_{it} \sim i.i.d.N(0, 1)$ . Serial correlation in the errors to such an extent does not infringe on Assumption 1(ii), as the process still remains stationary. However, as serial correlation is set to introduce additional estimation uncertainty and previous simulation studies in Section 4 show that such uncertainty complicates the classification mechanism, we choose to reduce the number of interior knots  $M^*$  for this exercise. We select  $M^* = 2$  for DGP 1 and  $M^* = 1$  for the two remaining DGPs.

When  $T = 100$ , the simulation results mirror largely the ones reported in section 4.3. However, as serially correlated errors effectively reduce the informational value contained in a time series, the performance in small samples is notably reduced. This does not just concern the grouping mechanism and the resulting estimation inaccuracy, but also the *RMSE* of the infeasible oracle estimator.

Table 4: Classification accuracy with serially correlated errors

	N	T	Freq. $\hat{K} = K_0$	Freq. $\hat{\mathcal{G}}_{\hat{K}} = \mathcal{G}_{K_0}^0$	ARI	$\bar{K}$
DGP 1	50	50	0.680	0.190	0.855	3.270
	50	100	0.927	0.753	0.978	3.080
	100	50	0.680	0.077	0.809	2.753
	100	100	1.000	0.720	0.990	3.000
DGP 2	50	50	0.140	0.027	0.577	2.130
	50	100	0.757	0.647	0.878	2.760
	100	50	0.073	0.007	0.501	1.940
	100	100	0.512	0.383	0.768	2.510
DGP 3	50	50	0.567	0.030	0.708	2.680
	50	100	0.903	0.560	0.937	2.990
	100	50	0.160	0.007	0.550	2.130
	100	100	0.933	0.433	0.951	2.970

Notes: Frequency of obtaining the correct number of groups  $\hat{K} = K_0$  and the correct grouping  $\hat{\mathcal{G}}_{\hat{K}} = \mathcal{G}_{K_0}^0$ , the ARI, and the average estimated number of total groups  $\bar{K}$  based on a Monte Carlo study with 300 replications. The errors are serially correlated with an autoregressive coefficient of 0.3.

## E.2 DGPs with Unbalanced Panels

Unbalanced panel datasets are a frequent occurrence in real world applications. Subsequently, we re-run our simulation study after discarding a randomly drawn 30% subset of each time series. This exercise gives an understanding how the classification performance and the estimation of the functional coefficients behave when some observations have to be interpolated. Furthermore, in line with the decreased informational value of an unbalanced panel dataset, we again deviate from the heuristic for the number of internal knots  $M^*$  provided in section 4 and set  $M^* = 2$  for DGP 1 and  $M^* = 1$  for the remaining two DGPs. Table 6 displays the classification metrics and Table 7 the *RMSE* values.

In large samples both the classification metrics and the *RMSE* are very similar to the ones reported in Section 4.3. However, just like the in the previous subsection, small samples suffer from the reduced number of observations. This dynamic is particularly apparent in DGP 2. Omitting observations, even on the interior of time series, seems akin to reducing  $T$  with respect to the classification performance and estimation accuracy of the *time-varying PAGFL*.

## E.3 Implementation of the *Time-varying C-Lasso*

In Section 4 we employ the *time-varying C-Lasso* by Su et al. (2019) as a benchmark, using Matlab replication files kindly provided by the authors. The *time-varying C-Lasso* and our methodology are exposed to the same simulated data, the DGPs following Su et al. (2019, sec. 6). The settings of the *time-varying C-Lasso* are specified as documented in Su et al. (2019, sec. 6): we set the polynomial degree to  $d = 3$ , the number of interior spline knots according to the heuristic  $M^* = \lfloor (NT)^{1(6)} \rfloor$  and the *C-Lasso* penalty tuning parameter to  $\lambda = (NT)^{-(2K+3)/24}$ . Furthermore, as the *C-Lasso* requires an explicit specification of the number of groups, we evaluate their IC for  $K = \{2, 3, 4\}$ , with  $\rho$  in the IC equaling  $\rho = M^* \log(NT)/(NT)$  (cf. Su et al., 2019, eq. 4.9).

Table 5: *RMSE* of coefficient estimates with serially correlated errors

		N	T	<i>PSE</i>	<i>post-Lasso</i>	oracle
DGP 1	$\hat{\alpha}_{k,0}(t/T)$	50	50	0.426	0.282	0.188
		50	100	0.346	0.226	0.165
		100	50	0.470	0.290	0.163
		100	100	0.339	0.212	0.15
DGP 2	$\hat{\alpha}_{k,1}(t/T)$	50	50	0.357	0.225	0.161
		50	100	0.275	0.158	0.137
		100	50	0.359	0.238	0.135
		100	100	0.309	0.149	0.095
DGP 3	$\hat{\alpha}_{k,2}(t/T)$	50	50	0.454	0.279	0.161
		50	100	0.314	0.162	0.120
		100	50	0.465	0.315	0.121
		100	100	0.385	0.184	0.088
DGP 3	$\hat{\alpha}_{k,3}(t/T)$	50	50	0.419	0.269	0.216
		50	100	0.339	0.230	0.222
		100	50	0.498	0.321	0.212
		100	100	0.364	0.226	0.219

*Notes:* *RMSE* of the *PSE*, the *post-Lasso*, and an infeasible oracle estimator based on a Monte Carlo study with 300 replication. The errors are serially correlated with an autoregressive coefficient of 0.3.

## F Details on the Empirical Illustration

The empirical illustration focuses on the 100 largest economies by GDP in 2022. The Global Carbon Budget provides CO<sub>2</sub> emission data for 99 of these economies, not tracking Puerto Rico. Additionally, we omit Azerbaijan (AZE), Iraq (IRQ), Kuwait (KWT), Luxembourg (LUX), Qatar (QAT), Turkmenistan (TKM), and the United Arab Emirates (ARE) from our study. These countries exhibit sever outliers and pronounced idiosyncratic volatility in their CO<sub>2</sub> intensity time series, predominantly attributable to extraordinary geopolitical events, such as conflicts and oil shocks, or unique economic structure, like those of tax havens or petro-economies. Figure 6 makes it apparent that the CO<sub>2</sub> intensity trajectories of these discarded economies diverge markedly from one another and from the estimated trend functions, further justifying their exclusion. The 92 countries included in the sample are listed in Table 9.

Table 8 presents descriptive statistics for the final sample of CO<sub>2</sub> emission intensities.

Table 9 provides a detailed report of the estimated group structure.

Table 6: Classification metrics in an unbalanced panel

	N	T	Freq. $\hat{K} = K_0$	Freq. $\hat{\mathcal{G}}_{\hat{K}} = \mathcal{G}_{K_0}^0$	ARI	$\bar{K}$
DGP 1	50	50	0.907	0.620	0.961	3.093
	50	100	1.000	0.973	0.998	3.000
	100	50	0.990	0.543	0.976	2.990
	100	100	1.000	0.980	0.999	3.000
DGP 2	50	50	0.477	0.090	0.713	2.530
	50	100	0.983	0.887	0.985	2.997
	100	50	0.337	0.050	0.620	2.260
	100	100	0.990	0.810	0.988	2.990
DGP 3	50	50	0.700	0.030	0.734	3.060
	50	100	0.910	0.467	0.939	3.057
	100	50	0.200	0.003	0.522	2.170
	100	100	0.853	0.277	0.906	2.873

Notes: Frequency of obtaining the correct number of groups  $\hat{K} = K_0$  and the correct grouping  $\hat{\mathcal{G}}_{\hat{K}} = \mathcal{G}_{K_0}^0$ , the ARI, and the average estimated number of total groups  $\bar{K}$  based on a Monte Carlo study with 300 replications. 30% of observations randomly discarded to create an unbalanced panel dataset.

Table 7: RMSE of coefficient estimates in an unbalanced panel

		N	T	PSE	post-Lasso	oracle
DGP 1	$\hat{\alpha}_{k,0}(t/T)$	50	50	0.370	0.235	0.226
		50	100	0.276	0.212	0.152
		100	50	0.371	0.218	0.153
		100	100	0.259	0.203	0.142
DGP 2	$\hat{\alpha}_{k,1}(t/T)$	50	50	0.316	0.201	0.142
		50	100	0.233	0.145	0.123
		100	50	0.334	0.225	0.124
		100	100	0.241	0.138	0.112
DGP 3	$\hat{\alpha}_{k,2}(t/T)$	50	50	0.403	0.240	0.149
		50	100	0.267	0.138	0.124
		100	50	0.413	0.278	0.127
		100	100	0.273	0.127	0.112
DGP 3	$\hat{\alpha}_{k,3}(t/T)$	50	50	0.304	0.162	0.109
		50	100	0.207	0.076	0.064
		100	50	0.402	0.228	0.068
		100	100	0.236	0.076	0.053

Notes: RMSE of the PSE, the post-Lasso, and an infeasible oracle estimator based on a Monte Carlo study with 300 replication. 30% of observations randomly discarded to create an unbalanced panel dataset.

Table 8: Descriptive statistics of the CO<sub>2</sub> intensity panel dataset

	Mean	Std.	Min	Q1	Median	Q3	Max
CO <sub>2</sub>	249.916	849.137	0.026	10.414	42.67	152.551	11953.218
GDP	395.621	1521.375	0.063	11.349	49.997	217.156	27360.935
CO <sub>2</sub> intensity	1.381	1.696	0.037	0.358	0.784	1.675	13.685
Observational horizon	56.511	12.48	29	55.5	64	64	64

Notes: Summary statistics on the panel dataset employed in the empirical illustration. CO<sub>2</sub> is measured in million tonnes, GDP in billion 2024 U.S. dollar, and the observational horizon in years.

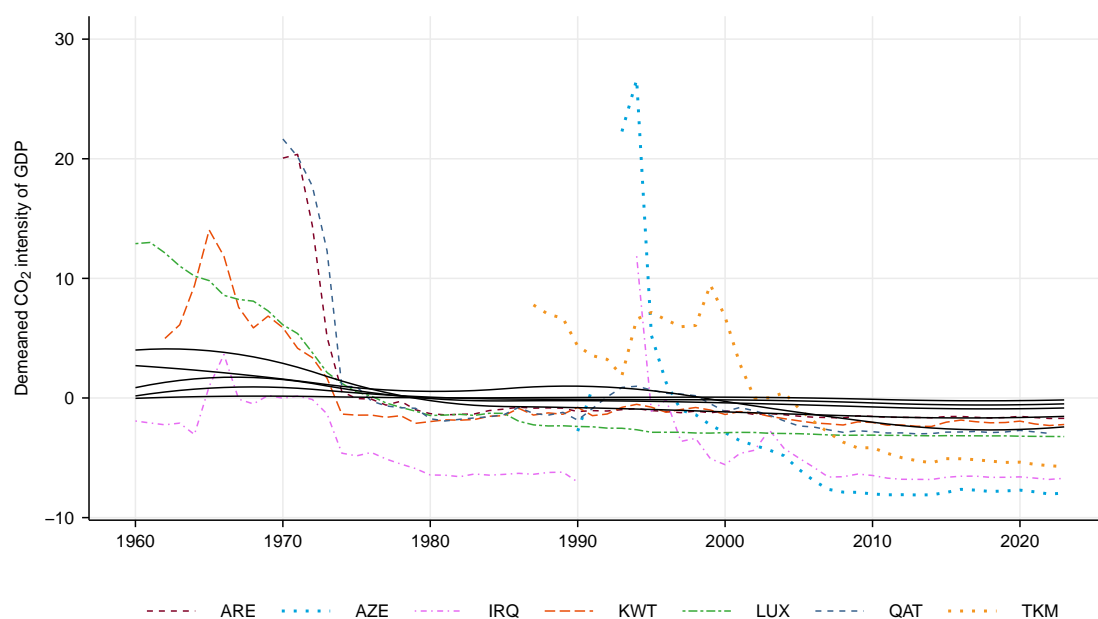


Figure 6: Demeaned CO<sub>2</sub> intensity of countries excluded from the analysis (colored) and the estimated group-specific trend functions (black, solid) based on the remaining panel dataset. The 1991 and 1992 observations for Iraq (1991: 103.51, 1992: 117.79) in addition to the 1992 and 1993 observations for Azerbaijan (1992: 99.06, 1993: 53.88) are omitted from the figure for ease of exposition.

Table 9: Group structure in the CO<sub>2</sub> emission intensity of GDP

Group 1 (18)	Angola	China	Kazakhstan	Serbia	Uruguay
	Belarus	Czechia	Poland	Slovakia	Uzbekistan
	Bulgaria	Estonia	Romania	Sweden	
	Chile	Italy	Russia	Ukraine	
Group 2 (28)	Algeria	Greece	Libya	Panama	Switzerland
	Argentina	Hong Kong	Malaysia	Philippines	Tunisia
	Bolivia	India	Mexico	Portugal	Turkey
	Dem. Rep. Congo	Indonesia	New Zealand	Saudi Arabia	Vietnam
	Egypt	Israel	Norway	Singapore	
	Finland	Kenya	Pakistan	Spain	
Group 3 (24)	Australia	Colombia	Hungary	Lithuania	South Africa
	Austria	Croatia	Iran	Myanmar	South Korea
	Bahrain	Denmark	Ireland	Netherlands	USA
	Belgium	France	Japan	Peru	United Kingdom
	Canada	Germany	Latvia	Slovenia	
	Group 4 (8)	Bangladesh	Cameroon	Ethiopia	Nepal
Brazil		Ecuador	Ghana	Tanzania	
Costa Rica		El Salvador	Morocco	Paraguay	Thailand
Group 5 (14)	Côte d'Ivoire	Guatemala	Nigeria	Sri Lanka	Uganda
	Dominican Republic	Jordan	Oman	Sudan	

Notes: Estimated group structure  $\hat{\mathcal{G}}_K$  in the trends of the CO<sub>2</sub> emission intensity. Group cardinalities are in parenthesis.